Mechanism of RanGTP dependent microtubule assembly during mitosis

Jacopo Scrofani

TESI DOCTORAL UPF - 2014

Thesis supervisor:

Dr. Isabelle Vernos

CELL AND DEVELOPMENTAL BIOLOGY PROGRAM

CRG (CENTER FOR GENOMIC REGULATION)

“Amico, alza lo sguardo dal microscopio.

Il mondo é grande, la natura immensa.”

Anonimo

Aknowledgments

This work would have never been possible without the following people:

Dr. Isabelle Vernos for giving me the opportunity to enjoy science in her Lab. I am really grateful for her kind and inspiring mentoring during all these four years of PhD.

Dr. Sylvain Meunier for mentoring, helping and encouraging me in all scientific and extra-scientific aspect of my PhD.

All the members of my thesis committee Dr. Manuel Mendoza, Dr. Luciano Di Croce and Dr. Jens Luders for their essential support and for helping me to keep the project right on tracks.

Dr. Pedro Carvalho, Dr. Jens Luders, Dr. Manuel Mendoza, Dr. Andreas Merdes and Dr. Joan Roig for the critical reading of this thesis.

Dr. Andrea Zecca for the inspiring conversations and friendly support in life and in science.

The people that inspired me during my first steps in science: Dr. Renata Tisi, Dr. Patrizia Lavia and Dr. Giulia Guarguaglini. Without them I would never have decided to leave my home to begin a PhD here in Barcelona.

All the peoples that, in the present and in the past, have shared with me the best and the worst of the lab experiences.

My family and my friends the best support ever.

Lady Blue, my “macroscope”, essential instrument to fully enjoy the beauty of nature.

Anna, always dreaming with me.

Summary

During mitosis, spindle assembly involves different sources of microtubules including centrosomes and chromosomes. While the role of centrosomes has been extensively studied over many years, we still do not fully understand how chromosomes trigger microtubule nucleation, stabilization and organization thereby contributing to the formation of the mitotic spindle. The chromosomal pathway is largely determined by a RanGTP gradient centered on the chromosomes that induces the local activation of spindle assembly factors by releasing them from importins. So far only few RanGTP targets have been identified. A prominent role is played by TPX2, known to be essential for microtubule nucleation around the chromosomes although the mechanism involved is still unclear. To get a better understanding on the RanGTP-dependent microtubule assembly during mitosis we aimed at:

i) Identifying and functionally characterize new RanGTP regulated proteins involved in spindle assembly. I will present here the approach we devised to select candidates from large proteomic data and to validate them experimentally. Our results pointed to three novel proteins with a putative mitotic role in the RanGTP pathway of microtubule assembly.

ii) Understanding how the RanGTP pathway regulates microtubule nucleation during mitosis. Combining HeLa cell lines with the *Xenopus laevis* egg extract system we found that TPX2 together with Aurora-A and RHAMM are part of a RanGTP-dependent complex that binds and strongly stimulates the γ-TuRC microtubule nucleation activity. Assaying *in vitro* microtubule nucleation we found that this regulatory mechanism requires two essential events both triggered by TPX2: a) the phosphorylation by Aurora-A of the γ-TuRC component NEDD1 on its S405 and b) the gathering of multiple γ-TuRCs.

iii) Investigating the contribution of the RanGTP pathway to spindle assembly. Particularly, our preliminary data provided new evidences to support a role for chromosomal nucleated MTs in k-fiber assembly.

Resumen

Durante la mitosis, el proceso de ensamblaje del huso mitótico implica diferentes fuentes de microtúbulos incluyendo centrosomas y cromosomas. Mientras que el rol de los centrosomas ha sido extensamente estudiado durante los últimos años, no se entiende en su totalidad como los cromosomas inducen la nucleación, la estabilización y la organización de microtúbulos contribuyendo de esta manera a la formación del huso mitótico. La vía de los cromosomas está mayormente determinada por un gradiente de RanGTP, centrado en los cromosomas, que induce la activación local de factores de ensamblaje del huso liberándolos de las importinas. Hasta el momento, solo unos pocos factores regulados por RanGTP han sido identificados. Aunque el mecanismo implicado no está todavía claro, el papel de TPX2 es esencial en la nucleación de los microtúbulos alrededor de los cromosomas. Para entender el mecanismo que promueve el ensamblaje de los microtúbulos vía RanGTP durante la mitosis, este trabajo tuvo los siguientes objetivos:

i) La identificación y caracterización funcional de nuevas proteínas reguladas por RanGTP que participan en el ensamblaje del huso. Se presenta la estrategia ideada para la selección experimental de los candidatos utilizando datos de proteómica y su posterior validación. Nuestros resultados apuntan a tres nuevas proteínas con un posible papel mitótico en la vía RanGTP de ensamblaje de los microtúbulos.

ii) El estudio de el mecanismo para el cual RanGTP regula la nucleación de microtúbulos durante la mitosis. La combinación de experimentos realizados con células HeLa junto con el sistema de extracto de huevos de *Xenopus*, mostró que TPX2 junto con Aurora-A y RHAMM son parte de un complejo RanGTP dependiente que estimula la actividad de nucleación de el γTuRC. Ensayando *in vitro* la nucleación de los microtúbulos mostramos que este mecanismo de regulación depende de dos eventos esenciales ambos desempeñados por TPX2: a) la fosforilación por Aurora-A del γTuRC en NEDD1 S405 y b) el reclutamiento de múltiples γTuRC.

iii) El estudio del papel de la vía de RanGTP en el ensamblaje del huso. En particular, nuestros datos preliminares proporcionan nuevas evidencias sobre la participación de los MTs nucleados alrededor de los cromosomas en el proceso del ensamble de fibras cinetocóricas.

Preface

The work presented in this thesis was carried out in the Cell and Developmental Biology Program at the Center for Genomic Regulation (CRG) and supervised by Dr. Isabelle Vernos.

The present work investigates the mechanism of the RanGTP dependent microtubule assembly during mitosis. It particularly provides new insight to the mechanism by which chromosomes regulate the γTuRC therefore triggering microtubule assembly in their close proximity. In this work I also obtained preliminar results strongly suggesting a link between chromosomal microtubule and k-fiber assembly.

Index

I. INTRODUCTION

1. The cell cycle

The cell cycle represents a basic mechanism of life, essential for all living beings to transmit their genetic identity. The transmission of the genetic material represents also the essential basic principle driving biological evolution. In fact, “it is cell’s dream to become two cells with identical copies of the genome” (Francois Jacob, 1965) and to satisfy it, along millions of years of evolution, cells developed a specific and accurate molecular machinery. More precisely, the cell cycle machinery orchestrates a sequential series of events that lead to division into two genetically identical daughter cells (Hartwell, 1978).

The cell cycle is classically divided into phases defined by specific events that need to occur before going to the next one. Different organisms have adopted different strategies during evolution however the same basic principles are conserved: the genetic material needs to be first replicated during the synthesis phase (S) and then the two identical copies faithfully segregated during mitosis. Between these two main events, two gap phases give the cell time to prepare for division. The two gap phases (G1 and G2) together with the DNA synthesis phase are defined as interphase (Fig. 1). Cell progression through the cell cycle involves the coordinated and consecutive execution of preparatory events for division. These events are subjected to an extremely precise regulation and are connected with the intra/extra cellular environment. Proliferative stimuli, like growth factors and nutrients, are essential for the cell to commit to divide. In absence of such stimuli cells can maintain themselves in a quiescent state (G0).

1.1. The cell cycle machinery

The basic mechanism driving cell cycle progression is the execution of specific processes interconnected by a sequential hierarchy. The rhythm of cell cycle progression is marked by the activity of the cyclin dependent kinases family (cdk). These are serine/threonine kinases with several substrates involved in the key cell cycle

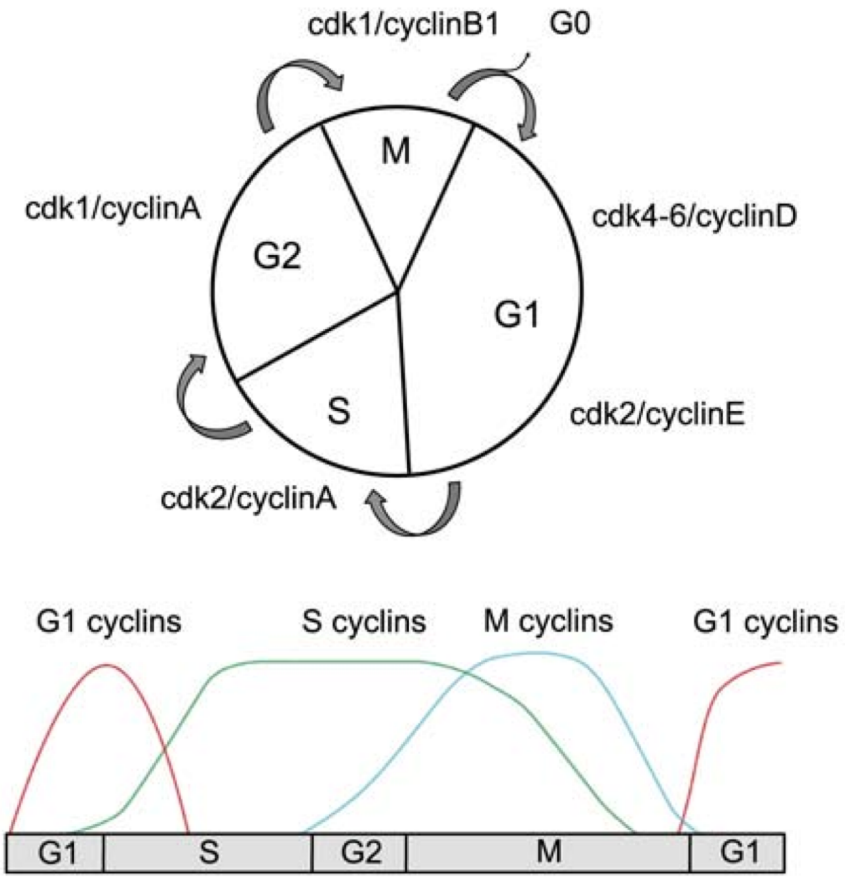

Figure 1. The cell cycle

A) Schematic representation of the human cell cycle and its main molecular machinery. The cell cycle is typically divided in phases: the interphase, constituted by two gap phases (G1 and G2) and one synthesis phase (S), and mitosis (M). The main cdk/cyclin complexes are indicated for each phase. Arrows represent the cell cycle transitions, characterized by synthesis and degradation of cyclins. B) Representation of the waves of activation of cdk/cyclin complexes. Cdk4-6/cyclinD promotes progression in G1 phase. Cdk2/cyclinE is responsible for the entry into S phase. Cdk2/cyclinA is essential for the S phase main events. Cdk1/cyclinA is responsible for G2. Cdk1/cyclinB triggers the entry into mitosis and its inactivation triggers anaphase and mitotic exit.

events (Golias et al., 2004). Cdk activity is subjected to a tight spatial and temporal regulation by the sequential synthesis and degradation of cyclins (Hunt, 1991). In this way specific cdk/cyclin complexes characterize every cell cycle phase. An example of this mechanism is the interphase to mitosis transition that in mammalian cells is mediated by the MPF (Maturation Promoting Factor; (Hunt, 1989; Schorderet-Slatkine and Drury, 1973). This factor is composed by cdk1 as catalytic subunit and the regulatory cyclinB1 and it is specifically activated by the completion of the previous

gap phase (Doree and Galas, 1994; Murray et al., 1989). The MPF activation triggers a signalling cascade that ends up in the spectacular morphologic rearrangement typical of the interphase to mitosis transition. Nuclear envelope break down, spindle assembly, chromosome condensation and segregation are examples of cell cycle regulated events essential for cell division. Mitosis exit requires cyclinB1 degradation and shut off cdk1 activity with the consequent establishment of the specific interphase cdk/cyclin complexes (Pines and Rieder, 2001). The basic mechanism, simplified in this paragraph, is based on the synthesis and degradation of specific cyclic regulators allowing the cell to orchestrate the temporal execution of all the processes essential for its division.

2. Mitosis

Mitosis is the final cell cycle phase and is characterized by a full morphological reorganization. The whole cell rearranges its structures to prepare for division. The most spectacular mitotic process is the reorganization of the interphase cytoskeleton into a dynamic microtubule (MT)-based and spindle-shaped structure: the mitotic spindle. Since the late 1870s, when cell division was described for the first time (Flemming, 1878), mitosis has been divided in sub-phases based on the morphological description of the process (Rieder and Khodjakov, 2003). In the following chapter I will provide a short description of the main events that characterize each mitotic phase from a microscopic point of view (Fig. 2). However, we have to consider that this description is much more complicated when we try to describe these events from a molecular point of view. Each step is in fact the result of precise biochemical events such as protein synthesis and degradation (Pines, 2006) or post translational modifications like phosphorylation and ubiquitination (Pines and Rieder, 2001). All these molecular events are under the tight control of the cell cycle machinery.

In prophase, the chromatin starts to compact and the two centrosomes start to assemble highly dynamic MTs. In the meantime pushing forces acting on MTs drive the separation of centrosomes that slide along the nuclear envelope. During prometaphase the nuclear envelope breaks down triggering initiation of spindle assembly.

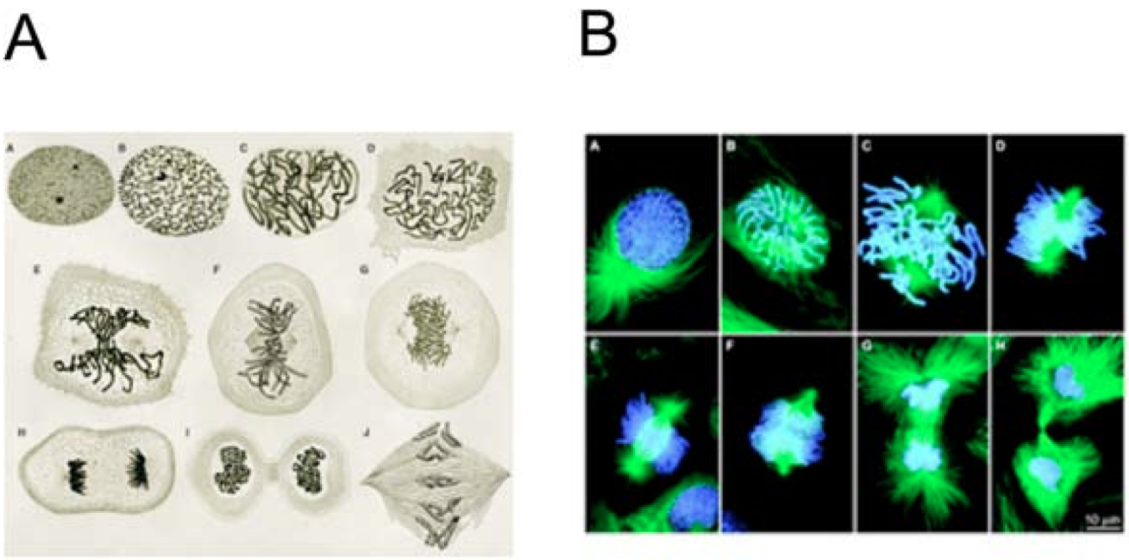

(Rieder and Khodjakov, 2003)

Figure 2. Mitosis

A) Drawings of mitotic phases by Fleming from the book "Zellsubstanz, Kern und Zelltheilung" written in 1882. During prophase the DNA condenses to form dense structures with high affinity for dyes: the chromosomes. After nuclear envelope breakdown, a spindle-shaped structure forms: Chromosomes attach to a spindle-shaped structure: the mitotic spindle to which chromosomes attach. During metaphase, chromosomes align on the cell equator, in the middle of the spindle. Once aligned the two chromatids of each chromosome detach and move toward the spindle poles. During late mitosis the cell divides and the two pools of chromosomes reconstitute the interphase nucleus. B) Immunofluorescence analysis of mitotic phases in newt lung cells. Microtubules (green) and chromosomes (blue) are stained with fluorescent dyes. Figure modified from (Rieder and Khodjakov, 2003).

Centrosomal MTs are free to explore the whole cell cytoplasm and chromosomes start to assemble MTs. During prometaphase, the kinetochores, multi-protein structures assembled at the centromere region of each chromosome (Cheeseman and Desai, 2008), attach to a specific class of MTs connecting each chromosome to the two spindle poles. The kinetochore MTs (K-fibers) (Rieder, 2005) work connecting sister chromatids to each pole of the cell aligning chromosomes on the cell equator. The mitotic spindle organizes in the typical bipolar shape. Metaphase is reached when all the chromosomes are attached to both spindle poles and aligned on the metaphase plate. Chromosome segregation is the main event that characterizes anaphase. Initially, k-fibers apply pulling forces that move chromatids to spindle poles. In this phase, a MT dense structure is assembled by the overlap of two anti parallel arrays of MTs: the central spindle. Subsequently, the sliding of these MTs one on each other triggers spindle elongation and further chromosome segregation. A contractile ring assembles around

the cleavage plane and once all the chromosomes are far away from this zone cytokinesis occurs. The ring contracts and membranes invaginate till two daughter cells are generated.

As shown in this short overview, a central event for cell division is the assembly of the mitotic spindle. The main components of this structure are the MTs whose properties are tightly regulated during the cell cycle. In the following chapters I will focus on MTs structure, function and regulation during mitosis.

3. The microtubules

MTs are essential components of the cell cytoskeleton, critically important in the spatial and temporal organization of eukaryotic cells. In fact MTs play a central part in a wide range of cellular processes such as intracellular transport, organelle positioning, cell motility, signalling and cell division (Kollman et al., 2011). This multitude of mechanic and regulatory functions requires MTs ability to rapidly re-arrange into different types of structures. Example of that is the dramatic reorganization of the interphase MT network, responsible for cell shape maintenance, into a bipolar spindle with dynamic functions in cell division. This high functional MT versatility is based on the intrinsic dynamic properties of these polymers.

3.1. Structure of the microtubule

To understand MT function, it is essential to get a proper description of their structure. MTs are constituted by large polymers, called protofilaments, of α and ß-tubulin laterally connected to form a hollow tube of around 25 nm (Fig. 3). The number of protofilaments per MT averages 13, however, MTs have been reported with as few as 11 or as many as 15 (Chretien et al., 1992; Pierson et al., 1978). The head to tail association between each α and ß-tubulin heterodimer confers to each protofilament as well as to the whole tube a polarity. Specifically, ß-tubulin is exposed at the MT "plus-end" whereas α-tubulin is at the "minus-end". The polarity is an essential property for the assembly and function of MTs. In fact, the two MT ends differ in polymerization

properties as the plus-end grows faster than the minus-end. Also the binding of some MAPs (Microtubule Associates Proteins) or the motility properties of motor proteins (Jiang and Akhmanova, 2011; Remy et al., 2013) are defined by MT polarity.

The understanding of the essential MT biology requires an accurate description of tubulin biochemical properties and structure. The α and β-tubulin monomers, which constitute the heterodimer subunit of a MT, are about 50% identical at the amino acid level, and each has a molecular mass of about 50 kDa (Burns, 1991). Tubulin has a GTP-ase activity that is stimulated by polymerization. In fact during polymerization, GTP bound to β-tubulin is hydrolyzed and the resulting GDP cannot exchange while β-tubulin remains in the polymer. Only when depolymerised, β-tubulin can exchange GDP for GTP and undergo a new cycle. Also α-tubulin binds to GTP, but this GTP is bound in a non-exchangeable manner and is not hydrolyzed during polymerization (Desai and Mitchison, 1997). GTP hydrolysis determines a curvature in the α–ß heterodimer structure that generates tension and instability inside the MT lattice (Vale et al., 1994).

3.2. The dynamics properties of microtubules

MTs are not stable polymers as they elongate and shrink continuously. This MT behaviour has been called dynamic instability as it is described by a stochastic switch between phases of slow growth and rapid shrinkage (Fig. 3). The transition between growth and shrinkage is called “catastrophe” whereas the transition between shrinkage and growth is called “rescue” (Mitchison and Kirschner, 1984a). The GTP hydrolysis inside the MT lattice explains this fundamental property. New incorporated GTP-bound tubulin subunits form a cap at the plus ends of growing MTs. This cap constituted of tubulin dimers in a stretched and low energy conformation stabilizes MTs protecting their plus ends from the GDP-bound unstable MT core. The loss of the GTP cap through GTP hydrolysis determines a catastrophic depolymerization of the MT plus end (Carlier, 1989). In the cellular environment many MAPs act on the dynamic properties of MTs therefore regulating their cellular functions.

In vitro studies showed that different dynamics at the two MT ends could determine preferential tubulin incorporation to one end and loss to the other end. This phenomenon

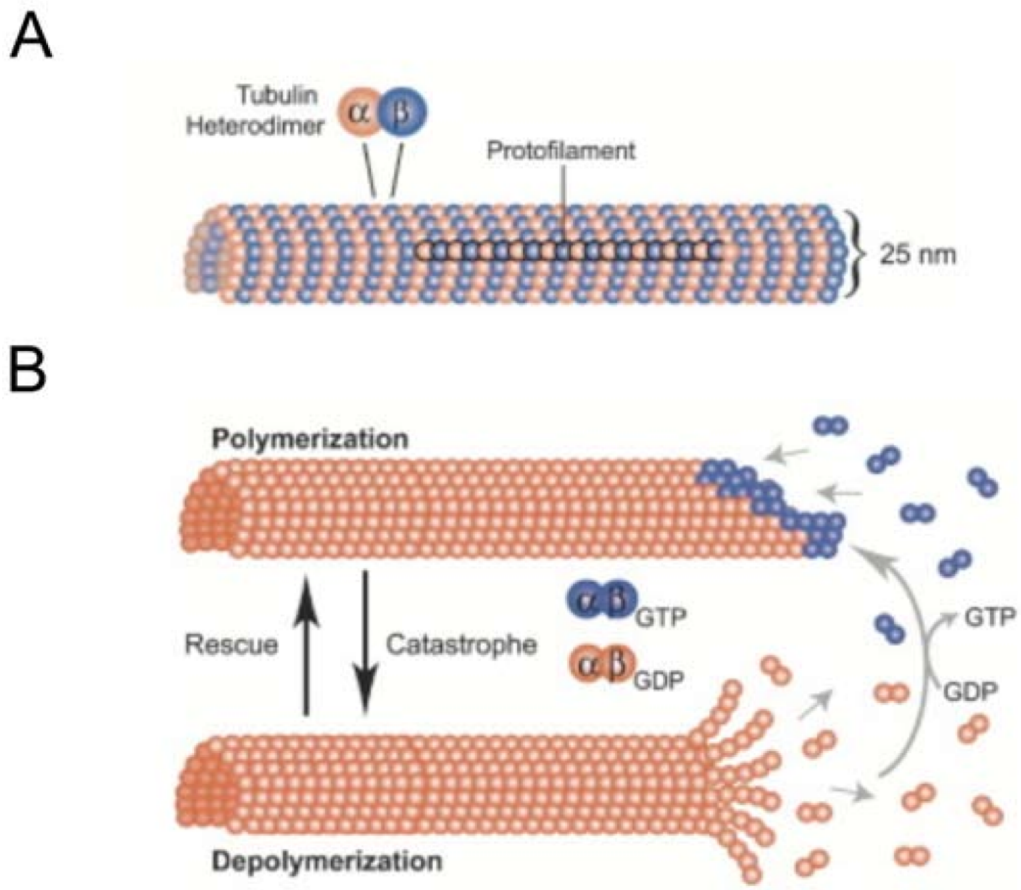

(Kline-Smith and Walczak, 2004)

Figure 3. Microtubule Structure and Dynamics

A) Illustration of MT structure. α-tubulin is represented in orange and β-tubulin in blue. α/β-tubulin dimers orientation defines the polarity of the MT. The plus-end exposes ß-tubulin. A single protofilament within the polymer lattice is outlined. B) The MTs alternate between stages of polymerization and depolymerization, a behavior central to dynamic instability. Dynamic instability can occur at both ends of the MT, however plus ends are more dynamic. GDP bound tubulin is in orange, and GTP bound tubulin, which generates the GTP cap, is in blue. Figure modified from (Kline-Smith and Walczak, 2004).

generates a flux of tubulin along the MT lattice (Margolis and Wilson, 1978). This intrinsic property is called MT flux as it presumes a unidirectional movement of incorporated tubulin between the two MTs ends. The flux can also be observed in mitotic living cells (Mitchison, 1989; Rogers et al., 2005) where it plays an essential role in many processes such spindle length maintenance, chromosomes alignment and segregation (Khodjakov and Kapoor, 2005).

In vitro MTs can spontaneously polymerize over certain tubulin concentration. MT growth *in vitro* must proceed through two phases. The first one is characterized by small

early assembly intermediates energetically unstable and with slow growth rate. A second phase starts when sufficiently large oligomers form. MT growth become energetically favourable and addition of tubulin proceeds rapidly (Rice et al., 2008). Specific nucleator complexes favour MT growth in living cells where tubulin concentration is not sufficient to promote spontaneous growth events. Their particular function is to bypass the initial slow growth phase providing the template function essential to promote energetically favourable MT growth events (Kollman et al., 2011).

4. The mechanism of microtubule assembly

As described before the MTs are essential polymers involved in many different cellular processes. Beyond their biological function MTs have intrinsic properties that simply emerge from their structural composition. This is extremely interesting in terms of biological evolution as cells "learned" how to take advantage from these structures evolving specific molecular machineries to regulate and control MT intrinsic properties. Here I will summarize the main cellular mechanisms involved in MT assembly.

4.1. Microtubule nucleation

As underlined before MT assembly in living cells cannot occur spontaneously as the initiation reactions in the assembly of the MT is energetically unfavorable. For that reason cells evolved a strategy to favour the MT assembly initiation reaction by mimicking the structure of stable MTs seeds therefore bypassing the first unstable intermediates (Rice et al., 2008). This "template" activity that initiates MT assembly is defined as nucleation (Fig. 4).

The first protein identified as "nucleator" is γ-tubulin, a member of the tubulin super family. It was related to MT nucleation because it localized to, and was essential for, all the known MTOCs in the cell (Oakley and Oakley, 1989). The crystal structure of γ-tubulin revealed an important similarity and possible interactions with both α and β-

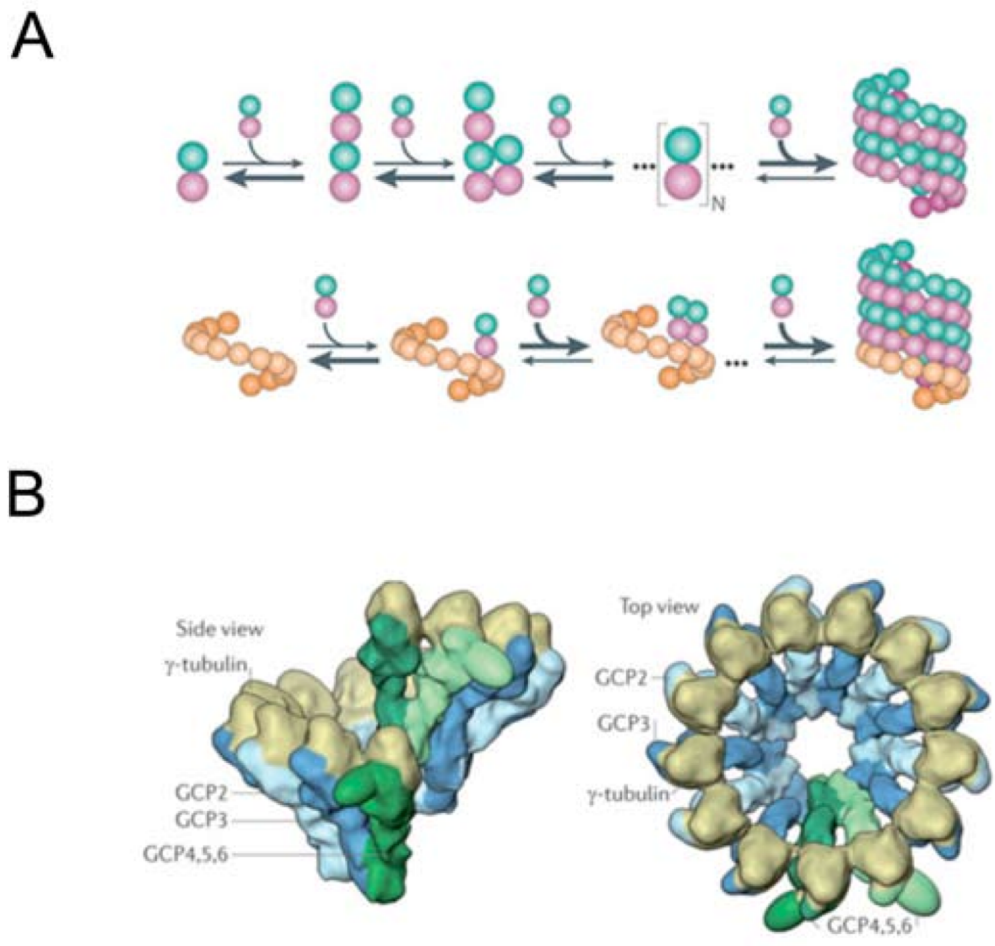

(Kollman et al., 2011)

Figure 4. Microtubule nucleation and γTuRC

A) Spontaneous microtubule nucleation *in vitro* (a) passes through energetically unstable intermediates. In a first phase depolymerization is favoured over polymerization. The kinetic of growth is slow during this phase and a variable number of steps (denoted by N) are required to form a sufficiently large polymer. In a second phase the newly nucleated MT assist the incorporation of new tubulin and the polymerization proceeds faster. (b) *In vivo,* MT nucleation is assisted by a specific complex that bypass the first unstable intermediates providing a spatial and temporal control. B) Side (left) and top (right) views of the γTuRC. The γTuSC (GCP2, GCP3 and γ-tubulin) provide an open ring template to favour MT nucleation. GCP4, GCP5 and GCP6 bind the γTuSC with lateral interactions constituting the γTuRC. Figure modified from (Kollman et al., 2011).

tubulin (Aldaz et al., 2005). Biochemical analysis revealed that at least seven other proteins co purified with γ-tubulin both in *Xenopus laevis* and human cell extracts (Murphy et al., 1998; Teixido-Travesa et al., 2010). Five of them, named gamma-tubulin complex proteins (GCP2-6), share high homology on two short fragments, the GRIPs motifs, that are unique for this family of proteins (Kollman et al., 2011). If depleted they destabilize the whole complex suggesting an important structural function

(Teixido-Travesa et al., 2012). In addition to the GCP family, three additional components of the γ-tubulin complex with no homology with the others, have been identified. These are GCP-WD (also called NEDD1 (Luders et al., 2006), MOZART1 (Hutchins et al., 2010) and GCP8 (also known as MOZART2 (Teixido-Travesa et al., 2010). All these components are considered part of the core complex, as in physiological conditions they are always associated to γ-tubulin. However, others proteins associate to the core components under specific condition with regulatory functions. Electron microscopy of purified γ-tubulin complexes revealed large ring shaped structures were therefore named γ-tubulin ring complexes (γTuRCs; (Zheng et al., 1995). These structures promote MT nucleation *in vitro* and several evidences in living systems demonstrated that the γTuRCs are essential to promote nucleation of MTs in the cell through different pathways (Teixido-Travesa et al., 2012). γ-tubulin complexes dissociate under high salt conditions to form a small sub complex constituted by γ-tubulin, GCP2 and GCP3 (Moritz et al., 1998; Oegema et al., 1999). This γ-tubulin small complex (γTuSC) is formed by one molecule of GCP2, one molecule of GCP3 and two molecules of γ-tubulin that are longitudinally bound to GCP 2 and 3 (Remy et al., 2013). Strikingly, γTuSCs show MT nucleation activity *in vitro* although it is lower than intact γTuRCs (Oegema et al., 1999). This observation suggests that the small complex works as catalytic core of the γTuRC. Stoichiometry revealed that a γTuRC is constituted by 12-13 molecules of GCP2 and GCP3, 2-3 copies of GCP4, 1 copy of GCP5 and 0-1 copies of GCP6 (Remy et al., 2013). Despite all these data, up to date, a clear vision of γTuRC 3D structure is still missing. However, new biochemical and crystallographic data about GCP4 support a model for γTuRC assembly (Guillet et al., 2011; Kollman et al., 2010). Based on that γTuRC assembles by lateral interactions between 13 γTuSCs into one helix and GCP4-6 occupying specific positions limiting its growth to one full turn (Fig. 4) (Kollman et al., 2011).

Considering the γTuRC structure, two main models have been proposed to explain how γTuRCs work in MT nucleation. The “protofilaments model” postulate that the γTuRC uncurls into linear γTuSCs oligomers that work as template protofilaments for the lateral attachment of α and β-tubulin to γ-tubulin. The “template model” suggests that the γTuSC helix works as template promoting longitudinal associations between γ-

tubulin and tubulin heterodimers with γ-tubulin always facing α-tubulin (Erickson, 2000). This last model is currently the more accepted one.

4.2. Microtubule dynamics

After nucleation, tubulin dimers integration in the tubular wall of the MT is energetically favoured. At this stage tubulin is in the GTP-bound straight conformation that facilitates its polymerization. Only after its integration tubulin starts to hydrolyze GTP to GDP. As trapped in the MT structure the consequent change in conformation generates high-energy tension. This is the force that trigger the MT catastrophe phase and consequently depolymerization (Dogterom et al., 2005). Many MAPs act as polymerising or depolymerising factors therefore the balance between these two opposite activities is essential for the regulation of MT growth and dynamics.

4.2.1. Microtubule stabilization

Polymerization is characterized by the addition of tubulin subunit to each of the 13 MT protofilaments. The kinetics of polymerization revealed that this reaction is limited by the diffusion of the dimers to the site of incorporation. Therefore this reaction is tightly dependent on tubulin concentration. To assist this process stabilizing agents could act as enzymes that speed the association reaction. XMAP215 (human ch-TOG) is a major example of this class of proteins (Gard and Kirschner, 1987). Interestingly two mechanisms have been proposed to explain the activity of such essential MT stabilizing agent. XMAP215, in fact, is a long and thin protein that can bind tubulin heterodimers assembled in small protofilaments (Cassimeris et al., 2001). The integration of these protofilaments could therefore efficiently promote MT growth. An alternative mechanism proposed to explain XMAP215 polymerase activity is a direct action at MT ends that could favour the integration of single tubulin dimers (Howard and Hyman, 2007).

Other MAPs with effect in MT stabilization differ from polymerases in the way they promote MT growth. One example is Tau that binds to the MT tip assembling a structure that is similar to the GTP-cap. Therefore, proteins like Tau work protecting MT from catastrophe stabilizing through lateral interactions their tips and promoting growth (Noetzel et al., 2005).

An interesting but less characterized MT stabilizing activity has been proposed to explain the role of CLASPs proteins. This family of proteins is commonly bound to MTs plus-ends where they promote repeated rescue events therefore playing a positive role for MT growth. CLASPs may work as movable clamps that locally promote rescues on dynamics MTs (Al-Bassam and Chang, 2011).

One important group of MAPs is characterized by its ability to bind and track growing MT plus-ends. Two prominent families of this group of proteins with a role in MT stabilization are the end binding EBs and the CLIPs (Akhmanova and Steinmetz, 2008). These proteins are incorporated into MT lattice at the plus-ends. Particularly EBs recognize specific features of tubulin in the GTP-bound state (Maurer et al., 2014) while CLIPs binding to tubulin dimers could be incorporated during polymerization (Slep, 2010). These proteins as integrated components of the MT lattice could directly change the structure of MTs ends acting as anti-catastrophe factors or through the recruitment of additional regulatory factors.

4.2.2. Microtubule destabilization

The GTP-bound integrated tubulin forms a cap at the plus-tip that prevents catastrophe and therefore MT depolymerization. The kinesin-13 family of depolymerases acts on this structure. MCAK, a member of that family, binds and acts at both ends of MTs removing specifically the GTP-bound tubulin heterodimers (Kinoshita et al., 2006). Removing the GTP-cap, the MCAK like depolymerases trigger catastrophe and therefore MT instability. Like MCAK also the kinesin-8 family member Kip3 acts as depolymerase but with a plus-end specificity (Varga et al., 2006). Other kinesins, such as Kif2A, Kif2B, Kif18A and Kif18B have been related to MT depolymerization however the mechanism is still unclear (Howard and Hyman, 2007).

Other strategies are adopted by MAPs to favour MT depolymerization. An interesting example has been proposed to explain stathmin/Op18 function in spindle assembly (Belmont et al., 1996). This protein has been shown to promote MT catastrophe both by sequestering tubulin heterodimers and stimulating the GTP-ase activity of tubulin at MT tips (Lawler, 1998). In addition to depolymerase activities a different class of proteins acts promoting MT destabilization. One example is the MT severing protein katanin that works removing tubulin subunit from MTs (Roll-Mecak and McNally, 2010).

4.2.3. Microtubule dynamics at the minus ends

In comparison with plus ends, much less is known about regulation of MT minus-ends. These are the place for MT nucleation and therefore have been considered protected by the MT capping activity of the γTuRC. The nucleation complex, in addition to its function in microtubule nucleation, has also a role in regulating the dynamics of the MT minus end by blocking both its growth and shrinkage (Anders and Sawin, 2011; Wiese and Zheng, 2000). However not all MTs are capped by γTuRCs and blunt and open minus-ends can be observed in cells by electron microscopy (Jiang and Akhmanova, 2011).

MCRS1 is a minus-end specific protein that associates to non-centrosomal MTs and k-fibers in cells. Its activity has been associated to the regulation of the dynamics at the chromosomal MT minus-ends. Strikingly MCRS1 executes these functions by specifically binding the MT minus ends and competing with the depolymerase MCAK (Meunier and Vernos, 2011). This suggests that another strategy adopted to stabilize MTs is the protection of the ends from MT destabilizing factors. Like MCRS1, the CAMSAPs family of proteins bind and stabilize MT minus-ends. Although they are not specific for non-centrosomal MTs, CAMSAPs proteins compete with MCAK for the binding to MTs minus ends therefore playing a stabilization role (Goodwin and Vale, 2010; Hendershott and Vale, 2014; Jiang et al., 2014).

4.3. Microtubule organization

As shown before MTs have many intrinsic dynamic properties that, in the cellular environment, are regulated trough different strategies by dedicated proteins. However to execute their mechanical and dynamic cellular functions MTs need to organize in specific structures such as the mitotic spindle. Interestingly recent *in vitro* studies revealed new MT emerging properties like autonomous motility, internally generated flows and self-organized beating (Sanchez et al., 2012; Sanchez and Dogic, 2013; Sanchez et al., 2011) or actively contracting rings (Aylett et al., 2011). Self-assembling, self-organizing as well as active mechanical properties stimulate consideration on the surprising amount of diverse intrinsic properties that MTs carry inside their structure. However like for the dynamics also the organization of MTs inside the cell needs a tight spatial and temporal regulation.

As organization requires the active movement of single MTs to form different types of structures motor proteins play an essential key role in this process. This wide and heterogeneous class of proteins is characterized by the ability to bind MTs and "walk" on their lattice through an active motor activity. Their active movement couples chemical cycle of ATP turnover in the active site to a mechanical cycle of tethered diffusion, MT binding, conformational changes and MT release (Cross and McAinsh, 2014). Interestingly motors can walk on MTs with a specific polarity toward plus or minus end or in some case in both directions. Another common feature of many motors is their ability to generate interactions with cargo proteins or different kinds of regulators. Combining both active movement and binding properties, motors unroll functions like sliding and moving MTs, transport cargo proteins or act on MT dynamics. An impressive number of motor proteins has been identified, all belonging to two main families with different features: kinesins and dyneins. Kinesins contribute to many events during mitosis such as centrosome separation, the self-organization of the mitotic spindle, pulling and pushing on kinetochores, lateral sliding of kinetochores, generation of polar ejection forces and anaphase chromosomes segregation (Cross and McAinsh, 2014). One particular class of kinesins, named chromokinesins, mediates interactions between MTs and the chromosomes arms. Adaptors proteins that localize on the chromatin mediate these interactions. Chromokinesins play many functions in spindle assembly particularly promoting chromosomes congression on the metaphase plate (Vanneste et al., 2011). Dyneins are the second large family of motor proteins. Particularly the cytoplasmic dynein1 operates in almost all the MT minus-end directed movements in eukaryotes essential for many mitotic process such spindle organization and orientation (Roberts et al., 2013).

5. The mitotic spindle

The eukaryotic cell developed an extremely complex machinery to spatially and temporally control MT assembly and organization. An example of that is the complete reorganization of the interphase MT network into an ordered and dynamic bipolar structure. This dramatic effect is due to a cell cycle dependent biochemical change that

generates a spindle assembly dedicated network of proteins (Belmont et al., 1990). The mitotic spindle is a complex spindle-shaped and MT-based structure that assembles when cells enter into mitosis and works in the mechanical segregation of the chromosomes in the two daughter cells. Its assembly is the result of a tight cellular regulation of MT intrinsic properties. Errors in the assembly of this structure are the molecular basis for a dramatic variety of pathologies such as cancers.

Different pathways contribute to spindle assembly as well as different classes of MTs compose the mitotic spindle. In the next section I will provide a general overview on the structure of the mitotic spindle and on the different pathways that cooperate to its assembly.

5.1. Mitotic spindle structure

Three main classes of spindle MTs have been defined by their position, origin and function during mitosis (Fig. 5). Astral microtubules emanate from the centrosomes in a radial pattern towards the closest cell membrane. Although their function is not essential for cell division (Khodjakov et al., 2000; Mahoney et al., 2006) they play an important role in many other processes. During prophase, astral MTs drive centrosome separation along the nuclear envelope to the opposites poles of the cell (Rosenblatt, 2005). Astral MTs are essential for cell division when the spindle needs to reach a proper orientation. This is typical in asymmetric cell division, essential process for cell differentiation and development. Here, astral MTs through contacts with the plasma membrane move the whole spindle in the right orientation. This process involves dedicated protein complexes on the cell cortex where motor proteins play an essential role generating pulling forces on MTs (Knoblich, 2010; Kotak and Gonczy, 2013).

The interpolar MTs are the most abundant and dynamic class of MTs in human mitotic cells. These MTs cover the entire spindle as they extend between the two poles. On the equator, some of the MTs coming from the two opposite poles overlap generating an antiparallel array. Another population of interpolar MTs makes contacts with chromosomes and kinetochores whereas others shorter MTs remain unattached. However, new advanced imaging techniques showed that in *Xenopus laevis* the interpolar MTs have a mean length of 40% of the spindle length suggesting therefore

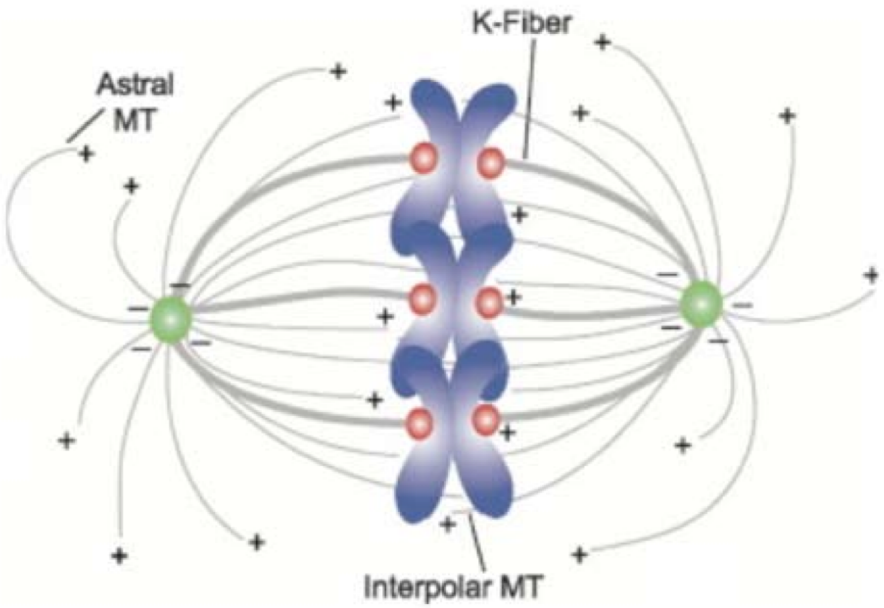

(Kline-Smith and Walczak, 2004)

Figure 5. The mitotic spindle

Different classes of MTs compose the mitotic spindle. Astral MTs assemble from the centrosomes (green dots) and are projected towards the cell membrane. Interpolar MTs cover the area between the two spindle poles overlapping in an antiparallel array at the spindle equator. K-fibers are bundles of MTs connecting kinetochores (red dots) to spindle poles. Figure modified from (Kline-Smith and Walczak, 2004).

that the spindle can be composed by a tiller array of short MTs cross linked together. This model also suggests that these MTs organize in a polar array of parallel MTs close to spindle poles and an antiparallel barrel shaped array close to the chromosomes (Yang et al., 2007). Antiparallel interpolar MTs have many functions during cell division. During early mitotic phases they are involved in spindle assembly and bipolarity maintenance. Their contacts with chromosomes are important for chromosome congression during metaphase. During anaphase interpolar MTs take also part in the formation of the central spindle, an antiparallel array of MTs involved in spindle elongation and chromosomes segregation (Meunier and Vernos, 2012).

K-fibers are bundles of cross-linked MTs that connect chromosomes to spindle poles. Unlike interpolar MTs, k-fiber minus-ends are not directly anchored to centrosomes and the plus ends make contact with the kinetochore surface (Rieder, 2005). The bundling of k-fibers involves many different MAPs with cross-linking activity like the TACC3/chTOG/clathrin complex. However, the exact molecular composition of these

structures is still unclear (Booth et al., 2011). The fact that this class of spindle MTs is organized in bundles confers them a particular resistance to depolymerising agents like nocodazole and low temperatures. The role of k-fibers is extremely important for cell division. During early mitosis pushing forces acting on kinetochores are essential for spindle bipolarization (Toso et al., 2009). In metaphase, k-fibers to kinetochores attachment generates pulling forces and tension between sister kinetochores. This tension is essential to trigger chromosome segregation. A dramatic change of the plus ends dynamics results in the fast shortening of k-fibers and generation of pulling forces on kinetochores that triggers chromosomes segregation. Despite their essential role, the origin of this class of MTs is really debated. In fact various observations in different systems suggested that the k-fibers are directly generated by the kinetochores (Maiato et al., 2004; Tulu et al., 2006). However, no direct proof really links the biogenesis of the k-fibers and the MTs that assemble on the kinetochores. The fact that cells without centrosomes are able to assemble functional k-fibers also suggest that a non centrosomal pathway is responsible for their assembly (Khodjakov et al., 2000). The chromosomes through the RanGTP pathway could therefore promote k-fiber assembly. This hypothesis opens an intriguing scenario, as chromosomes could then be considered auto-sufficient in terms of their own segregation.

5.2. Mechanism of spindle assembly

Since the first observations of mitosis centrosomes have always been described as prominent sources of MTs in the cell. Direct observations of purified centrosomes revealed highly dynamics cycles of MT growth and shrinking (Mitchison and Kirschner, 1984b). This observation lead to the formulation of the “search and capture” model for spindle assembly (Fig. 6) (Kirschner and Mitchison, 1986). In this model centrosomal MTs search for free kinetochores by repeated growing and shrinking cycles till they are captured and stabilized. This process stops when all the kinetochores are connected to MTs and all the chromosomes are correctly bioriented. However mathematical modelling revealed that such stochastic mechanism could not be efficient enough to get all the MT-kinetochore matches in a time scale compatible with spindle assembly (Wollman et al., 2005). Furthermore it cannot explain how spindle assembly occurs in systems lacking centrosomes such as higher plants and some vertebrate meiosis.

Injection of plasmid DNA into *Xenopus laevis* eggs strikingly triggers MTs and spindle assembly (Karsenti et al., 1984). Consistently also beads coated with plasmid-DNA triggers the formation of MTs in their close proximity (Heald et al., 1996). All these data pointed to a prominent role of chromatin during spindle assembly leading to the formulation of the "self organization" model (Fig. 6). In fact also without any MTOC (microtubule organizing center) chromosomes are able to properly assemble a functional bipolar spindle (Heald et al., 1997). Strikingly this is not only limited to systems lacking centrosomes as the inactivation of centrosomes does not seem to impair spindle assembly and bipolarization even in human somatic cells (Khodjakov et al., 2000). However also in absence of chromosomes, systems like Drosophila secondary spermatocytes can assemble morphologically normal spindles (Bucciarelli et al., 2003).
It is now well accepted that both centrosomes and chromosomes contribute to spindle assembly (Fig. 6). This cooperation can be observed during the recovery from nocodazole-induced MT depolymerization (Tulu et al., 2006). In cells released from nocodazole, centrosomes start immediately to assemble highly dynamic MTs that grow and shrink fast. With slower kinetic MTs asters appear close to chromosomes and start growing and interacting with centrosomal MTs. This cooperative process follows till a normal bipolar spindle is formed. The capture of the chromosomal MTs by the centrosomes has also been described and involves the activity of the molecular motor dynein and its partner NuMa (Khodjakov et al., 2000; Maiato et al., 2004; Rusan et al., 2002).

Despite the role of chromosomes and centrosomes, spindle assembly takes advantage of other sources of MTs. The observation that γ-tubulin not only localizes to MTOCs but is also present all along the spindle MTs lead to the discovery of a MT amplification mechanism (Goshima et al., 2008). New MTs branch out from the spindle MTs in a process that requires the γTuRC and a dedicated complex called Augmin/HAUS. Interestingly, the MT amplification pathway plays an important role during spindle assembly and bipolarization particularly in systems lacking functional centrosomes (Wainman et al., 2009).

The mitotic spindle is an extremely complicated machinery built up by the contribution of different assembly mechanisms. But things could be almost more complicate as other sources of MTs have been documented in the cell. In fact, peripheral non-centrosomal

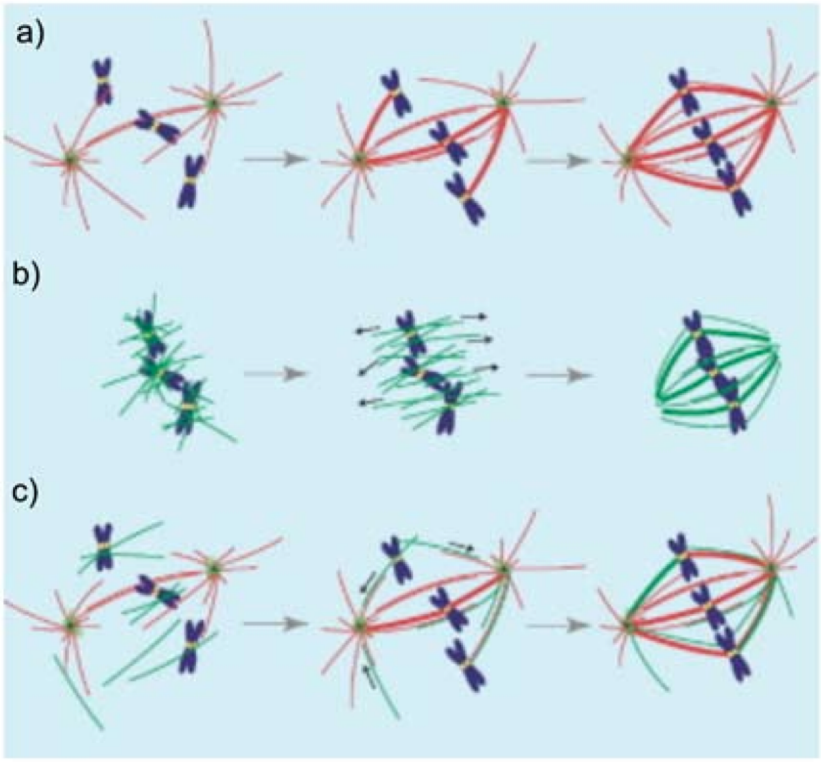

(Gadde and Heald, 2004)

Figure 6. Spindle assembly models

Different models have been proposed to explain spindle assembly. (a) In the search and capture model centrosomes nucleate highly dynamic MTs that elongate and shrink untill they are captured by kinetochores. (b) In the self-organization model, chromosomes nucleate an essential class of MTs that can organize a functional bipolar structure also in the absence of centrosomes. (c) In the combined model, chromosomal (green) and centrosomal MTs (red) cooperate to assemble the mitotic spindle. Figure modified from (Gadde and Heald, 2004) .

and non-chromosomal MTs can be recruited to the mitotic spindle (Moutinho-Pereira et al., 2009). Remnants of the nuclear envelop during *Drosophila* spermatogenesis are able to assemble microtubules (Rebollo et al., 2004). Interestingly the Golgi apparatus is also a significant source of MTs during interphase and its activity perpetuate also during mitosis (Maia et al., 2013). However whether these MTs play an active role during spindle assembly and function is not clear. Not only new sources of MTs could participate to spindle assembly but also unexpected cellular components could join this process. The "spindle matrix" idea has been proposed based on the observation that several large components with potential structural function have been observed on the spindle region. This structure could be considered as a spindle-associated scaffold that envelops and mechanically supports spindle assembly, maintenance and function (Schweizer et al., 2014).

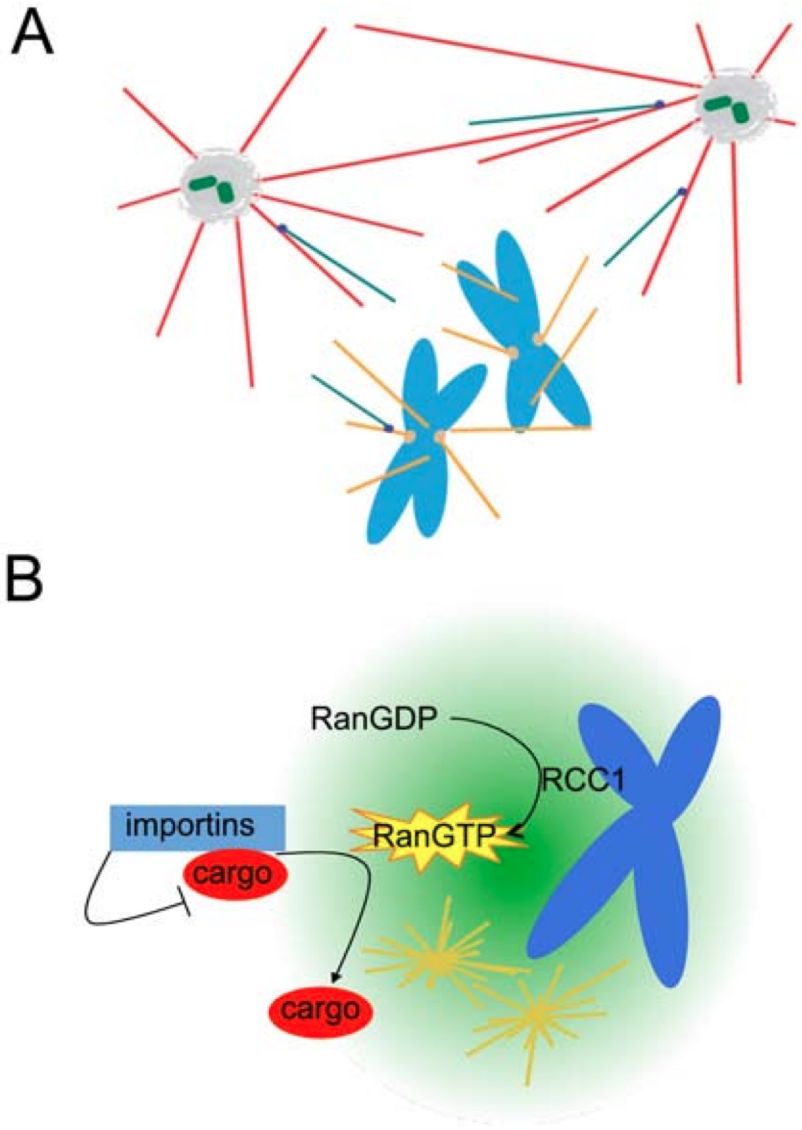

Figure 7. Microtubule assembly pathways

A) Schematic representation of the main spindle assembly pathway. Centrosomal MTs are represented in red, chromosomal MTs in yellow and branched MTs in green. Figure modified from (Meunier and Vernos, 2012). B) Model for the RanGTP pathway of MT assembly. RCC1 promotes the formation of a RanGTP gradient around chromosomes releasing cargo proteins from importins and promoting MT assembly.

5.3. Chromosomal pathways of microtubule assembly during mitosis

The MT assembly activity that resides on chromosomes depends on the function of the small GTPase Ran (Fig. 7) (Kalab et al., 2002). Interestingly Ran plays two completely different cellular functions during the cell cycle maintaining the same molecular activity. During interphase Ran regulates nuclear import and export of cargo proteins.

This process involves the karyopherins family members importin-α and β. Particularly, to be transported into the nucleus cargo proteins bind to importin-α or importin-ß through a specific NLS (Nuclear Localization Signal). Importin-β binds then to Importin-α stabilizing the complex and mediating the transport across the nuclear pore. Ran in its GTP-bound state (RanGTP) has high affinity with Importin-β triggering the dissociation of the complex and the release of the cargo. Because the GTP form of Ran is concentrated into the nucleus and the GDP form (RanGDP) outside, the release of cargo proteins occurs specifically inside the nucleus. This different distribution of Ran populations depends on the chromosomal localization of the GTP exchange factor (GEF) RCC1 and on the cytoplasmic localization of the GTPase activating protein (GAP) RanGAP1. A similar system works for nuclear export of specific NES (Nuclear Export Signal) containing cargoes. These are transported through their binding to exportins family of proteins and released in the cytoplasm after binding with RanGDP (Sorokin et al., 2007).

Strikingly adding a GTP-bound stable Ran to a mitotic arrested *Xenopus* egg extract is sufficient to promote MT assembly and organization in small spindle structures without chromosomes (Kalab et al., 1999). This first observation suggested that the RanGTP system plays an essential role also during mitosis particularly promoting spindle assembly and organization. FRET (Fluorescence Resonance Energy Transfer) experiments allowed visualizing a concentration gradient of RanGTP around mitotic chromosomes and lead to the formulation of the gradient model (Kalab et al., 2002). As RCC1 keeps its localization on chromatin during mitosis it generates RanGTP close to the chromosomes that diffuses in a gradient in the cell cytoplasm. This mechanism allows the local release of NLS proteins specifically at chromosome close proximity. With this system, chromosomes activate all the molecular functions required to assist MT nucleation, growth and their organization in spindle structures. For this reason the RanGTP pathway is an essential component of the "self organization" pathway (Karsenti and Vernos, 2001). Many RanGTP regulated proteins involved in spindle assembly have been identified however their exact role in the pathway is still not clear (Fig. 8) (Meunier and Vernos, 2012).

Protein	Transport receptors	Properties
MT nucleation		
TPX2	Importin-α, importin-β (Gruss et al., 2001; Wittmann et al., 2000)	Interacts with and activates Aurora A (Bayliss et al., 2003)
MEL-28	Importin-α, importin-β (Yokoyama et al., 2014)	Interacts with MTs and is required to localize γ-tubulin to MTOC (Yokoyama et al., 2014)
MT stabilization		
HURP	Importin-β (Silljé et al., 2006)	MT-bundling activity (Koffa et al., 2006; Silljé et al., 2006; Wong and Fang, 2006)
RAE1	Importin-β (Blower et al., 2005; Wong et al., 2006)	Ribonuncleoprotein complex involved in spindle assembly (Blower et al., 2005; Wong et al., 2006)
ISWI1	Importin-α, importin-β (Yokoyama et al., 2009)	MT-bundling activity (Yokoyama et al., 2009)
CDK11	Importin-β (Yokoyama et al., 2008)	Necessary for Ran-GTP-dependent MT stabilization(Yokoyama et al., 2008)
APC	Importin-β (Dikovskaya et al., 2010)	MT-bundling activity (Dikovskaya et al., 2010)
TACC3	Importin-β(Albee et al., 2006)	Phosphorylated by Aurora A(Barros et al., 2005; Peset et al., 2005)
MCRS1	Importin-β (Meunier and Vernos, 2011)	Binds and protects chromosomal MT minus-ends (Meunier and Vernos, 2011)
NUSAP1	Importin-α and/or importin-β, importin 7 (Ribbeck et al., 2006; Ribbeck et al., 2007)	Interacts with chromosomes and MTs (Ribbeck et al., 2006; Ribbeck et al., 2007)
CDH4	Importin-α, importin-β (Yokoyama et al., 2013)	Binds and stabilize MTs (Yokoyama et a., 2013)
Spindle organization		
NUMA1	Importin-β (Nachury et al., 2001; Wiese et al., 2001)	Pole focusing (Haren et al., 2009; Merdes et al., 2000; Merdes et al., 1996; Silk et al., 2009)
Kid	Importin-α, importin-β (Tahara et al., 2008)	Chromokinesin; additional MT-binding site (ATP independent) (Antonio et al., 2000; Funabiki and Murray, 2000; Tokai et al., 1996)
HSET	Importin-α, importin-β (Ems-McClung et al., 2004)	Minus-end directed motor; additional MT-binding site (ATP independent)(Walczak et al., 1997)

(Meunier and Vernos, 2012)

Figure 8. Known RanGTP regulated proteins involved in spindle assembly

Updated list of the known RanGTP targets involved in spindle assembly. The proteins are grouped according to their function in MT assembly. Table modified from (Meunier and Vernos, 2012).

The RanGTP pathway is not the only one active on the chromosomes. In fact, also kinetochores are able to promote MT assembly through a RanGTP and RCC1 independent mechanism (O'Connell et al., 2009). This pathway involves the chromosome passenger complex (CPC) that comprises the mitotic kinase Aurora-B (Sampath et al., 2004). The local activation of this kinase at the kinetochores could be the event triggering MT assembly. However it is still not clear if the CPC pathway promotes also MT nucleation in addition to stabilization as there are no proof of γ-tubulin involvement in the pathway (Meunier and Vernos, 2012). It is therefore possible that the CPC pathway promotes MT stabilization and that RanGTP nucleated microtubules can be stabilized and grow preferentially close to kinetochores. This idea

could also fit with the observation of MTs asters emanating from kinetochores (Maiato et al., 2004; Tulu et al., 2006).

6. Regulation of microtubule nucleation

In interphase as well as in mitosis, only a small pool of the whole cellular γTuRC is active in nucleating MTs. It has also been reported that the majority of the γ-TuRC is soluble in the cell whereas MT nucleation occurs only close to specific locations including the centrosomes, pre-existing MTs and the chromosomes (Kollman et al., 2011). How γ-TuRC MT nucleation activity is regulated to act in these different pathways is still very poorly understood.

6.1. Microtubule nucleation at MTOCs

The majority of γTuRCs are active only at the centrosomes. This suggests that localizing the γTuRC to specific MTOCs could be a way to regulate its activity. Consistently γ-tubulin recruitment to centrosomes is an essential event for centrosome maturation (Khodjakov and Rieder, 1999). Many proteins have been described to be essential for centrosomal γ-tubulin recruitment, many of them are structural components of the pericentriolar material and therefore not necessarily directly involved (Teixido-Travesa et al., 2012). Recently the new γTuRC component GCP8 has been shown to be required for the targeting of γ-tubulin to interphase centrosomes (Teixido-Travesa et al., 2010). However γTuRC targeting to mitotic centrosomes depends on the role of a specifically dedicated protein. NEDD1 is a component of the γTuRC that contains repeats of WD40 domains and is essential both for MT nucleation at centrosomes and chromosomes (Gunawardane et al., 2003; Luders et al., 2006). Regarding its function in centrosomal MT nucleation NEDD1 is essential for γ-tubulin recruitment in a process that requires the two mitotic kinases Plk1 and Nek9. Particularly Plk1 phosphorylation on Nek9 activates the kinase and triggers the phosphorylation on NEDD1 S377. This phosphorylation is essential for the function of NEDD1 to target the γTuRC to centrosomes. However the mechanism by which NEDD1 S377 phosphorylation

promotes the recruitment of the γTuRC to the centrosome is still unclear (Sdelci et al., 2012).

A similar γTuRC targeting mechanism has also been described to trigger branching MTs nucleation during the MT amplification pathway. This pathway involves the Augmin complex and promotes MT assembly from pre-existing MTs therefore inducing an amplification effect (Goshima et al., 2008). NEDD1 also plays an essential role in the targeting of γTuRCs to MT branching sites. In fact phosphorylation on NEDD1 S411 drives the recruitment of the γTuRC to the Augmin complex and therefore on MT branching sites (Johmura et al., 2011). Interestingly recent observations showed that the RanGTP pathway could also control Augmin dependent MT nucleation. Consistently TPX2 has been found associated both with Augmin and γTuRC (Petry et al., 2013).

MT nucleation at the centrosomes and pre-assembled MTs requires a targeting mechanism to localize the γTuRC. Whether the targeting is sufficient to promote MT nucleation or some other mechanism could directly act on the γTuRC promoting its activation is still not known. However recent data proposed a possible γTuRC activation mechanism driven by a conformational change of the γTuSC subunit GCP3. This switch could result in the closure of the γ-tubulin ring optimizing tubulin heterodimers attachment and therefore promoting nucleation (Kollman et al., 2011).

6.2. Microtubule nucleation around chromosomes

The mechanism described for MT nucleation at an MTOC cannot be valid for the chromosomal pathway. In fact, here, there is no evidence for the existence of specific sites for MT nucleation and therefore to target the γTuRC.

Only few proteins have been identified as players of the chromosomal dependent MT nucleation. In the following chapters I will provide an overview of all the proteins that could be part of the chromosomal dependent MT nucleation machinery.

7. Some players of the RanGTP dependent microtubule assembly pathway

7.1 TPX2

TPX2 was identified first as mitotic antigen and then described as a MAP that mediates the localization of the chromokinesin XKlp2 on the spindle microtubules (Wittmann et al., 1998; Wittmann et al., 2000). Apart from the human and the *Xenopus* proteins, TPX2 is widely conserved from mammals to plants (Goshima, 2011; Vos et al., 2008). TPX2 expression is cell cycle regulated. It is expressed during late S-phase and its NLS targets it to the nucleus through an Importin-α and β mediated transport (Gruss et al., 2001). TPX2 was the first RanGTP direct target identified as essential for spindle assembly both in human cells and *Xenopus* egg extract (Gruss et al., 2001; Gruss et al., 2002). After nuclear envelope breaks down, TPX2 binds to spindle MTs and spindle poles and, after anaphase onset, to the central spindle (Gruss et al., 2002). During mitotic exit, TPX2 is degraded through the recognition of its KEN-box by the APC/C complex (Stewart and Fang, 2005).

TPX2 depletion from *Xenopus laevis* egg extracts and silencing in cells have dramatic effects on the assembly of RanGTP induced MTs therefore affecting bipolar spindle formation (Brunet et al., 2004; Tulu et al., 2006). This phenotype is particularly severe suggesting that TPX2 function could be involved in the nucleation of chromosomal MTs. Consistently, TPX2 depletion does not affect the MT stabilization effect of RanGTP on centrosomal MTs in egg extract (Gruss et al., 2002). Furthermore, *in vitro* experiments showed that bacterially expressed TPX2 stimulates MT growth in pure tubulin solution suggesting that it could have a direct MT nucleation activity (Schatz et al., 2003). However, in *Xenopus laevis* egg extracts, it is well characterized that MT nucleation through the TPX2-RanGTP dependent pathway requires γ-tubulin. Interestingly, TPX2 interacts with γ-tubulin, the major MT nucleator in the cell suggesting a role in γTuRC mediated MT nucleation (Petry et al., 2013). Experiments aimed at exploring TPX2 function in MT nucleation defined a C-terminal region that is essential but not sufficient to promote microtubule nucleation in egg extracts (Brunet et al., 2004). Despite all these data, the mechanism by which TPX2 works in chromosomal

MT nucleation is still missing. Furthermore, TPX2 localization and phenotype on spindle pole integrity and organization suggests that its mitotic role could be even more complex (Garrett et al., 2002; Wittmann et al., 2000).

7.2. RHAMM

RHAMM (Receptor for Hyaluronan (HA) Mediated Motility) has been characterized as a cell surface and microtubule associated HA binding protein related to HA-dependent cell motility (Turley, 1992). In addition to its role in cell migration, RHAMM expression and overexpression have been related to tumor progression and metastasis (Hall et al., 1995). Interestingly RHAMM has also been described as a MT and actin associated protein (Assmann et al., 1999) that localizes to the mitotic spindle and centrosomes, playing a still unclear role in spindle assembly (Maxwell et al., 2003; Maxwell et al., 2008). Experiments in *Xenopus laevis* egg extract showed interactions between RHAMM, TPX2, γ-tubulin and the γTuRC component GCP3 (Groen et al., 2004). *In vitro* experiments showed that RHAMM promotes MT assembly both in egg extract and pure tubulin suggesting a function in RanGTP dependent MT nucleation (Groen et al., 2004). More recent data described a role of RHAMM in TPX2 localization to spindle poles. This RHAMM-TPX2 interplay could also be responsible for the activation of the mitotic kinase Aurora-A (Chen et al., 2014). All these data suggest that RHAMM and TPX2 functions could be closely related in the control of RanGTP dependent MT nucleation.

7.3. Aurora-A

Aurora-A has many diverse mitotic functions. It is involved in centrosome maturation where promotes γ-tubulin recruitment (Hannak et al., 2001). Aurora-A is also essential for spindle bipolarization, a process that requires the phosphorylation of the kinesin Eg5 (Barr and Gergely, 2007). The most clear and characterized role of Aurora-A is at the centrosome where it promotes MT assembly through a mechanism that involves the recruitment of the TACC family member TACC3. This event promotes the recruitment of the MT polymerase XMAP215 that antagonizes the binding at the MT minus-ends of the depolymerase MCAK (Barr and Gergely, 2007; Barros et al., 2005). Aurora-A has many different interactors that regulate its localization and activity consequently, many

different fractions of the kinase could be involved in different mitotic process. TPX2 is a well-established interactor and activator of the mitotic kinase Aurora-A. In fact a small peptide in the N-terminus of TPX2 (1-39 of *Xenopus* TPX2 and 1-43 of human TPX2) is sufficient to bind and activate the kinase (Bayliss et al., 2003; Kufer et al., 2002). Interestingly TPX2 is also required for the targeting of Aurora-A to the spindle poles although the absence of the kinase does not interfere with TPX2 localization (Bird and Hyman, 2008; De Luca et al., 2006; Kufer et al., 2002). TPX2 not only regulates Aurora-A activation and localization but also Aurora-A stability by protecting it from a proteasome dependent degradation (Giubettini et al., 2011). This close interplay between TPX2 and Aurora-A has also been linked to many different cancer types as the overexpression of the two proteins showed a significant correlation (Asteriti et al., 2010). The formation of the TPX2-Aurora-A complex is tightly regulated by RanGTP and therefore could be considered as a way to translate the RanGTP gradient into a phosphorylation gradient (Gruss and Vernos, 2004; Tsai et al., 2003). What is the role of the TPX2-Aurora-A complex during spindle assembly is still unclear. Experiments performed in egg extract suggest that TPX2-Aurora-A interaction is essential although not sufficient to promote RanGTP-dependent MT nucleation (Brunet et al., 2004). More recent data also showed that TPX2-Aurora-A interaction is essential for chromosomal induced MT nucleation in human cells (Bird and Hyman, 2008). The same results has also been observed directly silencing Aurora-A expression (Katayama et al., 2008). Strikingly Aurora-A coated beads can nucleate efficiently MTs in egg extract and pure tubulin in a RanGTP and TPX2 dependent manner (Tsai and Zheng, 2005). All these data suggest that through Aurora-A activation TPX2 could promote MT nucleation. However how the TPX2-Aurora-A complex promotes chromosomal dependent MT nucleation remains an interesting open question.

8. The *Xenopus laevis* egg extract system

The *Xenopus laevis* egg extract system is a well-established model for cellular biology. A large amount of egg cytoplasm can be easily prepared in controlled conditions. Therefore the extract represents an open system easy to manipulate and ideal to study and observe cell division (Fig. 9).

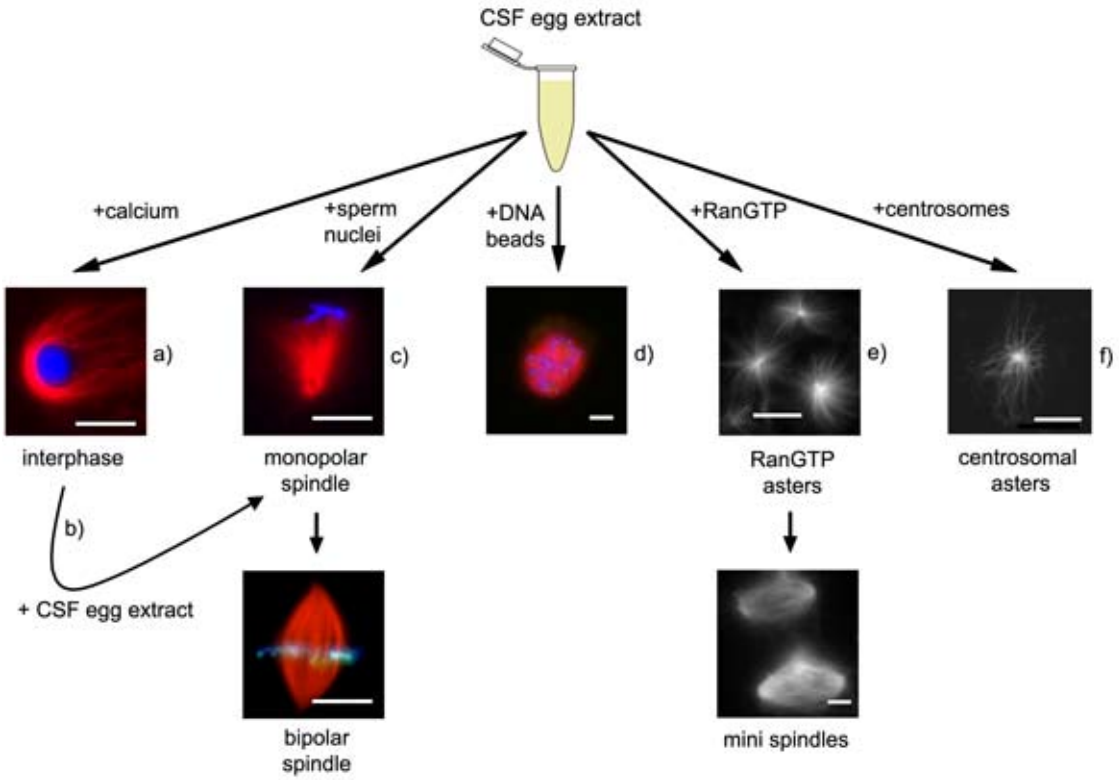

Figure 9. The *Xenopus laevis* egg extract system to study microtubule assembly during mitosis
Schematic representation of the different approaches that can be used to study microtubule assembly in *Xenopus laevis* egg extract system. Interphase can be induced adding calcium (a) to a CSF arrested egg extract. The interphase extract can cycle back to mitosis (b) by mixing it with fresh CSF egg extract. Sperm nuclei trigger the formation of monopolar and bipolar spindles(c). DNA beads (d) and RanGTP (e) are commonly used to study chromosome-dependent MT assembly. RanGTP asters can self-organize into mini spindle structures without DNA. Purified centrosomes also trigger MT assembly forming large asters. Pictures are selected examples. MTs are stained adding a small amount of rhodamine labelled tubulin. DNA and DNA beads (blue). Scale bars: 10 µm.

The extract is prepared from *Xenopus laevis* unfertilized eggs arrested in metaphase of the second meiotic division. Progesterone injection in female frogs induces maturation of a large amount of eggs. The eggs are then centrifuged and the cytoplasm separated from membranes and others large organelles. To keep the extract in a meiotic state cytostatic factor (CSF) degradation is inhibited. Calcium inactivates the CSF therefore promoting cell cycle progression and exit from meiosis. The extract will then cycle back to a mitotic state.

The egg extract system is particularly useful to study cell division and spindle assembly. Different protocols have been developed to dissect the different spindle assembly pathways that cooperate during mitosis. Bipolar spindle assembly can be observed after

the addition of sperm nuclei, bringing one immature centrosome, to the egg extract. Typically both the centrosome and the chromatin nucleate and assemble MTs that are efficiently organized in bipolar spindle structures with the DNA in the middle. The same extract can be switched to interphase triggering DNA synthesis and centrosome duplication. Addition of CSF will cycle back the extract into mitosis and bipolar structures assemble around chromosomes with a centrosome to each pole. Purified centrosomes can also trigger MT assembly in CSF arrested egg extract. Many systems are also available to study non-centrosomal spindle assembly. Adding plasmid DNA or beads coated with DNA triggers MT nucleation and assembly (Heald et al., 1997). MT assembly and organization into small spindle like structures can also be triggered in CSF egg extract adding a mutant of Ran unable to hydrolyze GTP (RanQ69L) (Heald et al., 1996). The study of the chromosomal pathway of spindle assembly takes advantage also of classical biochemistry in extract. Immunoprecipitations performed in extract treated or not with RanGTP are powerful tool to study the molecular events triggered by the pathway. Another advantage of the egg extract system is the possibility to easily deplete specific proteins by immunodepletion. The add back of the corresponding recombinant proteins is an easy way to perform rescue experiments aimed at identifying the specific molecular function of one protein. Altogether this application makes the extract the perfect system to dissect and study the different pathways that contribute to spindle assembly.

II. OBJECTIVES

The main aim of the thesis presented here was to provide new insights on the mechanisms of RanGTP dependent MT assembly.

The main objectives were:

i) Identify new proteins involved in the RanGTP pathway of MT assembly.

ii) Understand how the RanGTP pathway regulates chromosome dependent MT nucleation.

iii) Study the contribution of chromosomal MTs to spindle assembly.

III. RESULTS

1. Identification and functional characterization of novel proteins involved in the chromosomal pathway during spindle assembly

The current knowledge of the RanGTP dependent process that leads to microtubule nucleation, stabilization and organization around the chromosomes is still incomplete. Indeed only some targets of RanGTP have so far been identified (Meunier and Vernos, 2012) and previous work in our lab has suggested that other RanGTP regulated proteins are involved in the pathway (Meunier and Vernos, 2011). With the aim to identify novel proteins involved in the RanGTP pathway, we set up a screen based on (Fig.10A): i) an *in silico* approach to use large proteomics data, ii) the experimental validation of the candidates based on mitotic localization, iii) an *in vivo* screen for the putative role of the candidates in the RanGTP-dependent microtubule assembly pathway. In the next sections I will present the approach in detail and some preliminary results about the most promising candidates.

1.1. A proteomic approach to identify RanGTP regulated proteins involved in spindle assembly

With the aim to select a short number of candidate proteins we developed an *in silico* approach based on the integration of multiple proteomic data. Particularly our idea was to select a reasonable number of candidates using data obtained in our lab and others available in published bibliography (Fig.10B). We decided to focus on four different data sets. i) Two proteomes obtained from SILAC mass spectrometry experiments from the lab on two well-characterized RanGTP targets: TPX2 (Gruss et al., 2001; Wittmann et al., 2000) and MCRS1 (Meunier and Vernos, 2011). ii) The LIFEdb database, containing a large collection of nuclear proteins (Mehrle et al., 2006), because the RanGTP targets have a NLS (nuclear localization signal). iii) The mitotic spindle proteome containing the results of a proteomic analysis of the human mitotic spindle

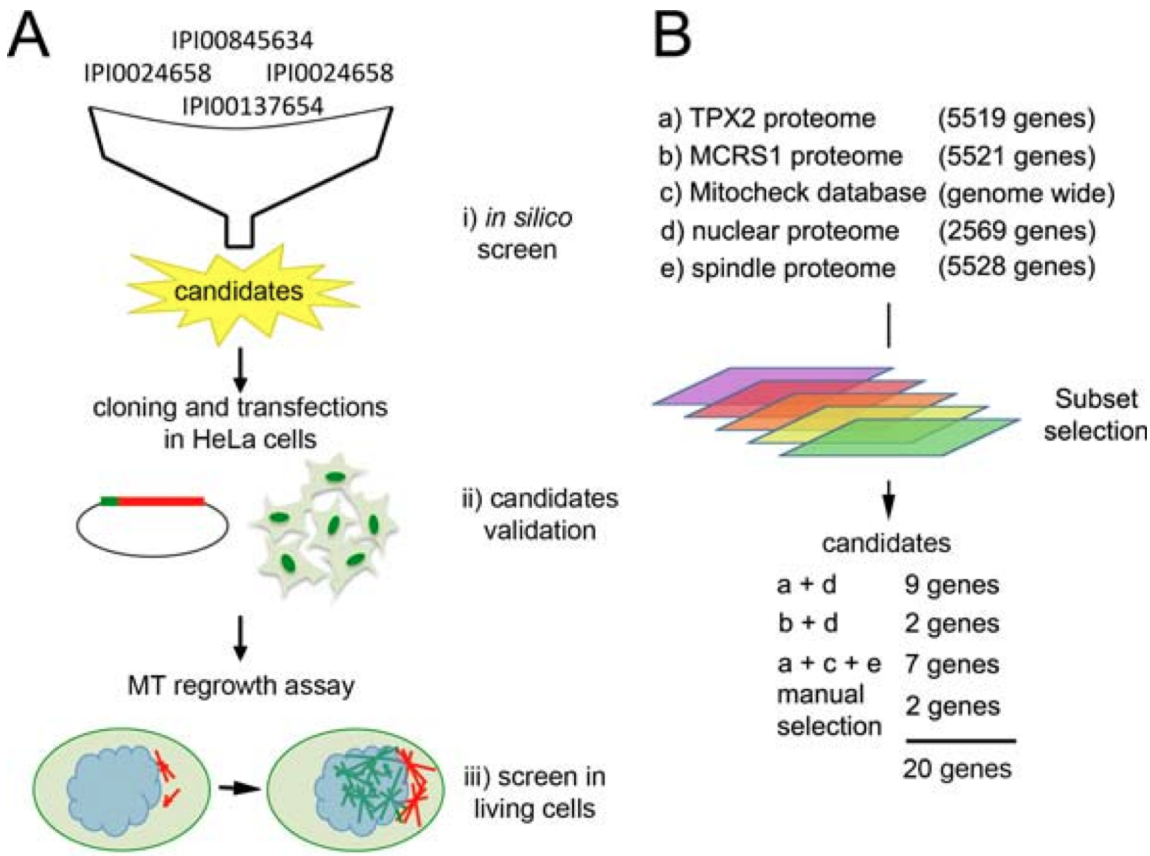

C

Ensemble Gene ID	Gene Name	Selection	Tag	Mitotic Localization
ENSG00000181904	UPF0461 protein C5orf24	TPX2/Nucleus/MitoCheck	Flag	Chromosomes
ENSG00000139620	Uncharacterized protein C12orf41	manual selection MCRS1/(Goshima et al., 2007)	/	Spindle poles
ENSG00000156261	chaperonin containing TCP1, subunit 8 (theta)	TPX2/Spindle/MitoCheck	Flag	Diffuse
ENSG00000108883	elongation factor Tu GTP binding domain containing 2	TPX2/Spindle/MitoCheck	Flag	Diffuse
ENSG00000196305	isoleucyl-tRNA synthetase	TPX2/Spindle/MitoCheck	Flag	Diffuse
ENSG00000110107	PRP19/PSO4 pre-mRNA processing factor 19 homolog	TPX2/Spindle/MitoCheck	Flag	Diffuse
ENSG00000144028	small nuclear ribonucleoprotein 200kDa (U5)	TPX2/Spindle/MitoCheck	Flag	Diffuse
ENSG00000120438	small nucleolar RNA, H/ACA box 29	TPX2/Spindle/MitoCheck	Flag	Diffuse
ENSG00000119335	SET nuclear oncogene	TPX2/Spindle/Nucleus	GFP	Spindle poles
ENSG00000174903	RAB1B, member RAS oncogene family	TPX2/Spindle/Nucleus	GFP	Poles
ENSG00000179409	gem (nuclear organelle) associated protein 4	MCRS1/Spindle/Nucleus	GFP	Diffuse
ENSG00000102119	emerin	TPX2/Spindle/Nucleus	GFP	Spindle
ENSG00000161800	Rac GTPase activating protein 1	TPX2/Spindle/Nucleus	GFP	central body
ENSG00000105993	DnaJ (Hsp40) homolog, subfamily B, member 6	MCRS1/Spindle/Nucleus	GFP	Spindle
ENSG00000158941	KIAA1967	TPX2/Nucleus	GFP	Diffuse
ENSG00000072062	protein kinase, cAMP-dependent, catalytic, alpha	TPX2/Nucleus	GFP	Diffuse
ENSG00000127483	heterochromatin protein 1, binding protein	TPX2/Nucleus	GFP	Diffuse
ENSG00000105618	PRP31 pre-mRNA processing factor 31 homolog	TPX2/Nucleus	GFP	Diffuse
ENSG00000106723	spindlin 1	TPX2/Nucleus	GFP	Diffuse
ENSG00000175792	RuvB-like AAA ATPase 1	manual selection MCRS1/(Ducat et al., 2008)	/	Spindle poles

Figure 10. Identification of novel RanGTP regulated proteins involved in spindle assembly

A) Schematic representation of the approach adopted to identify proteins involved in the RanGTP pathway of microtubule assembly. An *in silico* screen based on a proteomic approach was developed to identify candidate genes (top); the candidates were validated by experimental analysis of their localization

in HeLa cells (middle); The MT regrowth experiment can be used to determine whether the candidates have a role in the chromosomal pathway of MT assembly (bottom). B) Schematic representation of the proteomic approach adopted to identify candidate genes with putative role in the RanGTP pathway. Five proteomes were selected to look for candidates (top). The lists have been processed *in silico* to get a short list of candidates (middle). Four criteria were applied and a total of twenty genes selected (bottom). C) List of the selected candidates. Each gene has been cloned in fusion with different tags and the localization of the corresponding protein studied in HeLa cells. A total of eight candidates scored positively for their localization in mitosis. Three were selected for further analysis (highlighted in blue) .

(Sauer et al., 2005). More than 19000 proteins (repeated elements excluded) were contained into the whole lists. Because all these data are in the form of long lists of protein identification numbers (IPI, International Proteins Index) we took advantage of a specially developed bioinformatics tool to compare them. This script looks for common elements between two lists exploring all the possible combinations when the dataset is composed of multiple lists. The output is a manageable file to explore all the possible subsets coming from the systematic overlap of the five proteomes. To get a reasonable number of candidates we decided to focus only on the most promising subsets. Particularly, we selected the proteins that were TPX2 or MCRS1 interactors and also present in the nucleus proteome. We also selected TPX2 interactors with a putative localization to the mitotic spindle and having a reported mitotic phenotype. To do that we took advantage of the Mitocheck database reporting results of a human genome wide siRNA approach to identify genes with mitotic phenotypes (Neumann et al., 2006). In addition, two genes were also selected manually: C12orf41 (ENSG00000139620) and the RuvB-like AAA ATPase (ENSG00000175792) both in the MCRS1 proteome and having interesting mitotic features coming from previously published data. The C12orf41 coming from a genome wide screen was shown to be responsible for γ-tubulin localization to the mitotic spindle (Goshima et al., 2008). The RuvB-like AAA ATPase gene, also known as pontin, was reported to be essential for MT nucleation during mitosis (Ducat et al., 2008). A total of twenty genes were finally selected (Fig.10C).

1.2. Studying candidates localization in mitotic HeLa cells

To experimentally validate the candidates selected from the *in silico* screen we decided to consider only proteins having a specific mitotic localization. To obtain the corresponding cDNAs we used RT-PCR on the total HeLa cells RNA and we prepared

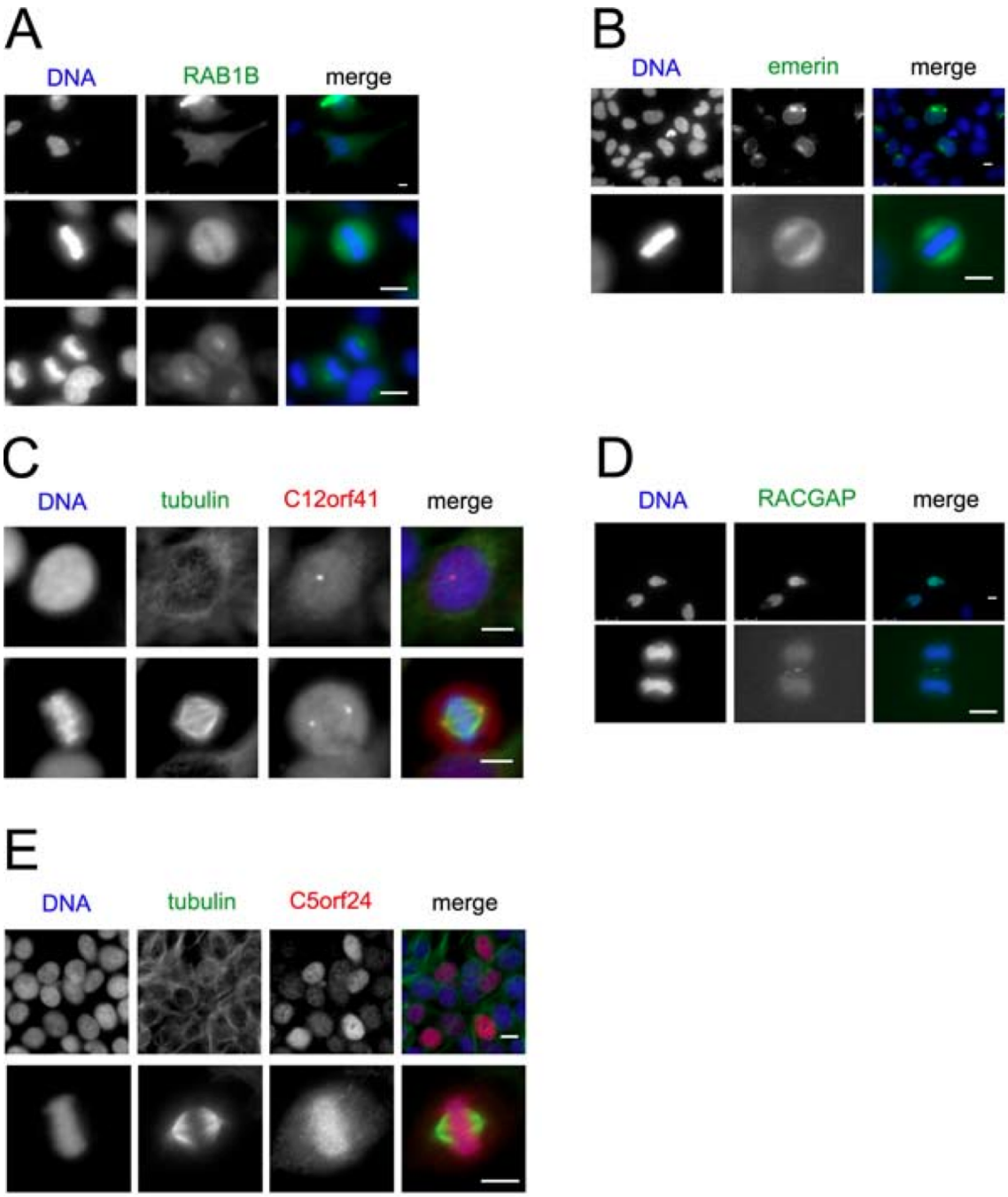

Figure 11. Candidate localization in interphasic and mitotic HeLa cells

Interphase and mitotic localization of five candidates. A) RAB1B (ENSG00000174903) shows a diffuse signal between nucleus and cytoplasm during interphase as well as a putative signal at the centrosomes and on unknown structures close to mitotic spindle poles. DNA (blue), GFP RAB1B (green). Scale bars: 10 µm. B) EMERIN (ENSG00000102119) is nuclear with an enrichment on the nuclear envelope during interphase and diffuse with enrichment around mitotic spindle poles. DNA (blue), GFP EMERIN (green). Scale bars: 10 µm. C) C12orf41 (ENSG00000139620) has a nuclear localization during interphase and a centrosomal localization during mitosis with a weak enrichment to spindle poles. DNA (blue), Flag C12orf41 (red), tubulin (green). Scale bars: 10 µm. D) RACGAP1 (ENSG00000161800) has a nuclear localization during interphase and at the cleavage plane during cytokinesis. DNA (blue), GFP RACGAP1 (green). Scale bars: 10 µm. E) C5orf24 (ENSG00000181904) has a nuclear localization during interphase

and a strong localization on chromosomes during mitosis. DNA (blue), Flag C5orf24 (red), tubulin (green). Scale bars: 10 µm.

Flag-tag constructs. For all the candidates coming from the nuclear LifeDB (Mehrle et al., 2006) we obtained CFP/EYFP-tag constructs (from Dr. Stefan Wiemann, DKFZ, Germany). The recombinant proteins were then expressed in HeLa cells and their mitotic localization analyzed by immunofluorescence (IF) microscopy. All the proteins showing a clear localization to any mitotic structure were finally selected for a further characterization. Strikingly, amongst the twenty selected candidates, seven showed a specific mitotic localization (Fig.10C and 11). We decided to focus on the three most promising ones because they clearly localized on the mitotic spindle. Short reviews on the published knowledge and our preliminary data on these three candidates are reported in the following paragraphs.

1.2.1 SET

SET (ENSG00000119335) is present in the TPX2, mitotic spindle and nuclear proteomes. It has been identified as an oncogene related to myeloid leukemia (Adachi et al., 1994; von Lindern et al., 1992). SET has also been shown involved in chromatin condensation (Leung et al., 2011), histone modification (Seo et al., 2001) and cell cycle regulation (Li et al., 1996), although its exact function is still unclear. Interestingly, we observed that the GFP-tagged protein clearly localizes to the nucleus of interphase HeLa cells and to centrosomes and spindle poles during mitosis (Fig.12A). Because this localization is similar to many RanGTP-regulated factors involved in spindle assembly, like TPX2, we decided to look for SET function during mitosis. To do that, we prepared specific polyclonal antibodies (Fig.12B and 12C) and look for a specific siRNA to silence its expression (Fig.12D). Preliminary siRNA experiments in HeLa cells suggest that SET could play an essential mitotic role during spindle assembly, however this result needs to be confirmed. Altogether our results suggest that it would be interesting to further investigate SET role in spindle assembly.

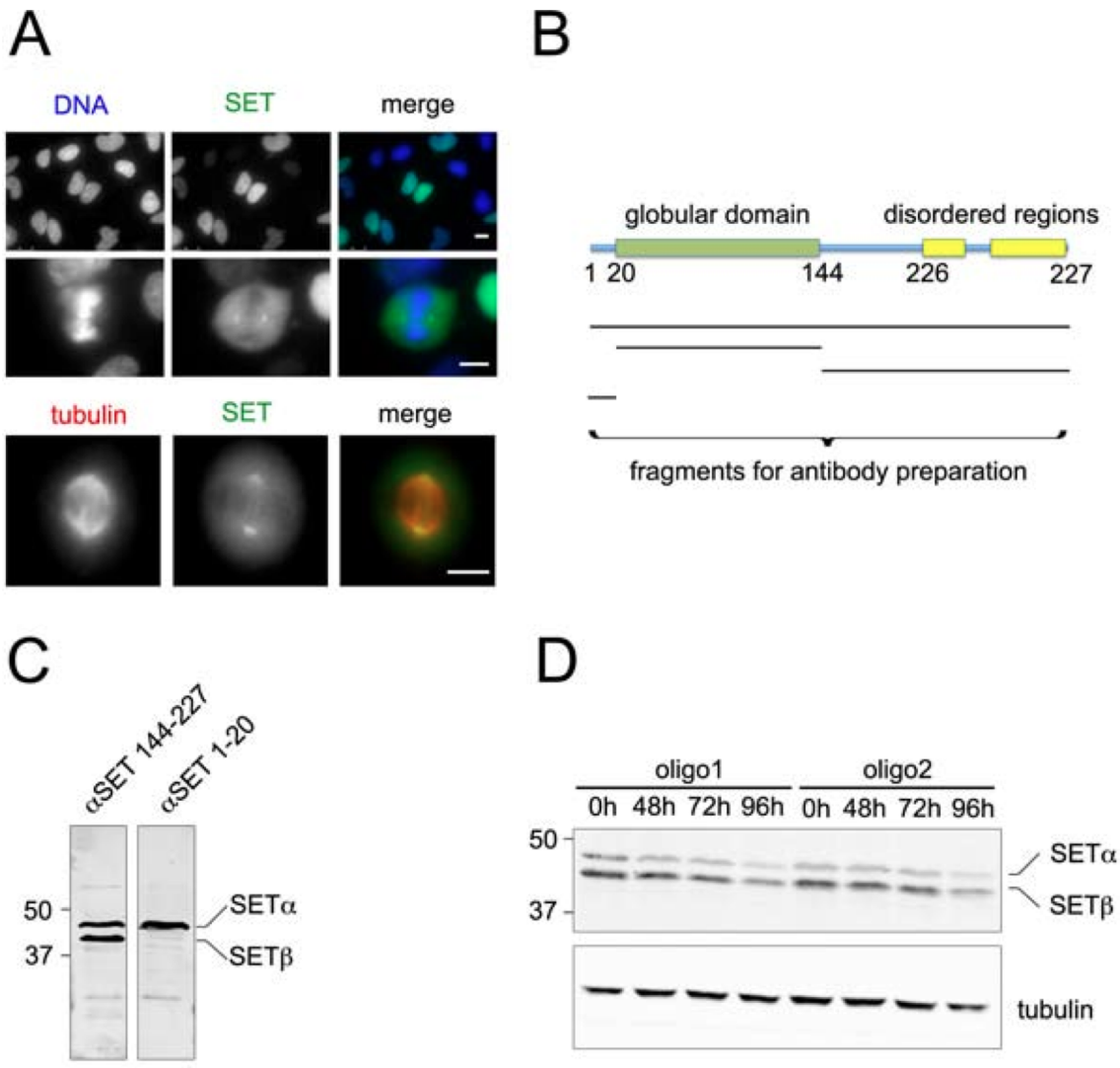

Figure 12. SET localization and tool preparation

A) Interphase and mitotic GFP-SET localization in transfected HeLa cells. DNA (blue), GFP-SET (green), tubulin (red). Scale bars: 10 µm. B) Preliminary analysis on SET primary sequence. ELM database (www.elm.eu.org) was used to predict structural domains. Black lines (bottom) define the fragments cloned to prepare specific polyclonal antibodies. C) Western blot on total HeLa cell extract showing the two best rabbit polyclonal antibodies. Anti-SET(144-227) recognises two different isoforms of SET while anti-SET(1-20) is specific for the α isoform (Seo et al., 2001). D) Western blot analysis on HeLa cells extract. HeLa cells were transfected with two different siRNA against SET and analyzed after 48, 72 and 96 hours. Anti-SET(144-227) antibody recognizes the α and β isoforms. Tubulin is a loading control.

1.2.2. Pontin (Tip49A)

Pontin (ENSG00000175792) was found to be MCRS1-interacting and nuclear protein. It localizes to spindle poles during mitosis (Sigala et al., 2005). Pontin is part of the AAA+ ATPases involved in chromatin remodeling and gene transcription

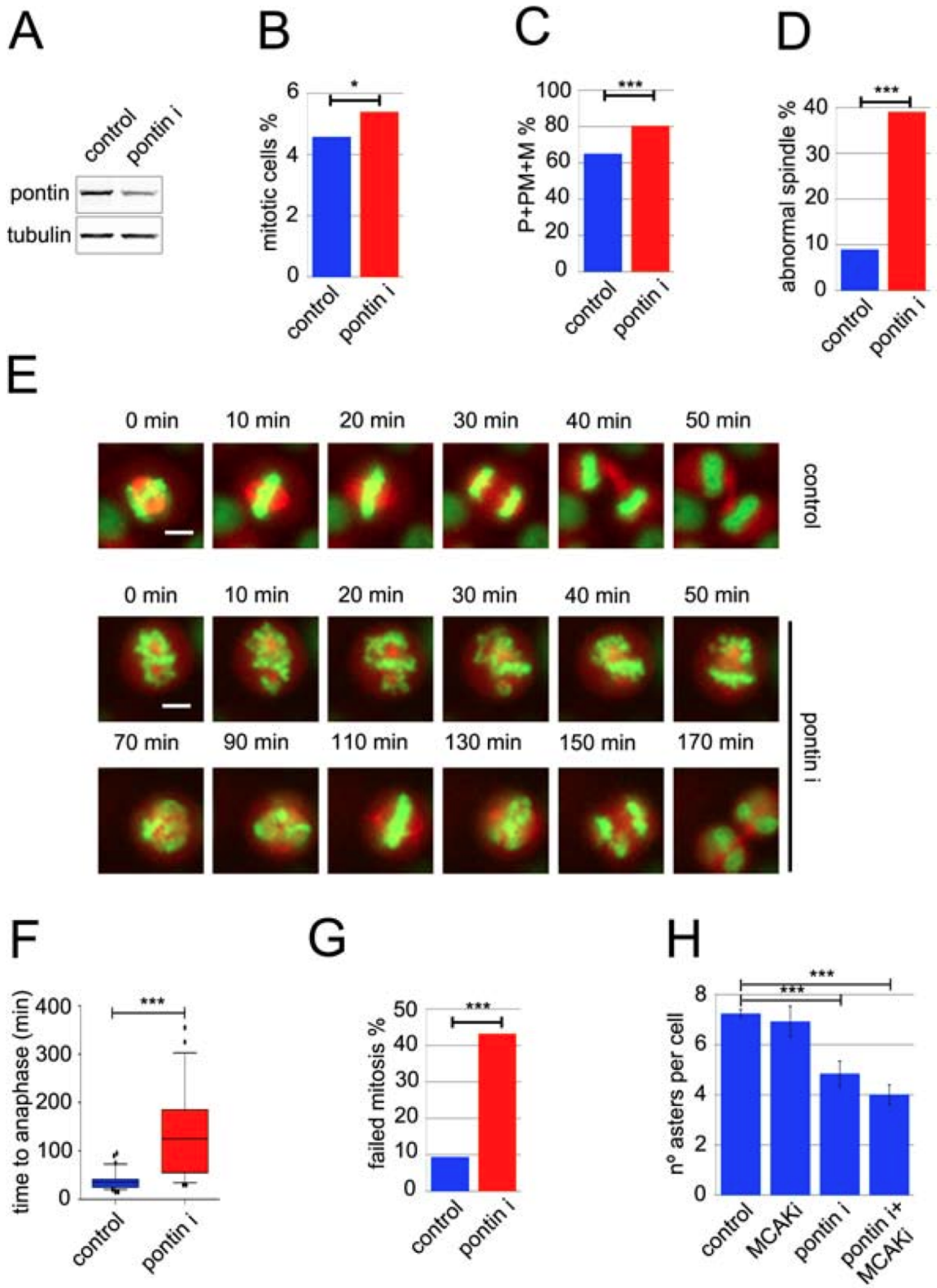

Figure 13. Pontin is involved in chromosome dependent microtubule nucleation in HeLa cells

A) Western blot analysis of control and pontin silenced HeLa cells after 72 hours of transfection. B) Quantification of mitotic cells (percentage over the total number of cells) in control and pontin silenced HeLa cells. More than 500 cells were counted for each condition in one representative experiment. * $0,1<p<0,5$ using X-squared test. C) Quantification of early mitotic cells (from prophase to metaphase; percentage over the total number of cells) in control and pontin silenced HeLa cells. More than 500 cells

were counted for each condition in one representative experiment. *** p<0,001 using X-squared test. D) Quantification of cells with abnormal spindles (percentage over the total number of cells) in control and pontin silenced HeLa cells. More than 500 cells were counted for each condition in one representative experiment. *** p<0,001 using X-squared test. E) Live microscopy on control and pontin silenced GFP-histone RFP-tubulin stably expressing HeLa cells. Scale bars: 10 μm. F) Quantification of time from prophase to anaphase onset in control and pontin silenced cells. The analysis has been performed on live microscopy. More than 30 cells were analysed for each condition in one representative experiment. *** p<0,001 using t-test. G) MT regrowth assay in control, pontin silenced, MCAK silenced and pontin/MCAK double silenced HeLa cells. Cells were fixed after 5 minutes from nocodazole washout. Quantifications represent the average number of asters per cell. More than 30 cells were analysed in each condition. Three independent experiments were performed. Error bars: standard deviation. *** p<0,001 using X-squared test.

(Gallant, 2007). Silencing in cells and depletion from egg extract causes strong spindle defects (Ducat et al., 2008). Pontin interacts with the γTuRC and is essential for its activity (Ducat et al., 2008). To better characterize pontin mitotic role we silenced its expression in HeLa cells. Interestingly, pontin silenced cells significantly accumulate in mitosis (Fig.13A and 13B). Quantifications of the mitotic progression in control and pontin silenced cells revealed a strong delay during the early mitotic stages suggesting defects in chromosomes alignment to the metaphase plate (Fig.13C). Consistently, IF analysis of pontin-silenced cells strikingly showed dramatic metaphase spindle defects (Fig.13D). Although we did not quantify such defects we noticed many monopolar structures and spindles with low MT density. To better define this mitotic phenotype we performed live microscopy on control and pontin-silenced cells. Strikingly, pontin silenced cells showed dramatic defects in chromosomes congression (Fig.13E). Consistently, quantifications revealed a strong delay to reach anaphase (Fig. 13F) and a dramatic increase of cells undergoing apoptosis after division (Fig.13G). To further investigate the mitotic role of pontin we asked if pontin was involved in the chromosomal pathway of spindle assembly. To do that we followed mitotic cells recovering from nocodazole-induced MT depolymerization. This assay, called “MT regrowth assay”, allows visualizing chromosomal MTs that appear like small asters close to the chromosomes (Tulu et al., 2006). Strikingly, the number of MT asters significantly decreased in pontin-silenced HeLa cells (Fig.13H). As previously shown, silencing MCAK can rescue stabilization defects on chromosomal MT assembly (Meunier and Vernos, 2011). Interestingly, MCAK silencing did not rescue pontin phenotype on chromosomal MT assembly suggesting that pontin could act upstream of

MT stabilization (Fig.4H). Altogether our data suggest that the mitotic defects observed in pontin-silenced cells could be due to problems in chromosomal dependent MT nucleation.

1.2.3. DNAJB6

DNAJB6 (ENSG00000105993) was found in the MCRS1, mitotic spindle and nuclear proteomes. DNAJB6 has a co-chaperone activity (Hunter et al., 1999; Chuang et al., 2002) although its mitotic function is still unknown. Interestingly DNAJB6 has been shown to interact with components of the IFT88 complex involved in the intra-flagellar transport and in the recruitment of non centrosomal asters to the spindle poles (Bhowmick et al., 2009; Delaval et al., 2011). GFP-tagged DNAJB6 localizes to the nucleus in interphase and on spindle MTs during mitosis in HeLa cells (Fig.14A). To better characterize DNAJB6 mitotic localization we prepared k-fibers by ice-cold MT depolymerization. Interestingly, DNAJB6 localizes on k-fiber MTs and only to their minus-ends (Fig.14B). To determine if the clear mitotic localization implies also a mitotic role we prepared polyclonal antibodies (Fig.14C and 14D) and looked for specific siRNA to silence its expression (Fig.14E). Preliminary data from IF experiments on DNAJB6 silenced HeLa suggest an essential mitotic role. Particularly, we detected an accumulation of cells in prometaphase and strong defects in spindle bipolarity. Preliminary observations revealed that DNAJB6 silenced cells normally assemble chromosomal MTs but strongly delay spindle assembly in MT regrowth assay. These experiments need to be repeated to confirm the result. These preliminary results suggest a role of DNAJB6 in spindle organization and indicate that the mitotic role of this new protein should be investigated.

1.3. Conclusions

Using a proteomic approach aimed at identifying novel proteins involved in the RanGTP pathway during spindle assembly we identified seven proteins that localize on mitotic structures but have uncharacterized mitotic roles. Preliminary experiments on three of them validate them as strong novel candidates for the RanGTP pathway during mitosis.

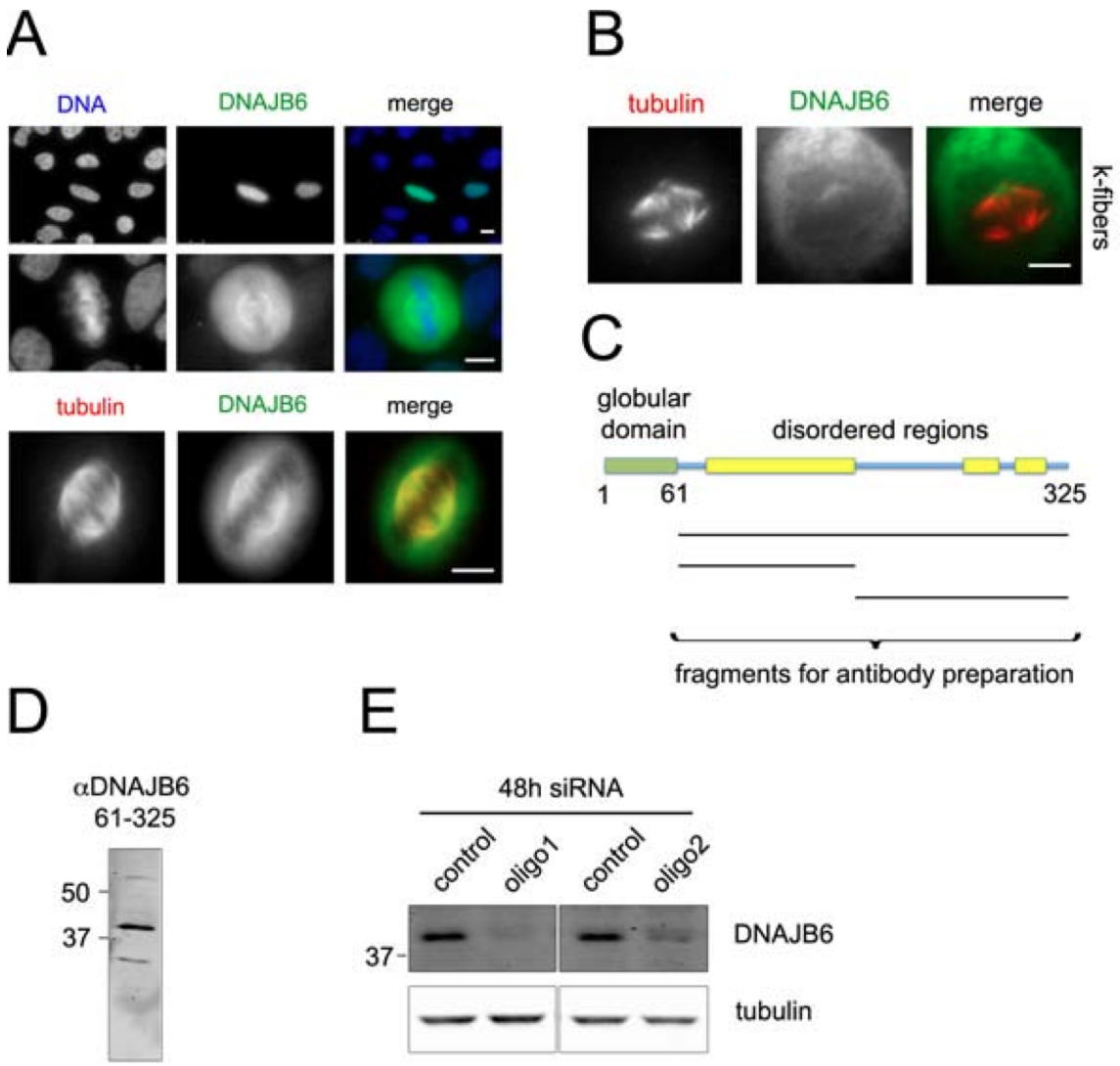

Figure 14. DNAJB6 localization and tool preparation

A) Interphase and mitotic GFP-DNAJB6 localization in transfected HeLa cells. DNA (blue), GFP-DNAJB6 (green), tubulin (red). Scale bars: 10 µm. B) GFP-DNAJB6 localization on k-fibers. Transfected HeLa cells were incubated 10 minutes on ice. Tubulin (red), GFP-DNAJB6 (green). Scale bar: 10 µm. C) Preliminary analysis on DNAJB6 primary sequence. ELM database (www.elm.eu.org) has been used to predict structural domains. Black lines (bottom) define the fragments cloned to prepare specific polyclonal antibodies. D) Western blot on total HeLa cell extract showing the best rabbit polyclonal antibody. E) Western blot analysis on HeLa cells extract. HeLa cells were transfected with two different siRNA against DNAJB6 and analyzed after 48 hours. Anti-DNAJB6(61-325) recognize the α and β isoforms. Tubulin is a loading control.

2. Mechanisms of RanGTP-dependent microtubule nucleation

In the previous chapter I described our approach to screen proteomic data looking for new players involved in the RanGTP pathway in mitosis. This wide approach is a powerful contribution to fill the gap of knowledge due to the limited number of known proteins involved in the RanGTP dependent MT assembly process. However we also decided to follow a more direct molecular approach to investigate how the RanGTP pathway regulates MT assembly close to the chromosomes. In this chapter I will show our advance in the investigation of the mechanisms driving the RanGTP dependent MT nucleation. The results reported in this chapter constitute the main body of one published paper and one submitted manuscript. Supplementary results follow providing additional unpublished informations.

2.1. The role of NEDD1 phosphorylation by Aurora-A in chromosomal microtubule nucleation and spindle function

The first manuscript ("The role of NEDD1 phosphorylation by Aurora-A in chromosomal microtubule nucleation and spindle function" Current Biology 2013 Jan 21; 23(2):143-9) reports the identification of a specific phosphorylation of the γTuRC targeting factor NEDD1 by Aurora-A. Through this phosphorylation Aurora-A plays an essential role promoting MT nucleation around chromosomes and thereby proper spindle assembly. My personal contribution in this work started by Roser Pinyol, former member of our lab, has been to describe the role of NEDD1 S405 phosphorylation in the *Xenopus laevis* egg extract system.

(Pinyol R, Scrofani J, Vernos I. The role of NEDD1 phosphorylation by Aurora-A in chromosomal microtubule nucleation and spindle function. Current Biology 2013 Jan 21; 23(2):143-9)

Pinyol R, Scrofani J, Vernos I. The role of NEDD1 phosphorylation by Aurora A in chromosomal microtubule nucleation and spindle function. Curr Biol. 2013 Jan 21; 23(2): 143-9. DOI: 10.1016/j.cub.2012.11.046

Current Biology 23, 143–149, January 21, 2013 http://dx.doi.org/10.1016/j.cub.2012.11.046

Report

The Role of NEDD1 Phosphorylation by Aurora A in Chromosomal Microtubule Nucleation and Spindle Function

Roser Pinyol,[1,2] Jacopo Scrofani,[1,2] and Isabelle Vernos[1,2,3,*]
[1]Centre for Genomic Regulation (CRG), Doctor Aiguader 88, 08003 Barcelona, Spain
[2]Universitat Pompeu Fabra (UPF), 08003 Barcelona, Spain
[3]Institució Catalana de Recerca i Estudis Avançats (ICREA), Passeig de Lluís Companys 23, 08010 Barcelona, Spain

Summary

Chromatin directs de novo microtubule (MT) nucleation in dividing cells by generating a gradient of GTP-bound Ran protein (RanGTP) that controls the activity of a number of spindle assembly factors (SAFs) [1]. It is now well established that these MTs are essential for the assembly of a functional bipolar spindle [2]. Although it has been shown that RanGTP-dependent MT nucleation requires γ-tubulin and a number of RanGTP-regulated proteins [3, 4], the mechanism involved is still poorly understood. We previously showed that the mitotic kinase Aurora A, which is activated in a RanGTP-dependent manner in mitotic cells, has a role in this pathway [5]. Here we show that Aurora A interacts with and phosphorylates the γTURC adaptor protein NEDD1 at a single residue, Ser405. Ser405 phosphorylation is not required for centrosomal MT nucleation but is critical for MT nucleation in the vicinity of the chromosomes in mitotic cells. Moreover, it is essential for RanGTP aster formation and chromatin-driven MT assembly in *Xenopus* egg extracts. Our data suggest that one important function of Aurora A in mitotic cells is to promote MT nucleation around the chromatin by phosphorylating NEDD1, and thereby to promote functional spindle assembly.

Results

Aurora A Interacts with the γTURC Adaptor Protein NEDD1

After nuclear envelope breakdown, chromosomes direct de novo microtubule (MT) assembly by generating a gradient of GTP-bound Ran protein (RanGTP) that promotes the release of various spindle assembly factors (SAFs) [1]. Very little is currently known about the mechanism that triggers MT nucleation through this pathway, but it involves basic components of the MT nucleation machinery like γ-tubulin [3] as well as the RanGTP-regulated protein TPX2 [4, 6] and the chromosomal passenger complex (CPC) [7, 8]. We previously showed that TPX2 activates the kinase Aurora A in a RanGTP-dependent manner [9] and in turn that Aurora A activity is required for RanGTP-dependent MT aster formation in *Xenopus* egg extracts [5]. Aurora A activity was also shown to be essential for kinetochore/chromatin-dependent MT assembly in human cells [7]. Recently, using a bioinformatics approach, we proposed that the γTURC adaptor protein NEDD1 could be one of its substrates [10], suggesting a direct link between Aurora A and the MT nucleation machinery.

To investigate this possibility, we first examined whether Aurora A and NEDD1 interact in egg extract and mitotic HeLa cells. Western blot analysis showed that Aurora A was coimmunoprecipitated by anti-NEDD1 antibodies both in cytostatic factor (CSF)-arrested *Xenopus* egg extracts and in mitotic HeLa cell lysates (Figure 1A). Consistently, anti-Aurora A antibodies coimmunoprecipitated NEDD1 from egg extracts (Figure 1B). We conclude that Aurora A interacts with the γTURC adaptor protein NEDD1 during M phase.

To confirm these data and map the domain (or domains) of NEDD1 involved in the interaction with Aurora A, we performed pull-down experiments in *Xenopus* egg extract using glutathione S-transferase (GST) fusion proteins corresponding to the N-terminal WD40 domain of NEDD1 (xNEDD1-NT) and the complementary C-terminal domain (xNEDD1-CT) (Figure 1D; see also Figure S1A available online). Western blot analysis showed that Aurora A was pulled down by GST-xNEDD1-CT, but not by GST-xNEDD1-NT or GST (Figure 1D). In vitro pull-down experiments using His-GFP-tagged xAurora A and the different GST-tagged NEDD1 fragments showed that there is a direct interaction between the C-terminal domain of NEDD1 and Aurora A (Figure S1B).

Double immunofluorescence analysis in mitotic HeLa cells showed that Aurora A and NEDD1 colocalized to the centrosomes and the spindle poles in metaphase (Figure 1C). Immunofluorescence studies in Aurora A- or NEDD1-silenced cells showed that they do not depend on each other for their localization (Figures S1C–S1E).

Altogether, we conclude that NEDD1 is a novel binding partner of Aurora A. It interacts directly with Aurora A through its C-terminal non-WD40 domain. Although the two proteins colocalize during mitosis, they are independently targeted to the centrosomes and spindle poles.

Aurora A Phosphorylates NEDD1 at Ser405

To determine whether Aurora A phosphorylates NEDD1 in vitro, we incubated Aurora A with each of the two NEDD1 fragments fused to GST (Figures S1F and S1G) in the presence of [^{32}P] ATP. Autoradiography showed that Aurora A efficiently phosphorylated GST-NEDD1-CT, but not GST-NEDD1-NT, for both the *Xenopus* and the human orthologs (Figures S1F and S1G). Mass spectrometry was then used to identify the Aurora A-dependent phosphorylated residue(s) in GST-xNEDD1-CT. A phosphopeptide containing Ser405 that is located in a consensus sequence for Aurora A phosphorylation [R/K]-X-[S/T]-[I/L/V] was identified [11] (Figure 1E). To confirm that NEDD1 Ser405 is the major site phosphorylated by Aurora A, we used site-directed mutagenesis to produce GST-NEDD1-CT S405A in which Ser405 was substituted by an alanine. In vitro kinase assays showed that this single amino acid substitution was sufficient to completely abolish the incorporation of ^{32}P upon incubation with xAurora A (Figure 1F). Altogether, this shows that Aurora A phosphorylates NEDD1 at Ser405 in vitro.

To determine whether Ser405 is phosphorylated during M phase in cells, we expressed Flag-hNEDD1 in HeLa cells and pulled down the protein from cells synchronized in mitosis. Mass spectrometry analysis of the hyperphosphorylated form of Flag-hNEDD1 identified a phosphorylated peptide containing Ser405 (Figure S2). Consistently, mass spectrometry analysis of xNEDD1 immunoprecipitated from

*Correspondence: isabelle.vernos@crg.eu

Current Biology Vol 23 No 2
144

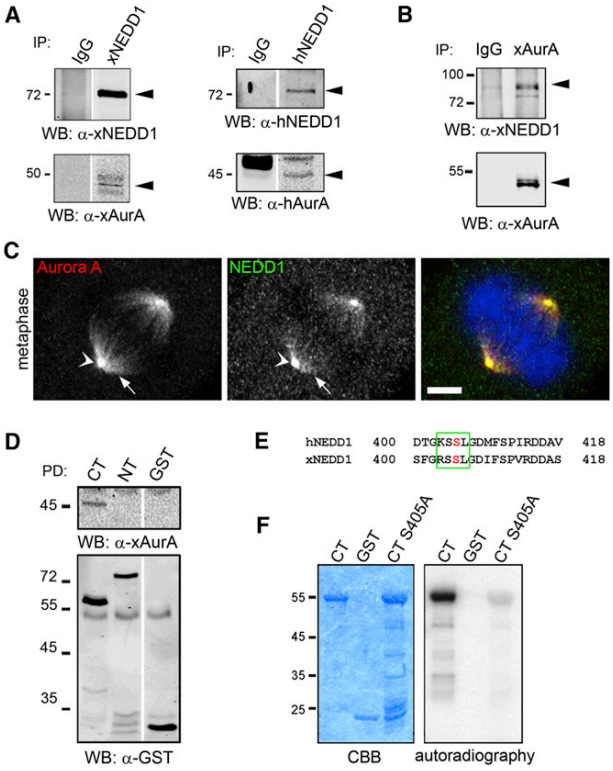

Figure 1. Aurora A Interacts With and Phosphorylates NEDD1 in Mitosis

(A) Western blot analysis of NEDD1 immunoprecipitations from CSF-arrested *Xenopus laevis* egg extracts (left) and mitotic HeLa cells lysates (right). Anti-xNEDD1 antibodies specifically immunoprecipitated xNEDD1 and xAurora A from egg extract. Mouse anti-hNEDD1 antibodies immunoprecipitated hNEDD1 and hAurora A from mitotic HeLa cells (the unspecific rabbit IgGs used as control are strongly recognized by the anti-rabbit secondary antibodies).

(B) Western blot analysis of xAurora A immunoprecipitation from CSF-arrested egg extracts. The anti-xAurora A antibodies specifically immunoprecipitate Aurora A and NEDD1.

(C) Confocal images of a HeLa cell in metaphase showing the localizations of Aurora A and NEDD1 by immunofluorescence. Aurora A and NEDD1 colocalize at the centrosome (arrowhead) and at the spindle MTs (arrow). A maximum projection is shown. In the merge image, Aurora A is in red, NEDD1 is in green, and DNA is in blue. Scale bar represents 5 μm.

(D) Western blot analysis of a pull-down experiment using GST-fusion proteins of the C-terminal (CT) and N-terminal (NT) domains of xNEDD1. GST-NEDD1-CT (CT), GST-NEDD1-NT (NT), or GST alone were immobilized on anti-GST antibody-coated beads and incubated in CSF-arrested egg extract. The beads were retrieved, washed, and resuspended in loading buffer. The recombinant proteins are visualized with anti-GST antibodies in the lower panel. Aurora A was specifically recovered only with GST-xNEDD1-CT, as shown on the western blot with anti-Aurora A antibodies in the upper panel.

(E) Alignment of the human and frog NEDD1 sequences containing the conserved Ser405 found to be phosphorylated in vitro by Aurora A. The conserved motif for Aurora A phosphorylation [R/K]-X-[S/T]-[I/L/V] is framed in green, with Ser405 highlighted in red.

(F) Coomassie brilliant blue (CBB)-stained gel and autoradiography of an in vitro kinase assay with His-xAurora A and GST, GST-xNEDD1-CT, and GST-xNEDD1-CTS405A. xAurora A phosphorylates GST-xNEDD1-CT specifically, but not xNEDD1 CT S405A. This shows that Aurora A phosphorylates NEDD1 at Ser405.

See also Figures S1 and S2.

CSF-arrested egg extracts detected a phosphorylated peptide containing Ser405 (Figure S2). These results are consistent with previous reports describing the phosphorylation of NEDD1 on Ser405 in mouse and mitotic U2OS cells [12, 13]. We conclude that Aurora A phosphorylates NEDD1 on Ser405 during M phase.

Phosphorylation of NEDD1 by Aurora A at Ser405 Is Required for Functional Spindle Assembly and Chromosome Alignment

As a first approach to examine the role for NEDD1 Ser405 phosphorylation during cell division, we expressed Flag-NEDD1, Flag-NEDD1 S405A, or Flag-NEDD1 S405D in HeLa cells. Overexpression of any of these NEDD1 variants did not interfere with spindle formation and chromosome segregation (data not shown).

Reducing NEDD1 levels by small interfering RNA transfection in HeLa cells resulted in a range of spindle defects, including monopolar and unorganized spindles, as previously described [14, 15]. We then expressed RNAi-resistant Flag-NEDD1, Flag-NEDD1 S405A, or Flag-NEDD1 S405D in the silenced cells. We first looked at the localization of the different NEDD1 variants by immunofluorescence with an anti-Flag antibody (Figure 2A). All of the recombinant NEDD1 variants localized both to the centrosomes and to the spindle MTs like the endogenous protein (Figure 2A; Figure S3A). Consistently, γ-tubulin localized to both the spindle poles and the spindle MTs in all the cells (Figure 2B; Figure S3B). As a control, we performed the same analysis on NEDD1-silenced cells expressing Flag-NEDD1-S411A (Figures S3A and S3B). As described previously and in contrast to the S405 phospho variants, neither the S411A variant nor γ-tubulin localized to the spindle MTs [14]. These results suggested that phosphorylation of NEDD1 at Ser405 is not required for NEDD1 and γ-tubulin localization to the centrosome and spindle MTs.

Expression of Flag-NEDD1, Flag-NEDD1 S405A, or Flag-NEDD1 S405D in the silenced cells rescued the formation of bipolar spindles. However, cells expressing Flag-NEDD1 S405A showed a striking chromosome misalignment phenotype, with only 19.5% ± 2.9% of the bipolar spindles showing fully aligned chromosomes, whereas 53.3% ± 5.4% of bipolar spindles in cells expressing Flag-NEDD1 and 42.7% ± 2.3% in cells expressing Flag-NEDD1 S405D had fully aligned chromosomes (Figure 2C). These data suggested that the phosphorylation of NEDD1 on Ser405 is important for the assembly of kinetochore fibers and their stable attachment to the chromosomes. To further test this idea, we monitored K-fiber stability using a cold-stable assay in NEDD1-silenced cells expressing the different NEDD1 variants (Figure 2D and 2E; Figure S3C). We found that silenced cells expressing Flag-NEDD1 S405A were more sensitive to cold-induced depolymerization than those expressing Flag-NEDD1 or Flag-NEDD1 S405D, indicating that their K-fibers were less stable (Figures 2D and 2E). Altogether, these results suggested that the phosphorylation of NEDD1 at S405 is important for the formation of functional K-fibers and chromosome alignment.

Phosphorylation of NEDD1 by Aurora A at Ser405 Is Essential for Chromatin-Dependent MT Assembly

The chromosome misalignment phenotype and K-fiber instability in silenced cells expressing Flag-NEDD1 S405A suggested that phosphorylation at this site could play a role in chromosomal MT nucleation [2, 7]. We therefore used a MT regrowth assay to clearly visualize the centrosomal and chromosomal

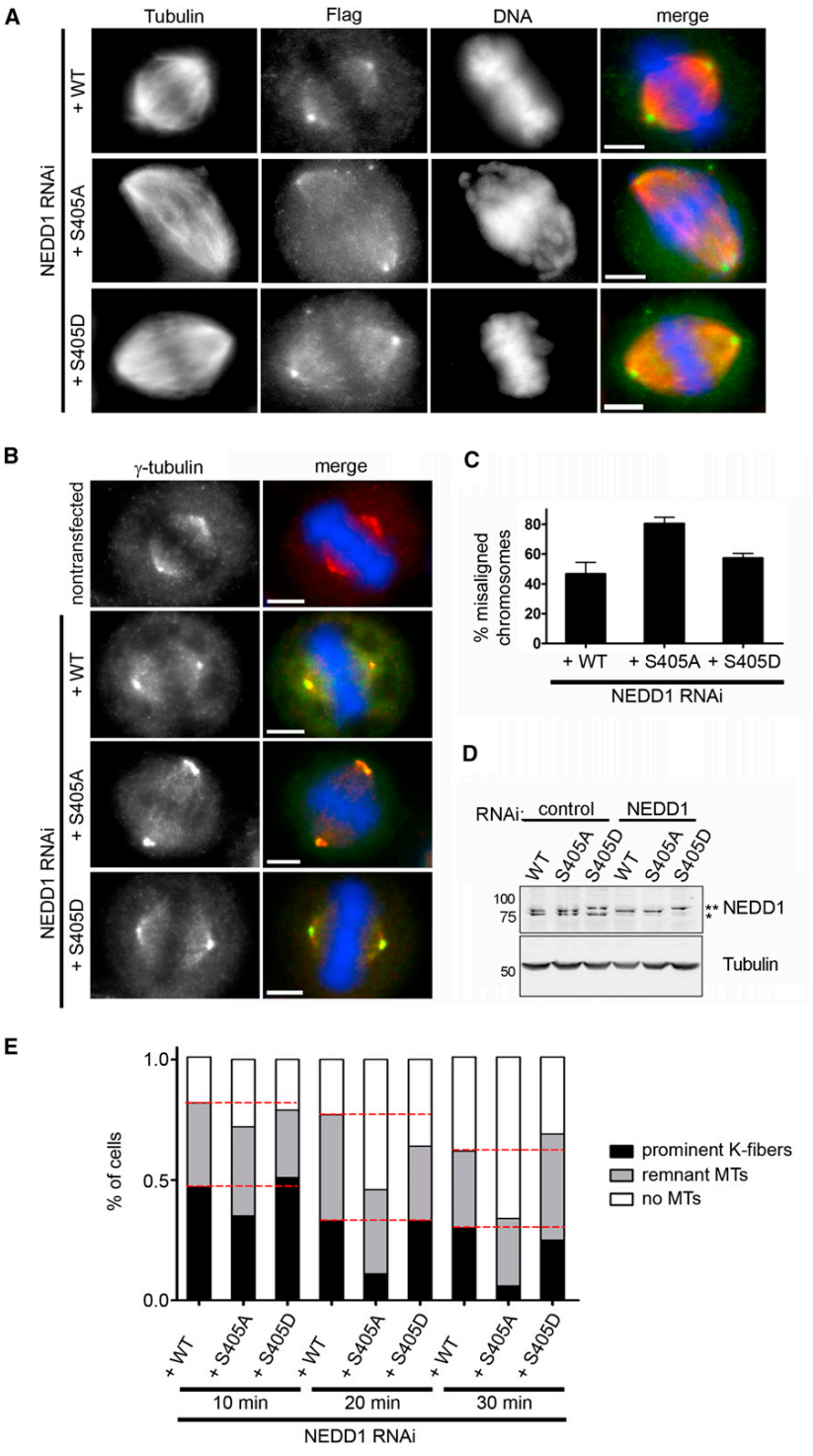

Figure 2. NEDD1 Phosphorylation Is Required for Chromosome Alignment, but Not for γ-Tubulin Targeting

(A) Immunofluorescence images of NEDD1-silenced cells transfected with RNAi-resistant Flag-NEDD1 wild-type (WT), Flag-NEDD1-S405A (S405A), or Flag-NEDD1-S405D (S405D). The exogenously expressed NEDD1 variants were detected with anti-Flag antibodies (in green). MTs are in red; DNA is in blue. Scale bar represents 5 μm.

(B) Immunofluorescence images of NEDD1-silenced cells transfected with RNAi-resistant Flag-NEDD1-WT (WT), Flag-NEDD1-S405A (S405A), or Flag-NEDD1-S405D (S405D) and processed for immunofluorescence to visualize γ-tubulin (red), the Flag-tagged recombinant proteins (green), and DNA (blue). Scale bar represents 5 μm.

(C) Quantification of the percentage of spindles with misaligned chromosomes in experiments similar to (B). Depicted is the average of two independent experiments and its SD.

(D) Western blot analysis of cell lysates from the different experimental conditions shown in (B). The anti-NEDD1 antibodies recognize both the endogenous and recombinant forms of NEDD1. In NEDD1-silenced cells, the endogenous protein (marked with one asterisk) is almost undetectable. The exogenously expressed recombinant proteins (marked with two asterisks) show levels comparable to endogenous NEDD1. Tubulin signal is shown as a loading control.

(E) Cold-stable assay to monitor K-fiber stability in NEDD1-silenced cells expressing Flag-NEDD1-WT (+WT), Flag-NEDD1-S405A (+S405A), or Flag-NEDD1-S405D (+S405D) as indicated. The quantification shows the percentage of metaphase-like cells with intact K-fibers (prominent K-fibers), K-fiber remnants (remnant MTs), or no MTs (no MTs). The red dashed lines mark the percent of each category for the control condition (silenced cells expressing Flag-NEDD1-WT). The graph shows a representative experiment out of three independent experiments (each with $n \geq 30$).

See also Figure S3.

MTs. Cells were incubated with nocodazole, released, and fixed. Immunofluorescence analysis showed that NEDD1 and Aurora A localized both to the centrosomal asters (as identified by the localization of the centrosomal marker Cep192) and to the chromosomal asters (Figure S4A) [14].

As described previously, control cells contained two prominent centrosome asters and a variable number of additional MT asters on the chromatin [2, 6] (Figure 3). In agreement with previous reports, NEDD1-silenced cells displayed a significant reduction in the number of asters and in their intensity, suggesting that both the centrosomal and chromosomal pathways were strongly impaired [14] (Figures 3A and 3C). We then expressed the different Flag-tagged NEDD1 variants in the silenced cells to evaluate their capacity to rescue the formation of centrosomal and/or chromosomal MT asters. Expression of Flag-NEDD1 or Flag-NEDD1 S405D in NEDD1-silenced cells rescued MT aster formation by both the centrosomes and the chromosomes in 54.3% ± 11.6% and 53.5% ± 8.1% of the cells, respectively (Figures 3B and 3C). Remarkably, the majority of the NEDD1-silenced cells expressing Flag-NEDD1 S405A contained only two prominent MT asters centered on the centrosomes as detected with GFP-centrin

Current Biology Vol 23 No 2
146

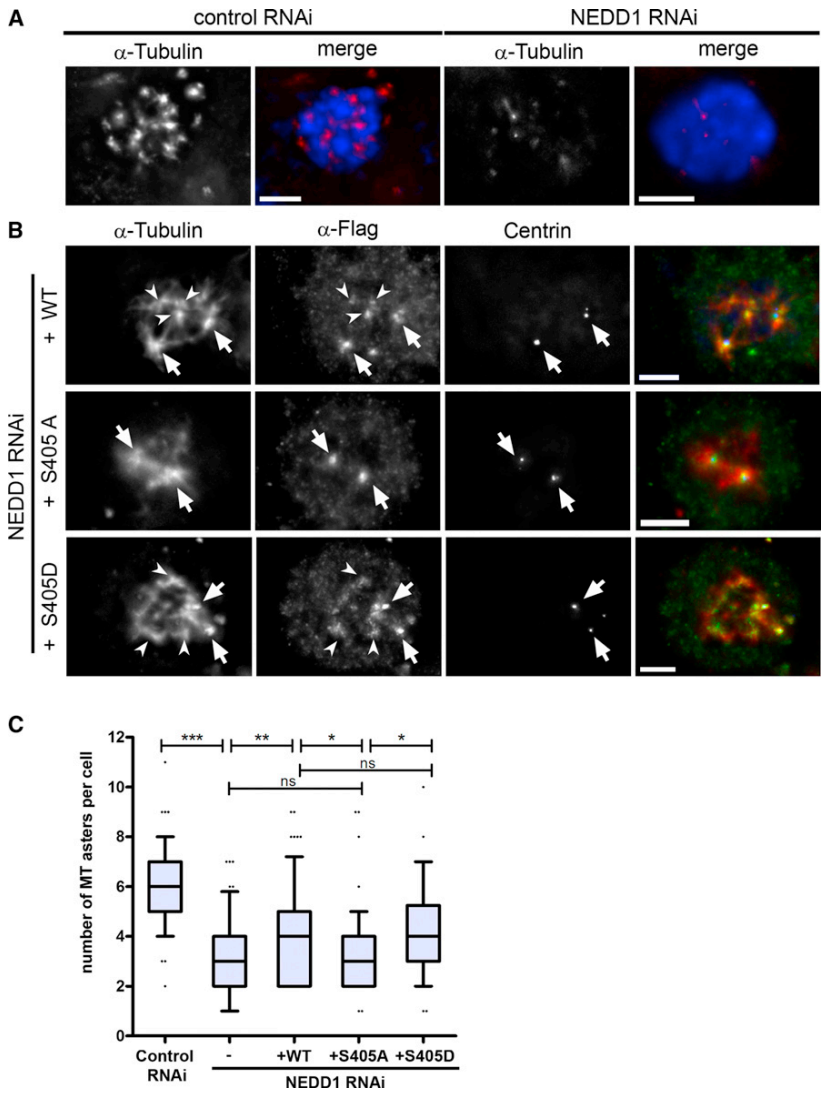

Figure 3. NEDD1 Phosphorylation at Ser405 Is Essential for Chromosome-Dependent MT Nucleation

(A) Immunofluorescence images of control and NEDD1-silenced HeLa cells incubated in nocodazole and fixed 5 min after washout. NEDD1-silenced cells are strongly impaired for MT regrowth. In the merge, MTs are in red and DNA is in blue. Scale bar represents 5 μm.

(B) Immunofluorescence images of NEDD1-silenced HeLa cells expressing RNAi-resistant Flag-hNEDD1 (+WT), Flag-hNEDD1 S405A (+S405A), or Flag-hNEDD1 S405D (+S405D) incubated in nocodazole and fixed 5 min after washout. The centrosomes (indicated by arrows) are visualized by GFP-centrin (here shown in blue) stably expressed in this HeLa cell line. The recombinant proteins are detected with anti-Flag antibodies (displayed in green), and tubulin is shown in red. Chromosomal MTs marked with arrowheads are absent in cells expressing Flag-hNEDD1 S405A. Scale bar represents 5 μm.

(C) Quantification of the number of MT asters per cell, 5 min after nocodazole washout. In the box-and-whiskers plot, boxes show the upper and lower quartiles (25%–75%) with a line at the median, whiskers extend from the 10th to the 90th percentile, and dots correspond to outliers. *$p \leq 0.05$; **$p \leq 0.01$; ***$p \leq 0.005$. The graph shows one representative experiment out of nine independent experiments (each with $n \geq 30$). See also Figure S4.

(Figure 3B). These results strongly suggested that NEDD1 phosphorylation on Ser405 by Aurora A is specifically required for the nucleation of chromosomal MTs.

We then examined cells at longer times after nocodazole washout to monitor spindle formation. Around 18% of control cells and Flag-NEDD1- or Flag-NEDD1 S405D-expressing cells had assembled a bipolar spindle with fully aligned chromosomes (Figure S4). By contrast, although Flag-NEDD1 S405A-expressing cells also rescued the spindle assembly defects due to NEDD1 silencing, only 5.2% formed a bipolar spindle with aligned chromosome (Figure S4). These data show that the phosphorylation of NEDD1 by Aurora A on Ser405 is essential for the nucleation of chromosomal MTs, and thereby for the assembly of a functional bipolar spindle.

Phosphorylation of NEDD1 by Aurora A at Ser405 Is Essential for RanGTP- and Chromatin-Dependent MT Assembly in *Xenopus* Egg Extracts

To gain further support for a role of phosphorylation of NEDD1 S405 by Aurora A in chromosome-dependent MT nucleation, we then turned to the *Xenopus* egg extract system. Depletion of NEDD1 strongly impaired the formation of MT asters induced by addition of RanGTP to the extract. Moreover, the capacity of DNA-coated beads to promote MT assembly when incubated in depleted egg extract was also impaired (Figure 4). Both phenotypes were fully rescued upon addition of recombinant NEDD1 or NEDD1 S405E to the depleted extract. By contrast, addition of NEDD1 S405A was unable to rescue RanGTP aster formation and MT assembly around DNA beads (Figure 4). These results provide strong support for an essential role of NEDD1 phosphorylation at Ser405 in the RanGTP-dependent MT assembly pathway during M phase.

Discussion

NEDD1 has recently emerged as a key targeting factor for the γTURC required in all the known pathways leading to MT assembly [14–17]. It does indeed target the γTURC to the centrosome, and to preexisting MTs through the augmin complex [17]. It is also required for chromosome-dependent MT assembly, although no mechanism for its targeting or activation in this pathway has been described so far. Interestingly, NEDD1 is hyperphosphorylated during M phase [14, 15]. Several studies have identified a number of sites phosphorylated by Cdk1 and Plk1 [12, 14, 16, 18, 19]. Phosphorylation at these sites plays important and complex regulatory functions at different levels, including the binding of NEDD1 to the γTURC [12, 16, 20] and its targeting to the spindle MTs [14] and the centrosome [21].

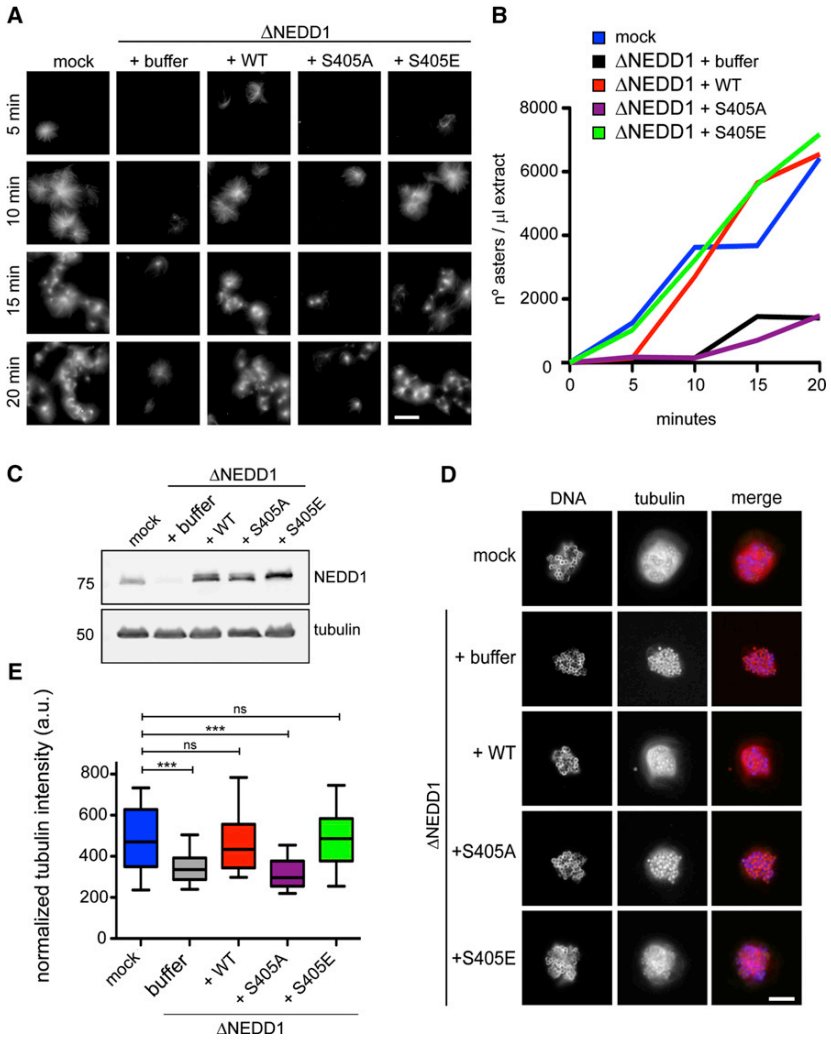

Figure 4. NEDD1 Ser405 Phosphorylation Is Essential for Chromatin- and RanGTP-Dependent MT Nucleation in *Xenopus laevis* Egg Extracts

(A) RanGTP asters formed in control mock-depleted egg extract (mock), NEDD1-depleted extract (+buffer), and depleted extract supplemented with human recombinant flag-NEDD1 (WT), Flag-NEDD1 S405A (+S405A), or Flag-NEDD1 S405E (+S405E). The images correspond to squashes taken at 5, 10, 15, and 20 min after RanGTP addition to a CSF extract. MTs are visualized by addition of rhodamine tubulin to the extract. Scale bar represents 25 μm.

(B) Quantification of the number of RanGTP asters in each experimental condition. The graph shows one representative experiment out of four independent experiments.

(C) Western blot analysis of the extracts used for (A) and (B) showing that endogenous NEDD1 in mock extract was efficiently depleted, and showing the different recombinant proteins that were added to the depleted extract. The tubulin signal is shown as loading control.

(D) Images of DNA-coated beads incubated in cycled extract as indicated for 30 min. Rhodamine tubulin was added to the extract for visualization. DNA was stained with Hoechst. Note that the beads are autofluorescent. Scale bar represents 25μm.

(E) Quantification of the DNA bead-dependent MT nucleation shown in (D). The total tubulin intensity around each DNA bead cluster was measured and normalized by the cluster size. In the box-and-whiskers plot, boxes show the upper and lower quartiles (25%–75%) with a line at the median. ***$p < 0.005$; ns, no statistical difference using Student's t test. The graph shows one of two independent experiments.

Here we show that Aurora A phosphorylates NEDD1 at a single residue in mitotic cells and that this phosphorylation is essential for the assembly of chromosomal MTs. Extensive work supports a role for Aurora A in promoting MT assembly in M phase, both at the centrosome, where it accumulates in G2/M, and around the chromosomes through the RanGTP- and TPX2-dependent pathway [4, 5, 7, 22, 23]. The substrates of Aurora A identified so far support a main role for this kinase in MT stabilization and organization [5, 10, 24]. Our findings provide for the first time a direct link between Aurora A and the MT nucleation machinery, suggesting a novel role for this kinase in controlling MT nucleation.

The localization of Aurora A and NEDD1 at both the centrosome and spindle MTs suggests that NEDD1 phosphorylation by Aurora A could have a general regulatory function on the MT nucleation machinery. However, both NEDD1 S405A and NEDD1 S405D localize to the centrosomes and fully rescue their MT aster formation capacity in NEDD1-silenced cells. These data indicate that Ser405 phosphorylation is required neither for the targeting of the γTURC to the centrosome nor for regulating its intrinsic MT nucleation activity. In line with these results, a previous report showed that Aurora A silencing does not interfere with the recruitment of γ-tubulin to the centrosome during MT regrowth experiments [7].

We provide evidence in two experimental systems for an essential role of NEDD1 phosphorylation by Aurora A in chromosomal MT assembly. The strong impairment of this pathway when NEDD1 cannot be phosphorylated on Ser405 is most likely due to defects at the level of MT nucleation. Although NEDD1 has also been implicated in another acentrosomal MT assembly pathway driving MT amplification through the augmin complex, our results do not indicate that this pathway is affected by NEDD1 S405 phosphorylation. Indeed, NEDD1 S405A localizes to the spindle MTs and does not interfere with the targeting of γ-tubulin to these spindle MTs, a process that has been shown to rely on NEDD1 and the augmin complex [17]. Moreover, we found that NEDD1 S405A pulled down FAM29A as efficiently as the wild-type protein in mitotic HeLa cell lysates (data not shown). In addition, in contrast to our results, it has been shown that the silencing of the augmin component FAM29A does not interfere with the early steps of chromosomal MT nucleation in cells released from nocodazole [17]. Our data therefore suggest that the phosphorylation of NEDD1 at Ser405 is specifically required for the direct nucleation of chromosomal MTs.

Although NEDD1 S405A strongly impairs chromosomal MT assembly, it supports the organization of the centrosomal MTs into a spindle-like configuration. Silencing the

Current Biology Vol 23 No 2
148

RanGTP-regulated protein TPX2 also impairs chromosomal MT assembly, but it has more dramatic consequences on spindle formation [25, 26]. Because TPX2 has additional functions related to spindle organization and complex interactions in particular with motor proteins [27–29], our results here may more specifically reflect the consequences of the absence of chromosomal MTs on spindle assembly and functionality. We recently showed that interfering with chromosomal MT assembly by silencing MCRS1 leads to defects in K-fiber formation and dynamics [2]. Altogether, our results indicate that although centrosomal asters can organize a bipolar-like spindle, these structures are not functional and cannot align the chromosomes. Moreover, they suggest that an active chromosomal MT assembly pathway is essential for the assembly and functionality of the K-fibers.

In summary, our work strongly supports the key role of NEDD1 in the spatial and temporal control of MT nucleation in mitotic cells. Moreover, it provides a specific mechanism for the regulation of MT nucleation around the chromosomes. Under the influence of the RanGTP gradient, TPX2 activates Aurora A, which in turn specifically phosphorylates the γTURC adaptor protein NEDD1 and triggers chromosomal-MT nucleation. This links for the first time the kinase Aurora A and the MT nucleation machinery and reveals a novel function for this kinase during mitosis.

Supplemental Information

Supplemental Information includes Supplemental Experimental Procedures and four figures and can be found with this article online at http://dx.doi.org/10.1016/j.cub.2012.11.046.

Acknowledgments

We thank S. Meunier and T. Sardon for discussion and critical comments on this work and N. Mallol, L. Ávila, and M. Sanz for technical support. We acknowledge the efficient help of the CRG/UPF Proteomics and the CRG Advanced Light Microscopy Core facilities. This work was supported by grants Consolider-Ingenio 2010 CENTROSOME_3D CSD2006-00023 and BFU2009-10202. J.S. is supported by a PhD student fellowship from La Caixa. All work involving animals was performed according to standard protocols approved by the CRG Ethics Committee.

Received: May 11, 2012
Revised: September 28, 2012
Accepted: November 21, 2012
Published: December 27, 2012

References

1. Clarke, P.R., and Zhang, C. (2008). Spatial and temporal coordination of mitosis by Ran GTPase. Nat. Rev. Mol. Cell Biol. *9*, 464–477.
2. Meunier, S., and Vernos, I. (2011). K-fibre minus ends are stabilized by a RanGTP-dependent mechanism essential for functional spindle assembly. Nat. Cell Biol. *13*, 1406–1414.
3. Wilde, A., and Zheng, Y. (1999). Stimulation of microtubule aster formation and spindle assembly by the small GTPase Ran. Science *284*, 1359–1362.
4. Gruss, O.J., and Vernos, I. (2004). The mechanism of spindle assembly: functions of Ran and its target TPX2. J. Cell Biol. *166*, 949–955.
5. Sardon, T., Peset, I., Petrova, B., and Vernos, I. (2008). Dissecting the role of Aurora A during spindle assembly. EMBO J. *27*, 2567–2579.
6. Tulu, U.S., Fagerstrom, C., Ferenz, N.P., and Wadsworth, P. (2006). Molecular requirements for kinetochore-associated microtubule formation in mammalian cells. Curr. Biol. *16*, 536–541.
7. Katayama, H., Sasai, K., Kloc, M., Brinkley, B.R., and Sen, S. (2008). Aurora kinase-A regulates kinetochore/chromatin associated microtubule assembly in human cells. Cell Cycle *7*, 2691–2704.
8. Sampath, S.C., Ohi, R., Leismann, O., Salic, A., Pozniakovski, A., and Funabiki, H. (2004). The chromosomal passenger complex is required for chromatin-induced microtubule stabilization and spindle assembly. Cell *118*, 187–202.
9. Bayliss, R., Sardon, T., Vernos, I., and Conti, E. (2003). Structural basis of Aurora-A activation by TPX2 at the mitotic spindle. Mol. Cell *12*, 851–862.
10. Sardon, T., Pache, R.A., Stein, A., Molina, H., Vernos, I., and Aloy, P. (2010). Uncovering new substrates for Aurora A kinase. EMBO Rep. *11*, 977–984.
11. Ohashi, S., Sakashita, G., Ban, R., Nagasawa, M., Matsuzaki, H., Murata, Y., Taniguchi, H., Shima, H., Furukawa, K., and Urano, T. (2006). Phospho-regulation of human protein kinase Aurora-A: analysis using anti-phospho-Thr288 monoclonal antibodies. Oncogene *25*, 7691–7702.
12. Gomez-Ferreria, M.A., Bashkurov, M., Helbig, A.O., Larsen, B., Pawson, T., Gingras, A.-C., and Pelletier, L. (2012). Novel NEDD1 phosphorylation sites regulate γ-tubulin binding and mitotic spindle assembly. J. Cell Sci. *125*, 3745–3751.
13. Huttlin, E.L., Jedrychowski, M.P., Elias, J.E., Goswami, T., Rad, R., Beausoleil, S.A., Villén, J., Haas, W., Sowa, M.E., and Gygi, S.P. (2010). A tissue-specific atlas of mouse protein phosphorylation and expression. Cell *143*, 1174–1189.
14. Lüders, J., Patel, U.K., and Stearns, T. (2006). GCP-WD is a gamma-tubulin targeting factor required for centrosomal and chromatin-mediated microtubule nucleation. Nat. Cell Biol. *8*, 137–147.
15. Haren, L., Remy, M.H., Bazin, I., Callebaut, I., Wright, M., and Merdes, A. (2006). NEDD1-dependent recruitment of the gamma-tubulin ring complex to the centrosome is necessary for centriole duplication and spindle assembly. J. Cell Biol. *172*, 505–515.
16. Zhang, X., Chen, Q., Feng, J., Hou, J., Yang, F., Liu, J., Jiang, Q., and Zhang, C. (2009). Sequential phosphorylation of Nedd1 by Cdk1 and Plk1 is required for targeting of the gammaTuRC to the centrosome. J. Cell Sci. *122*, 2240–2251.
17. Zhu, H., Coppinger, J.A., Jang, C.Y., Yates, J.R., 3rd, and Fang, G. (2008). FAM29A promotes microtubule amplification via recruitment of the NEDD1-gamma-tubulin complex to the mitotic spindle. J. Cell Biol. *183*, 835–848.
18. Johmura, Y., Soung, N.K., Park, J.E., Yu, L.R., Zhou, M., Bang, J.K., Kim, B.Y., Veenstra, T.D., Erikson, R.L., and Lee, K.S. (2011). Regulation of microtubule-based microtubule nucleation by mammalian polo-like kinase 1. Proc. Natl. Acad. Sci. USA *108*, 11446–11451.
19. Haren, L., Stearns, T., and Lüders, J. (2009). Plk1-dependent recruitment of gamma-tubulin complexes to mitotic centrosomes involves multiple PCM components. PLoS ONE *4*, e5976.
20. Manning, J.A., Shalini, S., Risk, J.M., Day, C.L., and Kumar, S. (2010). A direct interaction with NEDD1 regulates gamma-tubulin recruitment to the centrosome. PLoS ONE *5*, e9618.
21. Sdelci, S., Schütz, M., Pinyol, R., Bertran, M.T., Regué, L., Caelles, C., Vernos, I., and Roig, J. (2012). Nek9 phosphorylation of NEDD1/GCP-WD contributes to Plk1 control of γ-tubulin recruitment to the mitotic centrosome. Curr. Biol. *22*, 1516–1523.
22. Kufer, T.A., Silljé, H.H., Körner, R., Gruss, O.J., Meraldi, P., and Nigg, E.A. (2002). Human TPX2 is required for targeting Aurora-A kinase to the spindle. J. Cell Biol. *158*, 617–623.
23. Brunet, S., Sardon, T., Zimmerman, T., Wittmann, T., Pepperkok, R., Karsenti, E., and Vernos, I. (2004). Characterization of the TPX2 domains involved in microtubule nucleation and spindle assembly in Xenopus egg extracts. Mol. Biol. Cell *15*, 5318–5328.
24. Peset, I., Seiler, J., Sardon, T., Bejarano, L.A., Rybina, S., and Vernos, I. (2005). Function and regulation of Maskin, a TACC family protein, in microtubule growth during mitosis. J. Cell Biol. *170*, 1057–1066.
25. Gruss, O.J., Wittmann, M., Yokoyama, H., Pepperkok, R., Kufer, T., Silljé, H., Karsenti, E., Mattaj, I.W., and Vernos, I. (2002). Chromosome-induced microtubule assembly mediated by TPX2 is required for spindle formation in HeLa cells. Nat. Cell Biol. *4*, 871–879.
26. Garrett, S., Auer, K., Compton, D.A., and Kapoor, T.M. (2002). hTPX2 is required for normal spindle morphology and centrosome integrity during vertebrate cell division. Curr. Biol. *12*, 2055–2059.
27. Ma, N., Tulu, U.S., Ferenz, N.P., Fagerstrom, C., Wilde, A., and Wadsworth, P. (2010). Poleward transport of TPX2 in the mammalian mitotic spindle requires dynein, Eg5, and microtubule flux. Mol. Biol. Cell *21*, 979–988.

28. Gable, A., Qiu, M., Titus, J., Balchand, S., Ferenz, N.P., Ma, N., Collins, E.S., Fagerstrom, C., Ross, J.L., Yang, G., and Wadsworth, P. (2012). Dynamic reorganization of Eg5 in the mammalian spindle throughout mitosis requires dynein and TPX2. Mol. Biol. Cell *23*, 1254–1266.
29. Vanneste, D., Takagi, M., Imamoto, N., and Vernos, I. (2009). The role of Hklp2 in the stabilization and maintenance of spindle bipolarity. Curr. Biol. *19*, 1712–1717.

Current Biology, Volume *23*

Supplemental Information

The Role of NEDD1 Phosphorylation by Aurora A in Chromosomal Microtubule Nucleation and Spindle Function

Roser Pinyol, Jacopo Scrofani, and Isabelle Vernos

Supplemental Inventory

Supplemental Experimental Procedures

DNA Constructs and siRNAs

The cDNA of *Xenopus laevis* NEDD1 (xNEDD1, GI:148223468) was amplified by PCR from a *Xenopus laevis* cDNA library (*Xenopus laevis* embryo stage 26) using the primers 5'-CGGTCGACTTCAAAAATTGGCCC-3' and 5'-GCGAATTCATGCAGGATAACATCAGAC-3' and cloned into a TOPO vector. xNEDD1-CT (aa 371-655) and xNEDD1-NT (aa 1-370) were cloned into the TOPO vector and subcloned into pGEX-6P1. The cDNA of human NEDD1 (hNEDD1, GI:206597464) was obtained from RZPD - German Science Centre for Genome Research. Full-length hNEDD1 (1-660 aa) was cloned into pFLAG-CMV^{TM}-2 (Sigma-Aldrich) using the primers 5'-CCATAGATCTGATGCAGGAAAACCTC-3' and 5'-AAGTCGACTCAAAAGTGGGCCCGTAAT-3'. hNEDD1 CT (aa 372-660) was cloned into pGEX. In order to generate an RNAi-resistant NEDD1 clone several silent mutations (GG(G/T)CA (A/G) AA(G/A) CA(G/A) AC(A/G) TG(T/C) GTC AA(T/C) TTA; mutations underlined) were introduced by several rounds of PCRs. xNEDD1 and hNEDD1 Ser405 and Ser411 were mutated to alanine, aspartate or glutamate through site directed mutagenesis. All constructs were confirmed by sequencing.

siRNAs were synthesized by Dharmacon Inc. The Aurora A and NEDD1 siRNA were previously described [1, 2].

Expression and Purification of Recombinant Proteins

GST alone and GST-fusion proteins of NEDD1 were expressed in *E. coli* and purified by glutathione affinity chromatography using standard protocols. Recombinant His-GFP-xAurora A and His-hAurora A were previously described [3, 4]. Flag-tagged hNEDD1 was expressed and purified from HEK293 cells. Cells were transfected with X-tremeGENE 9 DNA Transfection Reagent (Roche) according to the manufacturer's instructions. 48h post-transfection, cells were lysed in Lysis Buffer: 50 mM Tris (pH 7.1), 100 mM NaCl, 1 mM DTT, 1 mM EDTA, 1 mM EGTA, 10 mM beta-glycerophosphate, 2 mM Na_3VO_4, 1% TX100, protease inhibitors (EDTA-free tablets; Roche). Lysates were centrifuged for 20 minutes and the supernatants incubated with anti-FLAG M2 Affinity Gel (Sigma-Aldrich) for 2h at 4°C. After several washes, the recovered proteins were eluted from the beads by competition with Flag peptide (Sigma-Aldrich) according to the manufacturer instructions, and dialyzed against PBS.

Antibodies

Polyclonal anti-xNEDD1 and anti-hAurora A antibodies were raised in rabbits by injection of recombinant GST-xNEDD1 CT or His-hAurora A respectively. Polyclonal anti-γ-tubulin antibodies were generated against the peptide AATRPDYISWGTQDKC conjugated to KHL. Polyclonal anti-Cep192 antibodies were generated against the following peptides: CGGNVSLDVLPVKGPQ, CASEEPWTVLPEHLIL and CFQDELLVTEVYDLPQ. All antibodies were affinity-purified. Monoclonal anti-Flag M2, anti-tubulin (DM1A) and anti-γ-tubulin (GTU-88) antibodies were from Sigma-Aldrich. Monoclonal anti-hNEDD1 was from Abnova. The 1C1 monoclonal anti-xAurora A antibodies were a gift from C. Prigent (CNRS, Rennes, France). Polyclonal anti-xAurora A and anti-GST antibodies were described previously [5]. Alexa Fluor anti-mouse and anti-rabbit secondary antibodies used for immunofluorescences and western blot were from Invitrogen.

Cell Culture, Immunofluorescence Microscopy, and Immunoprecipitations

HEK293T and Hela cells were maintained and transfected as described in [6]. To express RNAi-resistant Flag-NEDD1 constructs in NEDD1 depleted cells, 10^5 cells per cm^2 were plated and transfected after 24h with Flag-NEDD1 plasmids and after 48h with NEDD1 siRNAi. 72h after the first transfection, coverslips were washed with PBS containing 0.1% Triton. Cells were fixed in MeOH at -20^0C and processed for immunofluorescence with the antibodies indicated in each figure. Images were recorded digitally using a Leica DMI6000B microscope equipped with a Leica DFC 350FX camera and processed with Adobe Photoshop.

The stable HeLa cell line expressing GFP-centrin was a kind gift from A. Khodjakov. To facilitate visualization and comparisons with other figures, the colour code for immunofluorescence images performed in this cell line was modified in Photoshop to show Centrin in blue, Tubulin in red and Flag-NEDD1 in green.

Immunoprecipitation experiments from *Xenopus laevis* egg extract were performed as described in [5], except for immunoprecipitations using anti-xNEDD1 antibodies for which beads were finally washed with 0.1 % Tween-20 in PBS instead of Triton X-100.

For immunoprecipitations from HEK293T or Hela cells, cells were lysed in Lysis Buffer. Lysates were centrifuged for 20 minutes and the supernatants were incubated with antibody-coated resin for 2h at 4°C. After several washes, the immunoprecipitated proteins were eluted from the beads with SDS sample buffer and analyzed by western blot.

***Xenopus laevis* Egg Extract**

Cytostatic factor arrested extracts (CSF extracts) from *Xenopus laevis* eggs were prepared as previously described [5]. For NEDD1 immunodepletion, one volume of anti-xNEDD1 coated protein A dynabeads (Life Technologies) were incubated in 2.5 volumes of CSF extract. Two rounds of immunodepletion, of 30 min each, at 4°C were enough to completely deplete the endogenous protein from the CSF extract. Mock control depletions were performed in the same conditions using anti-rabbit IgG coated protein A dynabeads.

Pull-Downs and In Vitro Binding Assay

GST-fusion proteins were immobilized onto magnetic beads coated with anti-GST antibodies and incubated in CSF extract for 1h at 4°C. Beads were retrieved and washed twice with CSF-XB buffer and twice with PBS with 0.1 % Triton X-100. Samples were analyzed by SDS-PAGE and western blot.

For in vitro binding assays, immobilized GST-fusion proteins were incubated for 1h at 4°C with 250 µl of 0.2 µM of His-GFP-xAurora A in 5% BSA. Beads were washed with PBS containing 0.1% Triton X-100 and analyzed by western blot.

In Vitro Kinase Assay

5 µM of GST alone or GST-fragments of xNEDD1 or hNEDD1 and mutants thereof were incubated with 0.1 µM of purified His-xAurora A or His-hAurora A in kinase buffer (20 mM HEPES, 0.2 M KCl, 5 mM $MgCl_2$, 0.5 mM EGTA, 0.05 % Triton X-100, 0.1 mM ATP) in the presence of [γ-^{32}P]-ATP. The reactions were incubated at 30°C for 10 to 15 min and stopped by addition of SDS-PAGE loading buffer. Proteins were resolved by SDS-PAGE and visualized by CBB

staining. Autoradiographies were obtained by exposing the gel to an Imaging Plate (Fuji Film) that was later scanned with a Typhoon Trio Imager (Amersham Biosciences).

Mass Spectrometry Analysis

To identify phosphopeptides liquid chromatography-tandem mass spectrometry (LC-MS/MS) was performed. For that, purified NEDD1 proteins were resolved in SDS-PAGE, stained with Coomassie Blue, bands excised and samples reduced, alkylated, and digested in-gel with trypsin (Promega). For each sample, 20% was analyzed without enrichment while the reminder of the sample was subjected to a titanium dioxide (TiO) phosphopeptide-enrichment strategy. For LC-MS/MS analysis, peptides were either analyzed on a LTQ Orbitrap XL mass spectrometer (Thermo Fisher Scientific) or in a LTQ Orbitrap Velos Pro (Thermo Fisher Scientific). For each MS scan, the 10 to 20 most intense ions where selected for fragmentation in the LTQ linear ion trap. MS/MS fragmentation was performed using phosphopeptide-focused multistage activation. MS/MS data were queried against *Xenopus laevis* NCBI database or IPI_Human database using Mascot v2.3 (Matrix Science).

Microtubule Regrowth and Cold-Stable Assays

MT regrowth and cold-stable experiments were performed as previously described [6]. In short, MT were depolymerized by incubating cells in media containing 3µM of nocodazole for 3h and washed extensively. Cells were then incubated in pre-warmed medium for 5 to 45 min and fixed in MeOH for 10min at -20^{0}C. The assay was quantified with ImageJ, counting the number of microtubule asters per cell in 9 independent experiments (n ≥ 30 cells, each). For cold-stable assays, cells were washed twice with PBS and incubated on ice for 10, 20 and 30 min in L15 medium (Sigma) supplemented with 20 mM HEPES at pH 7.3. Cells were fixed in MeOH at -20^{0}C and processed for immunofluorescence to visualize MTs and DNA. To quantify the phenotypes, cells were classified into the different categories for each experimental condition (two independent experiments, n ≥ 30 cells, each).

RanGTP-Induced and DNA-Coated Beads-Induced Microtubule Nucleation

Recombinant RanQ69L-GTP was expressed and purified as described in [7]. RanGTP asters were induced by adding 15 µM of RanQ69L-GTP to CSF extracts containing 0.2 mg/ml of Rhodamine-labeled tubulin. Extracts were incubated at 20ºC and squashes of 2 ml were collected every 5min to monitor aster formation. Quantifications were made counting the total number of asters per field in 50 random fields (40X magnification). Data were normalized to obtain the number of aster per ml of extract.

DNA-coated beads were prepared as described [7]. To induce the DNA beads dependent spindle assembly reaction, CSF extracts containing 0.2 mg/ml of Rhodamine-labeled tubulin were incubated with DNA-coated beads and sent to interphase by adding 0.4 mM Ca^{2+} before incubation for 90 min at 20°C. The extract was then cycled back into mitosis by addition of one volume of CSF extract and spindle assembly was followed collecting squashes every 10 minutes. Quantifications were made at 30 minutes. Pictures of bead-clusters of similar dimensions were taken at 40X magnification. The total Rhodamine-labeled tubulin signal for each cluster was measured and normalized to the cluster size.

Supplemental References

1. Kufer, T.A., Sillje, H.H., Korner, R., Gruss, O.J., Meraldi, P., and Nigg, E.A. (2002). Human TPX2 is required for targeting Aurora-A kinase to the spindle. J Cell Biol *158*, 617-623.
2. Haren, L., Remy, M.H., Bazin, I., Callebaut, I., Wright, M., and Merdes, A. (2006). NEDD1-dependent recruitment of the gamma-tubulin ring complex to the centrosome is necessary for centriole duplication and spindle assembly. J Cell Biol *172*, 505-515.
3. Sardon, T., Pache, R.A., Stein, A., Molina, H., Vernos, I., and Aloy, P. (2010). Uncovering new substrates for Aurora A kinase. EMBO Rep *11*, 977-984.
4. Sardon, T., Peset, I., Petrova, B., and Vernos, I. (2008). Dissecting the role of Aurora A during spindle assembly. Embo J *27*, 2567-2579.
5. Peset, I., Seiler, J., Sardon, T., Bejarano, L.A., Rybina, S., and Vernos, I. (2005). Function and regulation of Maskin, a TACC family protein, in microtubule growth during mitosis. J Cell Biol *170*, 1057-1066.
6. Meunier, S., and Vernos, I. (2011). K-fibre minus ends are stabilized by a RanGTP-dependent mechanism essential for functional spindle assembly. Nature cell biology *13*, 1406-1414.
7. Brunet, S., Sardon, T., Zimmerman, T., Wittmann, T., Pepperkok, R., Karsenti, E., and Vernos, I. (2004). Characterization of the TPX2 domains involved in microtubule nucleation and spindle assembly in Xenopus egg extracts. Molecular biology of the cell *15*, 5318-5328.
8. Luders, J., Patel, U.K., and Stearns, T. (2006). GCP-WD is a gamma-tubulin targeting factor required for centrosomal and chromatin-mediated microtubule nucleation. Nature cell biology 8, 137-147.

Supplemental Figure Legends

Figure S1. Aurora A Binds Directly and Phosphorylates the C-Terminal Half of NEDD1 in Egg Extract and In Vitro

(A) Schematic representation of the NEDD1 fragments used in this work.

(B) Western blot analysis of an in vitro binding assay. GST- xNEDD1 CT (CT) or GST- xNEDD1 NT (NT) were immobilized on anti GST-antibodies coated beads and incubated with purified His-GFP-xAurora. The beads were retrieved, washed and resuspended in loading buffer. Aurora A was found strongly associated to GST-xNEDD1 CT but not to GST-xNEDD1 NT.

(C) The silencing of Aurora A does not alter the localization of NEDD1 to the centrosomes and spindle poles. Immunofluorescence images of control (left) and Aurora A (right) silenced Hela cells 24h after siRNA transfection. Aurora A is in red and DNA in blue. Scale bar, 5 µm.

(D) The silencing of NEDD1 does not alter the localization of Aurora A to the centrosomes and spindle poles. Immunofluorescence images of control (left) and NEDD1 (right) silenced Hela cells 48h after siRNA transfection. NEDD1 is in red and DNA in blue. Scale bar, 5 µm.

(E) Western Blot of cell lysates from control and Aurora A or NEDD1 silenced cells showing the efficiency of depletion of the corresponding proteins. Tubulin was used as a loading control.

(F) In vitro kinase assay with Xenopus proteins: His-xAurora A phosphorylates specifically the C-terminal domain of xNEDD1 (CT). Control GST and the N-terminal domain of xNEDD1 (NT) are not phosphorylated. The CBB stained gel and the corresponding autoradiography are shown. The asterisk indicates a degradation product of GST-xNEDD1 NT.

(G) In vitro kinase assay with human proteins: His-hAurora A phosphorylates specifically the C-terminal fragment of hNEDD1 (CT) and not GST. The CBB stained gel and the corresponding autoradiography are shown.

Figure S2. NEDD1 S405 Is Phosphorylated in CSF-Arrested *Xenopus* Egg Extracts and in Mitotic HeLa Cells

(A) Representative MS/MS spectra of the identified phosphorylated peptides for the human and *X. laevis* NEDD1. Flag-NEDD1 was expressed in HeLa cells and pulled down with anti-Flag coated beads from lysates of cells synchronized in mitosis. Endogenous NEDD1 was immunoprecipitated from CSF arrested Xenopus egg extracts.

(B) Peptide sequences, Mascot score and PhosphoRS [1] score of identified phosphosites. In case of ambiguous phosphorylation assignment all possible sites are shown.

Figure S3.

(A) Quantification of the tubulin and Flag fluorescence signal along the width of spindles assembled in NEDD1 silenced Hela cells expressing Flag-hNEDD1 WT (WT), Flag-hNEDD1 S405A (S405A) or Flag-hNEDD1 S411A (S411A) corresponding to the experiment shown in Figure 2A. The fluorescence signal intensity of tubulin (red lines) and the different Flag-tagged NEDD1 variants (green lines) were quantified along the lines across the half spindles (as indicated) using the “Plot Profile” function of ImageJ software. The fluorescence intensities were plotted as a function of the line length. Flag-NEDD1 wt and Flag-NEDD1 405A localize to the spindle MTs whereas Flag-NEDD1 411A does not, as previously described [8]. Scale bars, 5 µm.

(B) Quantification of the γ-tubulin and Flag fluorescence signal along the width of spindles assembled in NEDD1 silenced Hela cells expressing Flag-hNEDD1 WT (WT), Flag-hNEDD1 S405A (S405A) or Flag-hNEDD1 S411A (S411A) corresponding to the experiment shown in Figure 2B. The fluorescence signal intensity of γ-tubulin (blue lines) and the different flag-tagged NEDD1 variants (green lines) were quantified along the lines across the half spindles (as indicated) using the "Plot Profile" function of ImageJ. The fluorescence intensities were plotted as a function of the line length. Flag-NEDD1 wt and Flag-NEDD1 405A localize to the spindle MTs similarly to γ-tubulin. In silenced cells expressing Flag-NEDD1 411A, neither γ-tubulin nor the recombinant NEDD1 variant localize to spindle MTs. Scale bars, 5 µm.

(C) Representative images of the categories used for the quantification of K-fiber stability shown in Figure 2E. The images correspond to NEDD1 silenced Hela cells expressing Flag-hNEDD1 WT incubated in the cold. MTs are shown in red, anti-Flag is shown in green and the DNA in blue. Scale bar, 5 µm.

Figure S4.

(A) NEDD1 and Aurora A colocalize at sites of MT nucleation. Immunofluorescence images of mitotic HeLa cells treated with nocodazole for 3h and fixed 5 min after nocodazole washout. The upper panel shows that Aurora A (green) localizes to all the MT asters (red). The medium panel shows that NEDD1 (red) localizes to both chromosomal and centrosomal asters. Centrosomes (arrows) were visualized with antibodies against the centrosomal marker Cep192 (green). The lower panel shows that Aurora A (red) colocalizes with NEDD1 (green). DNA was stained with Hoechst (blue). Scale bar, 5 µm.

(B) NEDD1 phosphorylation at Ser405 is essential for chromosome alignment. Representative images of NEDD1 silenced Hela cells incubated in nocodazole and fixed 45 min after nocodazole washout. Cells expressing Flag-hNEDD1 S405A showed a strong chromosome misalignment phenotype. MTs are shown in red, the Flag-hNEDD1 proteins (as detected with anti-Flag antibodies) in green and DNA in blue. Scale bar 5 µm.

(C) Quantification of the percentage of cells with a bipolar spindle and fully aligned chromosomes in the different experimental conditions shown in (B). The graph shows the averages from 3 independent experiments. The bars correspond to the standard error of the mean.

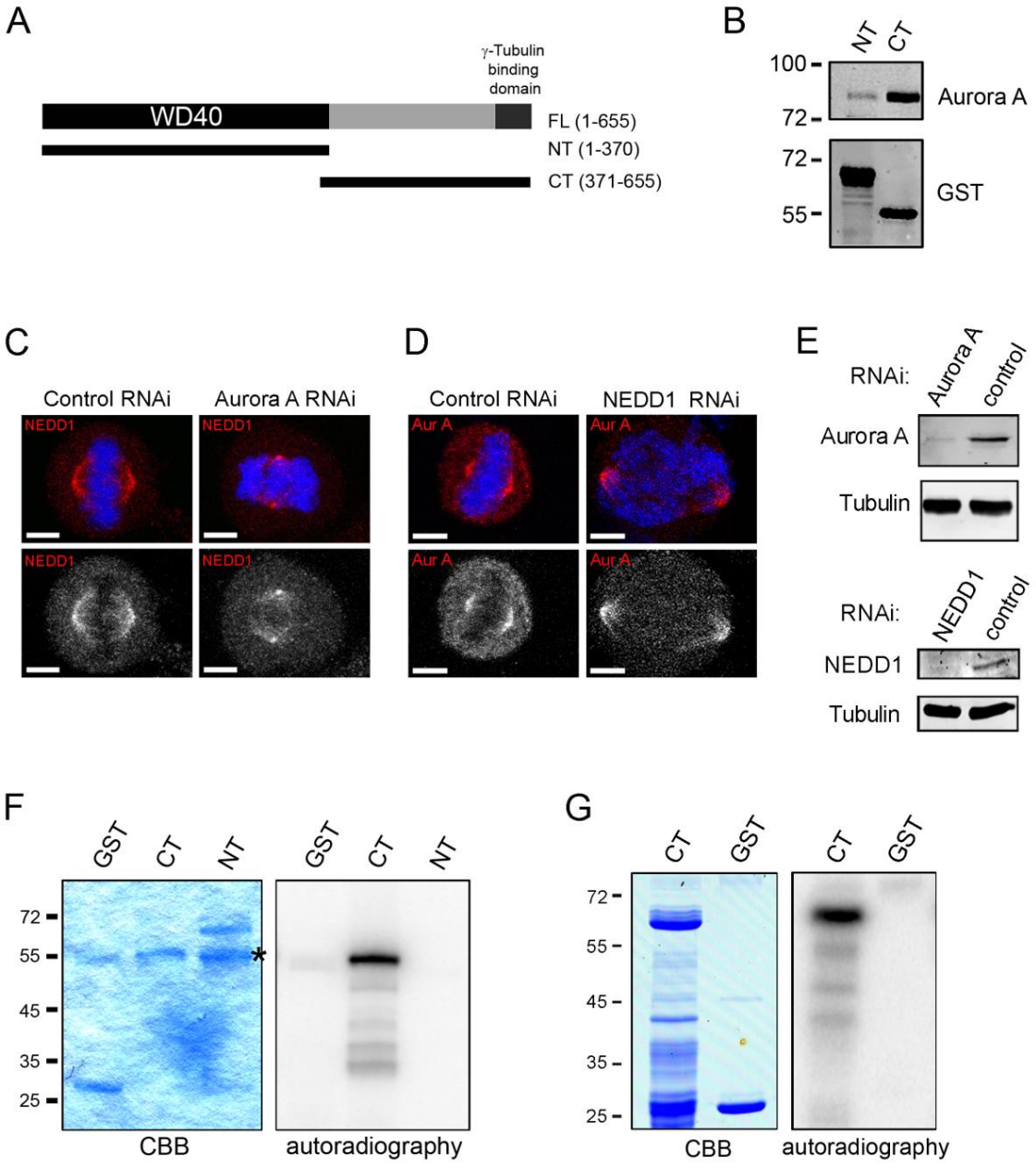
A
γ-Tubulin binding domain
WD40
FL (1-655)
NT (1-370)
CT (371-655)
B
NT
CT
100
72
Aurora A
72
55
GST
C
Control RNAi
Aurora A RNAi
NEDD1
D
Control RNAi
NEDD1 RNAi
Aur A
E
RNAi:
Aurora A
control
Aurora A
Tubulin
RNAi:
NEDD1
control
NEDD1
Tubulin
F
GST
CT
NT
72
55
45
35
25
CBB
autoradiography
G
CT
GST
72
55
45
35
25
CBB
autoradiography

Figure S1

A

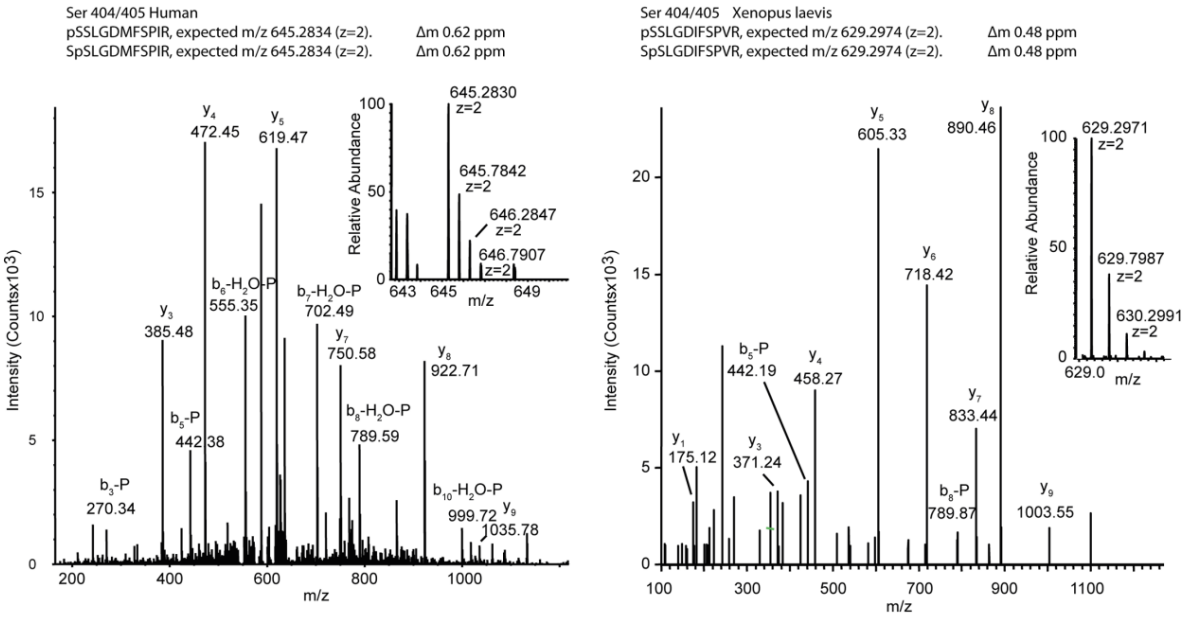

B

Modified residue	Sequence	MASCOT Score	pRS Score
Ser 404/405 Human	pSSLGDMFSPIR SpSLGDMFSPIR	30	59
Ser 404/405 Xenopus	pSSLGDIFSPVR SpSLGDIFSPVR	51	59

Figure S2

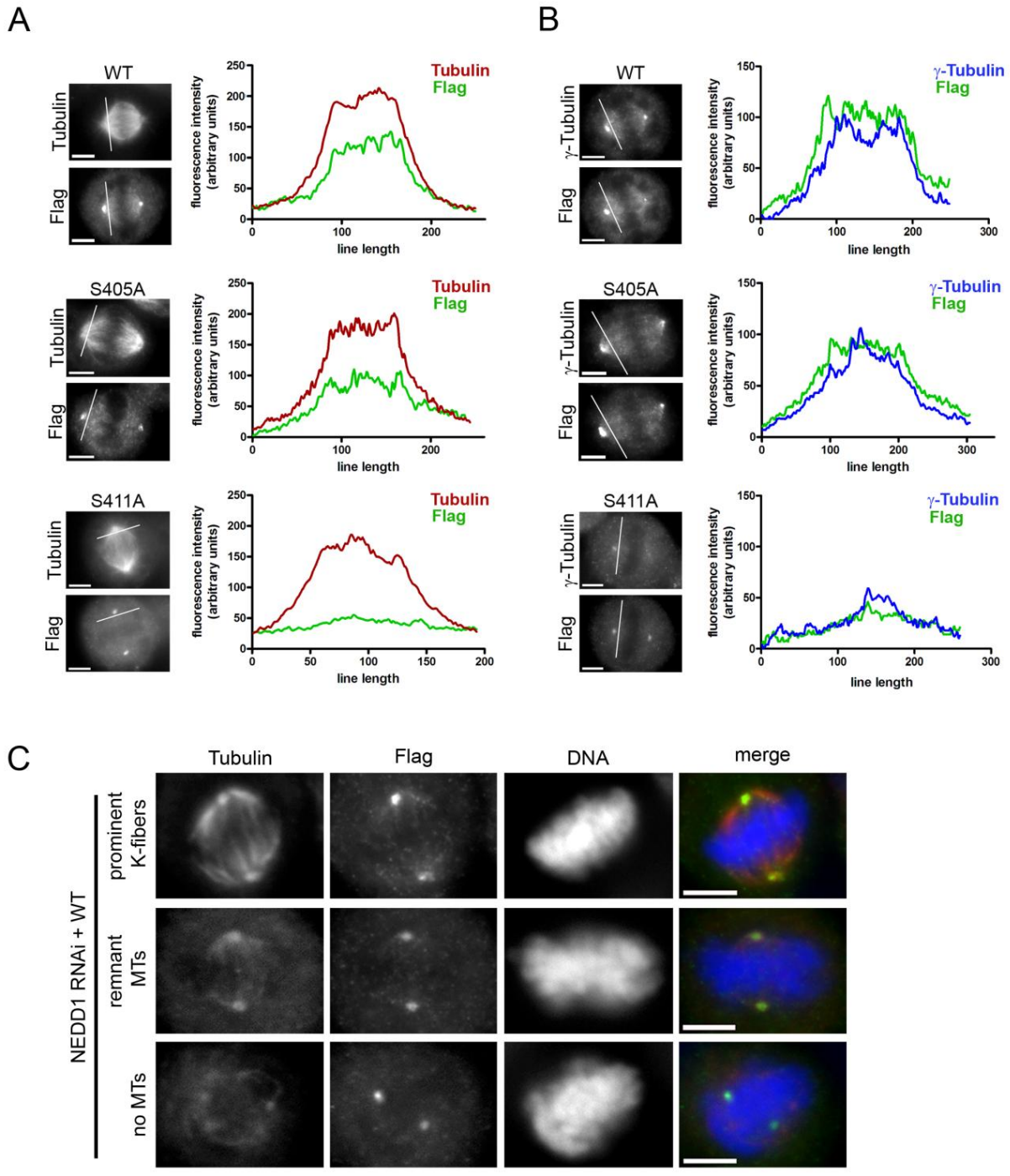
A
WT
Tubulin
Flag
fluorescence intensity (arbitrary units)
line length
Tubulin
Flag
S405A
S411A
B
γ-Tubulin
C
Tubulin
Flag
DNA
merge
NEDD1 RNAi + WT
prominent K-fibers
remnant MTs
no MTs

Figure S3

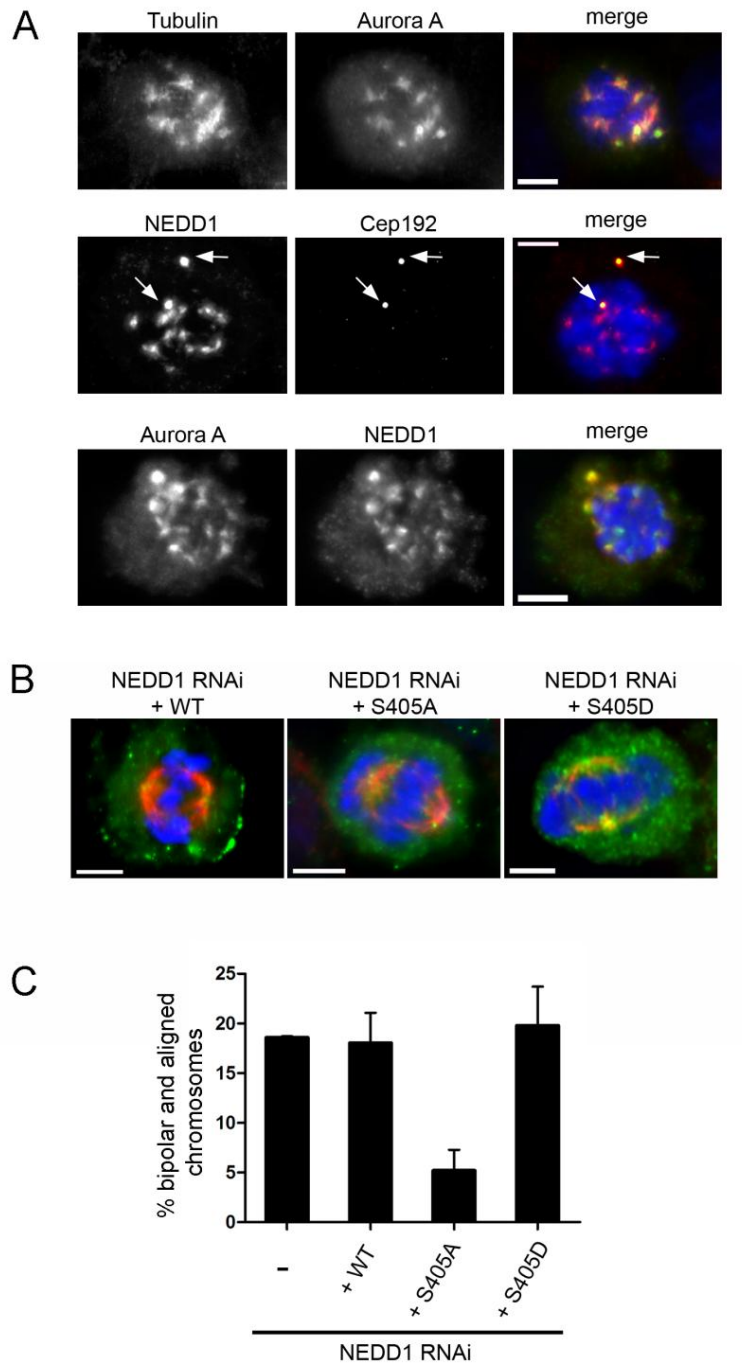
A
Tubulin
Aurora A
merge
NEDD1
Cep192
merge
Aurora A
NEDD1
merge
B
NEDD1 RNAi
+ WT
NEDD1 RNAi
+ S405A
NEDD1 RNAi
+ S405D
C
% bipolar and aligned chromosomes
25
20
15
10
5
0
-
+ WT
+ S405A
+ S405D
NEDD1 RNAi

Figure S4

2.2. Microtubule nucleation in mitosis by a RanGTP-dependent protein complex

The essential role of Aurora-A phosphorylation on NEDD1 S405 for RanGTP dependent MT nucleation opens new interesting questions on how the different MT assembly pathways spatially and temporally regulate MT nucleation. It particularly suggests that a chromosome specific mechanism could act through Aurora-A on the MT nucleation machinery. We therefore decided to further investigate this hypothesis.

The following manuscript ("Microtubule nucleation in mitosis by a RanGTP-dependent protein complex" Submitted, under revision) directly follows the first one focusing on the mechanism driving RanGTP dependent MT nucleation. Here we showed how the RanGTP pathway, through its effector TPX2, regulates the MT nucleation activity of the γTuRC. Particularly we described how TPX2 provides all the essential requirements to trigger MT nucleation by γTuRC activation. My personal contribution to this story covers the entire experimental work except the TPX2-TPX2 interaction described by Teresa Sardon, former member of our lab. The manuscript has unpublished supplementary figures and associated paragraphs that expand specific aspects of the story.

(Scrofani J, Sardon T, Meunier S and Vernos I. Microtubule nucleation in mitosis by a RanGTP-dependent complex. Submitted Manuscript)

Microtubule nucleation in mitosis by a RanGTP-dependent protein complex

Jacopo Scrofani, Teresa Sardon, Sylvain Meunier* and Isabelle Vernos[1*]

Cell and Developmental Biology program, Centre for Genomic Regulation (CRG) and UPF, Dr. Aiguader 88, 08003 Barcelona, Spain

[1] Institució Catalana de Recerca i Estudis Avançats (ICREA), Pg. Lluis Companys 23, 08010 Barcelona, Spain

*correspondence:

Isabelle Vernos: e-mail: Isabelle.Vernos@crg.eu, phone: +34 93 316 02 77, fax: +34 93 316 00 99 (communication with Editorial and Production offices)

Sylvain Meunier: email: Sylvain.Meunier@crg.eu, phone: +34 93 316 02 75, fax: +34 93 316 00 99

Running title: Chromosomal microtubule nucleation

Characters: 19.899

Abstract

The γTuRC (γ-tubulin Ring Complex) is a multi-subunit complex responsible for microtubule nucleation in eukaryotic cells. During mitosis, its spatial and temporal regulation underlies the activation of different microtubule assembly pathways that all participate in spindle formation. Understanding this regulation is therefore key to understand cell division. Although it is currently accepted that the RanGTP-dependent MT assembly pathway is essential for functional spindle assembly, how chromosomes and RanGTP regulate MT nucleation is not clear. Here, we show that RanGTP induces the formation of a complex between a pool of γTuRC associated with RHAMM and two major spindle assembly factors TPX2 and Aurora-A. Within this complex, TPX2 is responsible for γTuRC recruitment and through Aurora-A activation promoting the phosphorylation of the γTuRC-adaptor NEDD1. We show that these two events are necessary and sufficient to explain γTuRC activation by the RanGTP pathway and thereby MT nucleation in the vicinity of the chromosomes.

Introduction

During mitosis, different microtubule (MT) nucleation pathways drive the assembly of dynamic MTs to organize a bipolar spindle. One of them relies on a gradient of GTP-bound Ran centered on the chromosomes, that promotes the dissociation of nuclear localization signal (NLS)-containing proteins from karyopherins, thereby driving MT nucleation, stabilization and organization around the chromosomes (Clarke and Zhang, 2008). Chromosomal MTs are essential for building a functional bipolar spindle (Meunier and Vernos, 2011), therefore understanding how these MTs are nucleated is essential to fully understand cell division.

MT nucleation relies on the γ-TuRC (γ-tubulin ring complex) a multi-subunit complex constituted by multiple copies of γ-tubulin and associated proteins (Kollman et al., 2011; Zheng et al., 1995). The γ-TuRC is required for all the known pathways of MT nucleation in animal mitosis (Moudjou et al., 1996; Teixido-Travesa et al., 2012) and its regulation involves the adaptor protein NEDD1 (Gunawardane et al., 2003; Luders et al., 2006; Sdelci et al., 2012; Zhu et al., 2008). Chromosomal MT assembly requires NEDD1 phosphorylation by Aurora A (Pinyol et al., 2013), and TPX2 (Wittmann et al., 2000), a RanGTP regulated protein with multiple functions during spindle assembly (Gruss and Vernos, 2004; Neumayer et al., 2014) and a main Aurora A activator in mitosis (Bayliss et al., 2003; Sardon et al., 2008). However, the mechanism by which RanGTP spatially and temporally regulates γ-TuRC MT nucleation is still fragmentary (Gruss et al., 2001; Gruss et al., 2002; Tulu et al., 2006).

Here, taking advantage of the *Xenopus laevis* egg extract system, we have determined the essential requirements for RanGTP/chromosome-dependent MT nucleation in M-phase.

Results and discussion

RanGTP activates MT nucleation by NEDD1-γTuRC

To investigate the mechanism by which RanGTP drives MT nucleation in M-phase, we used *Xenopus laevis* egg extracts in which the whole pathway can be triggered by addition of a GTP hydrolysis deficient form of Ran (RanQ69L) bound to GTP (RanGTP) (Bischoff et al., 1994; Ohba et al., 1996). Previous data showed that the γTuRC adaptor protein NEDD1 is essential for RanGTP-dependent MT nucleation (Luders et al., 2006; Pinyol et al., 2013). To determine whether the association of NEDD1 with the γTuRC is regulated by RanGTP, we immunoprecipitated NEDD1 from extracts in the presence or absence of RanGTP. In both conditions, NEDD1 co-immunoprecipitated the components of the γTuRC XGrip109 (GCP3), γ-tubulin and XGrip195 (GCP6) (Fig. 1A). These results suggest that in extracts, NEDD1 associates with intact γTuRCs in a RanGTP-independent manner. We then addressed the functionality of this complex. Surprisingly, the NEDD1 beads only generated MT asters in extracts containing RanGTP (Fig. 1B, C). To determine whether RanGTP was acting at the level of MT nucleation or stabilization, the NEDD1-γTuRC beads were retrieved from the egg extract and incubated in pure tubulin (Fig. 1B). As in the previous experiment, beads pre-incubated in RanGTP-containing egg extract promoted MT assembly but not those incubated in control extract (Fig. 1D). Altogether these results indicate that the M-phase egg cytoplasm contains inactive or poorly active NEDD1-γTuRC complexes that become activated through a RanGTP dependent mechanism.

RHAMM has a conserved function in RanGTP dependent MT nucleation in M-phase

In addition to NEDD1 and γ-tubulin, two proteins, TPX2 and XRHAMM, have been reported as essential for RanGTP-induced MT assembly (Groen et al., 2004; Gruss et al., 2001;

Wittmann et al., 2000). TPX2 has been extensively characterized and since it does not stabilize MTs, it has been proposed to play a role in MT nucleation (Gruss et al., 2002; Tulu et al., 2006). However, the role of RHAMM in the chromosomal pathway is less clear and was only examined in egg extracts (Groen et al., 2004). To determine whether RHAMM has a conserved role in the pathway, we examined its function in Hela cells. Immunofluorescence analysis showed that RHAMM localized to the spindle (Maxwell et al., 2003) and to both chromosomal and centrosomal MT asters in MT regrowth experiments (Fig. S1A). To determine whether RHAMM is required for chromosomal MT assembly, we performed MT regrowth assays in control and RHAMM silenced cells (Fig.2A, Fig. S1B). RHAMM silencing dramatically reduced the number of asters formed in the mitotic cells, mimicking the TPX2 silencing phenotype (Tulu et al., 2006). To discriminate between MT nucleation and stabilization, we tested whether MCAK silencing could rescue the RHAMM silencing phenotype during regrowth, as it does in cells silenced for the MT stabilization factor MCRS1 (Meunier and Vernos, 2011). Indeed, MCAK silencing did not rescue MT aster formation in cells silenced for RHAMM. Since this lack of rescue was also observed for cells silenced for the MT nucleation factors TPX2 and NEDD1 (Fig.2B, Fig. S1C), this strongly suggested that RHAMM has also an essential conserved role in chromosomal MT nucleation. We therefore investigated further its role using the Xenopus egg extract system.

As previously shown, the γTuRC components XGrip109 and γ-tubulin co-immunoprecipitated with XRHAMM in egg extract (Fig. 2C) (Groen et al., 2004). In addition, NEDD1 and XGrip195 were also present in the IP suggesting that XRHAMM interacts with full γTuRCs (Fig.2C). Interestingly, these interactions are not regulated by RanGTP (Fig. 2C), suggesting that the mitotic Xenopus egg extract contains a stable XRHAMM-NEDD1-γTuRC complex.

To determine whether this complex is the general MT nucleation complex in egg extracts, we monitored MT nucleation by the sperm-associated immature centrosome upon incubation in

control or depleted egg extracts (Fig. 2D and S1D) (Felix et al., 1994). As expected, NEDD1 depletion prevented MT nucleation at the centrosome. In contrast depletion of XRHAMM or TPX2 had no consequences on centrosomal MT nucleation (Fig. 2D), indicating that both proteins are specifically required for the RanGTP pathway.

Altogether, our data show that XRHAMM forms a complex with NEDD1-γTuRC not directly regulated by RanGTP but specifically required for chromosomal MT nucleation.

RanGTP promotes the interaction between TPX2 and the RHAMM-NEDD1-γTuRC complex

XRHAMM was shown to co-immunoprecipitate with TPX2 in a RanGTP-independent manner (Groen et al., 2004). Immunoprecipitations with anti-XRHAMM or anti-TPX2 antibodies in egg extracts showed that their interaction is in fact strictly RanGTP-dependent (Fig. 3A). TPX2 also co-immunoprecipitated with NEDD1 and γ-tubulin in a RanGTP-dependent manner (Fig.3B). Since XRHAMM interacts with the γTuRC (Fig. 2C) (Groen et al., 2004), we then tested whether it is required for TPX2 - γTuRC interaction. Indeed, TPX2 did not co-immunoprecipitate with NEDD1 in XRHAMM-depleted extracts (Fig. 3C). Therefore, RanGTP induces a specific interaction between TPX2 and the XRHAMM-NEDD1-γTuRC complex.

To test whether the TPX2-XRHAMM-NEDD1-γTuRC complex is essential for RanGTP induced MT nucleation, anti-NEDD1-coated beads were incubated in control or XRHAMM-depleted extracts with or without RanGTP. The beads were retrieved, washed and their MT nucleation activity tested in pure tubulin (Fig. 3D). Although the NEDD1-beads carried γ-tubulin in all conditions (Fig3C), in contrast to the control, those retrieved from XRHAMM-depleted extracts were unable to trigger MT assembly in pure tubulin (Fig. 3D).

We conclude that the RanGTP pathway promotes an interaction between the RHAMM-NEDD1-γTuRC complex and TPX2 thereby triggering MT nucleation. However, the specific function of TPX2 in this complex is unclear.

NEDD1 phosphorylation on S405 is essential but not sufficient for RanGTP-dependent MT nucleation

We recently reported that the phosphorylation of NEDD1 on S405 by Aurora A is essential for RanGTP-dependent MT nucleation (Pinyol et al., 2013). RanGTP promotes TPX2 interaction with Aurora A leading to the activation of the kinase (Bayliss et al., 2003; Sardon et al., 2008). Consistently, we found that NEDD1 interaction with Aurora-A was strongly enhanced by RanGTP (Fig. 4A). Therefore, by promoting the interaction of TPX2 with the γTuRC, RanGTP may indirectly favor the phosphorylation of NEDD1 on S405 by Aurora A.

To determine whether this is the essential mechanism underlying RanGTP dependent MT nucleation, we used a recombinant TPX2 mutated in its NLS (TPX2-ΔNLS) (Fig. 4B) that promotes MT nucleation and activates Aurora A in the absence of RanGTP (Brunet et al., 2004; Schatz et al., 2003). Egg extracts were depleted of TPX2 and NEDD1. TPX2-ΔNLS was then added back in combination with either NEDD1 wild type (WT), NEDD1-S405A or NEDD1-S405D (Fig. S1D, E) (Pinyol et al., 2013). MT aster formation was then monitored in the absence of RanGTP. As previously described, TPX2-ΔNLS did promote MT aster formation (Schatz et al., 2003). However this was strictly dependent on NEDD1 (Fig.4C). This strongly indicated that TPX2 is the only RanGTP-regulated factor required for the pathway but that it cannot induce MT nucleation directly as it does in vitro (Schatz et al., 2003). Moreover and in agreement with our previous data (Pinyol et al., 2013), NEDD1-S405A did not support MT aster formation at all. These result suggest that the main mechanism by which TPX2 triggers MT nucleation is by promoting NEDD1 phosphorylation

by Aurora A. To test this idea, we monitored MT aster formation in TPX2 and NEDD1-depleted egg extract upon addition of TPX2ΔNLS that lacks the first 39 amino acids (Δ39TPX2ΔNLS) (Fig. 4B, S1E) and is therefore unable to activate Aurora A (Bayliss et al., 2003). Consistently, Δ39TPX2ΔNLS was unable to trigger MT nucleation except in the presence of the phospho-mimicking NEDD1-S405D (Fig. 4D).

Altogether our data strongly suggest that RanGTP dependent MT nucleation involves TPX2-dependent Aurora A activation and thereby NEDD1 phosphorylation on S405. Moreover, this critical phosphorylation is specific for the RanGTP pathway, as it does not interfere with MT nucleation at the centrosome (Fig. S2A). Finally, our data show that TPX2 is the only RanGTP target needed for RanGTP-dependent MT nucleation.

To determine whether TPX2 may have additional roles in the pathway, we then tested whether TPX2 requirement could be bypassed by activating Aurora A or by the phospho-mimicking NEDD1-S405D. Addition of the first 39 amino-acids of TPX2 (TPX2-N39) that are sufficient to fully activate Aurora A (Sardon et al., 2008) to a TPX2-depleted extract did not rescue MT aster formation (Fig. 4E). Consistently, neither did NEDD1-S405D when added to a NEDD1-depleted extract in the absence of RanGTP (Fig. 4F).

Altogether, these results suggest that NEDD1 phosphorylation on S405 by Aurora A is essential but not sufficient for RanGTP MT nucleation. TPX2 has additional functions that go beyond Aurora A activation.

TPX2 provides an essential function for the recruitment of the MT nucleation complex

Pull-down experiments in egg extract using GFP-TPX2 full length (GFP TPX2 FL) or its C-terminal part (GFP TPX2 CT) showed that RanGTP promotes TPX2-TPX2 interactions (Fig. 5A). This suggested that TPX2 could generate a scaffold controlled by RanGTP to efficiently recruit the nucleation complex. We reasoned that the absence of this putative scaffolding

activity could explain why NEDD1-S405D does not drive MT nucleation in egg extract in absence of RanGTP (Fig. 4F). To explore this idea we decided to test whether the putative TPX2 scaffolding activity could be substituted by beads. Magnetic beads were coated with recombinant NEDD1 phospho-variants and incubated in egg extract with or without RanGTP. The beads were retrieved from the extract and their MT nucleation capacity tested in pure tubulin. NEDD1-WT beads nucleated MTs only when retrieved from an extract containing RanGTP (Fig. 1D and 5B) whereas NEDD1-S405A beads did not promote MT nucleation in any condition (Fig. 5B). Strikingly, the NEDD1-S405D beads did trigger MT nucleation in a RanGTP-independent manner (Fig. 5B). Western blot analysis showed that the NEDD1-S405D beads associated with γTuRC components but not with TPX2 and Aurora A in absence of RanGTP (Fig. S2B). Therefore these results suggest that NEDD1 phosphorylation on S405 alone is sufficient to trigger MT nucleation in absence of RanGTP as long as the nucleation complex is recruited onto a scaffolding element (here provided by beads). In further support of this idea, NEDD1 beads retrieved from a TPX2-depleted extract containing the Aurora A activating protein TPX2-N39 triggered MT nucleation in pure tubulin independently of RanGTP (Fig. 5C).

Altogether these data show that TPX2 provides a scaffolding activity for the recruitment of the RHAMM-NEDD1S405D-γTuRC that is essential for RanGTP induced MT nucleation (Fig. 5D).

Conclusion

Here, we have shown that RanGTP induces the activation of a specific pool of γTuRC associated with RHAMM, dramatically increasing its MT nucleation activity. RanGTP, by releasing TPX2 from its binding to importins, promotes its association with the RHAMM-NEDD1-γTuRC complex. In this complex, TPX2 provides two essential requirements for

RanGTP-dependent MT nucleation: the activation of Aurora A promoting the phosphorylation of NEDD1 on S405, and a scaffolding activity for the recruitment of the MT nucleation complex. Our data show that the RanGTP MT nucleation pathway functions through a unique direct target, TPX2 and a unique Aurora A substrate, NEDD1. TPX2 is therefore the central player of the RanGTP-dependent γTuRC activation mechanism leading to the nucleation of MTs around the chromosomes in mitosis.

Materials and methods

DNA constructs, expression and purification of recombinant proteins

All hNEDD1 constructs and protein expression and purification methods were previously described (Pinyol et al., 2013). The constructs for TPX2ΔNLS, Δ39TPX2ΔNLS, GST-N39 TPX2 and TPX2-CT and the methods for protein expression and purification were previously described (Bayliss et al., 2003; Brunet et al., 2004).

Cell culture and siRNA

HeLa cell lines were maintained and transfected as described previously (Meunier and Vernos, 2011). The stable HeLa cell line expressing GFP–centrin-1 was a gift from Alexey Khodjakov (Wadsworth Center, Albany, NY). The silencing of MCAK, MCRS1, TPX2, RHAMM and NEDD1 was performed as described previously (Gruss et al., 2002; Maxwell et al., 2005; Meunier and Vernos, 2011; Pinyol et al., 2013). In short, cells were transfected with Lipofectamine 2000 (Invitrogen) using 100 pmol of siRNAs per well in six-well plates according to the manufacturer's protocol and analyzed 48 h after transfection. The control (scrambled) siRNA was: 5'-CGUACGCGGAAUACUUCGAUU-3'. All siRNA were from Dharmacon Inc.

MT regrowth was performed as previously described (Meunier and Vernos, 2011). In brief, MTs were depolymerized by incubating cells in media containing 3μM of nocodazole for 3h and washed extensively. Cells were then incubated in pre-warmed medium from 2 to 40 min, fixed in MeOH for 10 min at -20 ºC and processed for immunofluorescence.

Antibodies

The rabbit polyclonal antibodies against *Xenopus* TPX2 and *Xenopus* NEDD1 were

previously described (Sdelci et al., 2012; Wittmann et al., 2000), and the mouse monoclonal antibody anti *Xenopus* TPX2 was produced by Abyntek Biopharma.

The following commercial antibodies were used : a monoclonal mouse antibody against γ-tubulin (GTU-88) (Sigma-Aldrich), a monoclonal anti-human NEDD1 (that cross-reacts with *Xenopus* NEDD1) (Abcam) ; a mouse monoclonal anti tubulin (12G10) (Developmental Studyes Hybridoma Bank (Thazhath et al., 2002) ; the monoclonal mouse antibody against tubulin (DM1A) (Sigma-Aldrich).

The rabbit polyclonal antibody against *Xenopus* RHAMM was raised against a GST-RHAMM-CT (corresponding to the last 137 amino acids) and affinity purified. The rabbit polyclonal antibody against human RHAMM was made against a mixture of three peptides (1. CAPSPGAYDVKTLEVL ; 2. CKVLGIKHFDPSKAFH ; 3. CYDSMVQSLEDVTAQF) and affinity purified. Anti-GFP polyclonal antibodies were affinity purified from rabbit sera.

The mouse 1C1 monoclonal antibody against *Xenopus* Eg2 (Aurora-A) was a kind gift from C. Prigent (CNRS Université de Rennes, Rennes, France). Polyclonal antibodies against XGrip195 and XGrip109 were kind gifts from Yixian Zheng (Carnegie Institution for Science, Baltimore, USA).

Secondary antibodies were anti-rabbit or anti-mouse conjugated to Alexa-488, 568 or 680 (Life Technologies) and were used at 1:1000 for IF and 1:10000 for western blot.

Immunofluorescence and microscopy

Cells grown on coverslips were fixed in −20 °C methanol for 10 min. The blocking and antibody dilution buffer was PBS with 0.5% BSA (Sigma), 0.1% Triton-X100 (Sigma). Coverslips were mounted in Mowiol (Calbiochem).

Fixed cells were visualized with a ×63 objective on an inverted DMI-6000 Leica wide-field fluorescent microscope equipped with a Leica DFC 350FX camera. Confocal images were

acquired on a Leica TCS SP5 confocal microscope with a ×63 oil-immersion 1.4 numerical aperture objective lens. All pictures were acquired with the Leica Application Suite software. Images were processed with ImageJ or Photoshop (Adobe) and mounted using Photoshop (Adobe).

Xenopus laevis egg extract

Cytostatic factor arrested egg extracts from *Xenopus laevis* were prepared as previously described (Peset et al., 2005). Recombinant RanQ69LGTP was expressed and purified as previously described (Brunet et al., 2004).

RanGTP asters were induced by adding 15 µM of RanQ69L-GTP to egg extract containing 0.2 mg/ml of rhodamine-labelled tubulin. Extracts were incubated at 20ºC and squashes of 3 µl were collected at the indicated time points. Quantifications were made counting the total number of MT asters in 10 random lines for each cover slip (40X magnification with Leica DMI6000B microscope equipped with a Leica DFC 350FX camera). Data were normalized to obtain the number of aster per µl of extract.

Centrosome MT assembly was studied adding demembranated Xenopus sperm nuclei at a concentration of ≈500 nuclei/µl to egg extracts containing 0.2 mg/ml of rhodamine-labelled tubulin. Extracts were incubated at 20ºC and squashes of 3 µl were collected after 6, 8 and 10 minutes of incubation. MT nucleation from sperm centrosomes was evaluated counting 100 nuclei for each condition.

Immunodepletions and immunoprecipitations

For NEDD1, TPX2 and XRHAMM immunodepletions, one volume of antibody-coated protein A dynabeads (Life Technologies) was incubated in 2,5 volumes of egg extract. Dynabeads were prepared following manufacturer's recommendations. Two rounds of

immunodepletion of 30 min each at 4°C completely depleted the endogenous proteins from the egg extract. Mock control depletions were performed in the same conditions using unspecific anti-rabbit IgG coated protein-A dynabeads. After immunodepletions, RanGTP or buffer was added to the extract for 15min at 20˚C). Add-backs of NEDD1, NEDD1 phospho variants. TPX2-ΔNLS and Δ39TPX2ΔNLS were performed as previously described (Pinyol et al., 2013 ; Brunet et al., 2004 ; Bayliss et al., 2003). TPX2-N39 was added to the egg extract as previously described (Sardon et al., 2008).

For immunoprecipitations 1 volume of protein-A dynabeads (Life Technologies) was coated with the indicated antibodies (6 µg for 20 µl of beads) and incubated for 1h on ice in 2,5 volumes of CSF-arrested extract. To detect NEDD1-XRHAMM, NEDD1-TPX2 and XRHAMM-TPX2 interactions beads were washed without detergent (four times in TBS). For all the others IPs, beads were washed in TBS 0,1% Triton-X100. Proteins were eluted from beads directly in SDS-PAGE loading buffer 2X. All the immunoprecipitations were performed in egg extract previously incubated for 15 min at 20˚C with RanGTP or CSF-XB buffer (10 mM Hepes [pH 7,7], 50 mM sucrose, 100 mM KCl, 0,1 mM CaCl2, and 5mM EGTA).

Bead experiments

To assay the γ-TuRC MT nucleation activity, beads coated with anti-NEDD1 antibodies were incubated in egg extract. For analyzing the MT nucleation activity of NEDD1 phospho-variants, NEDD1-depleted egg extract were complemented with the corresponding recombinant proteins for 20min at 20C. The NEDD1 variants and associated proteins were then recovered with anti-NEDD1 antibody coated beads..

To evaluate MT nucleation in egg extract, beads were washed 4 times in CSF-XB buffer (10 mM Hepes [pH 7,7], 50 mM sucrose, 100 mM KCl, 0,1 mM CaCl2, and 5mM EGTA) and

then resuspended in the same initial volume of beads. Beads were then diluted 200-400 times in 20 µl CSF-arrested extract and incubated at 20ºC for 20-30 min, depending on the extract.

To study MT nucleation *in vitro*, beads were washed twice in CSF-XB, twice in BRB80 (80 mM PIPES (pH 6.8), 1 mM EGTA, 1 mM MgCl2) and resuspended in the same initial volume in BRB80. 1-2 µl of beads was then added to a 30µM pure tubulin solution and incubated for 10 minutes at 37ºC.

For both approaches the reaction mixture was fixed in 1% glutaraldehyde (in BRB80), spun down through a 10% glycerol in BRB80 cushion onto a coverslip and fixed in methanol for 10' at -20ºC. MTs were then visualized by immunofluorescence using anti-tubulin antibody. The quantifications were performed by evaluating the proportion of beads associated with MTs in 30 random fields for each condition.

Supplementary material.

Figure S1.

A- Confocal images showing RHAMM localization in HeLa cells. The upper panel sho
cell in metaphase, the lower panel shows a mitotic cell during MT regrowth RHAMM is shown in red, DNA in blue, and tubulin in green. Scale bars 10 µm.

B- Western blot analysis of control and RHAMM-silenced (RHAMMi) HeLa cells after 48 hours of transfection. Tubulin was used as a loading control.

C- Western blot analysis of control and RHAMM and MCAK (RHAMMi + MCAKi) double silenced HeLa cells at 48 hours after transfection. Tubulin was used as a loading control.

D- Western blot analysis of control (mock), XRHAMM, TPX2 and NEDD1 depleted egg extract. Aurora-A is shown as loading control.

E- Western blot analysis showing TPX2 depletion and the add-backs of TPX2ΔNLS and Δ39TPX2ΔNLS to the depleted extract. Control is a mock-depleted extract. Tubulin is shown as loading control.

Figure S2.

A- Centrosome MT nucleation assay in control and NEDD1-depleted egg extract complemented with NEDD1 WT and NEDD1-S405 phospho-variants. Demembranated sperm nuclei that are associated with an immature centrosome were incubated in egg extract at 20ºC. The fluorescent images (left) are representative sperm nuclei after 10' of incubation. The graph on the right shows the quantification of the proportion of active centrosomes in one representative experiment out of two. More than 30 nuclei were counted at each time point.

B- Pull down of NEDD1-S405 phosphorylation mutants from egg extract with or without RanGTP. NEDD1 depleted extract was complemented with NEDD1WT, NEDD1S405A or NEDD1S405D phospho-variants and these proteins were pulled-down by IP. Controls were performed in parallel with unspecific IgGs. In the upper panel, a Western blot shows the interaction of the NEDD1 variants with the γTuRC components XGrip195 and XGrip109. In the lower panel a Western blot shows their interaction with TPX2.

Acknowledgements

JS was supported by La Caixa. This work was supported by the Spanish ministry grants BFU2009-10202 and BFU2012-37163. We thank Y.Zheng for the anti-XGrip195 and XGrip109 antibodies. We thank N. Mallol and L. Ávila for excellent technical support and members of the lab for their useful comments.

Abbreviations list

γ-TuRC, gamma tubulin ring complex

IF, immunofluorescence

IP, immunoprecipitation

MT, microtubule

References

Bayliss, R., T. Sardon, I. Vernos, and E. Conti. 2003. Structural basis of Aurora-A activation by TPX2 at the mitotic spindle. *Mol Cell*. 12:851-62.

Bischoff, F.R., C. Klebe, J. Kretschmer, A. Wittinghofer, and H. Ponstingl. 1994. RanGAP1 induces GTPase activity of nuclear Ras-related Ran. *Proc Natl Acad Sci U S A*. 91:2587-91.

Brunet, S., T. Sardon, T. Zimmerman, T. Wittmann, R. Pepperkok, E. Karsenti, and I. Vernos. 2004. Characterization of the TPX2 domains involved in microtubule nucleation and spindle assembly in Xenopus egg extracts. *Mol Biol Cell*. 15:5318-28.

Clarke, P.R., and C. Zhang. 2008. Spatial and temporal coordination of mitosis by Ran GTPase. *Nat Rev Mol Cell Biol*. 9:464-77.

Felix, M.A., C. Antony, M. Wright, and B. Maro. 1994. Centrosome assembly in vitro: role of gamma-tubulin recruitment in Xenopus sperm aster formation. *J Cell Biol*. 124:19-31.

Groen, A.C., L.A. Cameron, M. Coughlin, D.T. Miyamoto, T.J. Mitchison, and R. Ohi. 2004. XRHAMM functions in ran-dependent microtubule nucleation and pole formation during anastral spindle assembly. *Curr Biol*. 14:1801-11.

Gruss, O.J., R.E. Carazo-Salas, C.A. Schatz, G. Guarguaglini, J. Kast, M. Wilm, N. Le Bot, I. Vernos, E. Karsenti, and I.W. Mattaj. 2001. Ran induces spindle assembly by reversing the inhibitory effect of importin alpha on TPX2 activity. *Cell*. 104:83-93.

Gruss, O.J., and I. Vernos. 2004. The mechanism of spindle assembly: functions of Ran and its target TPX2. *J Cell Biol*. 166:949-55.

Gruss, O.J., M. Wittmann, H. Yokoyama, R. Pepperkok, T. Kufer, H. Sillje, E. Karsenti, I.W. Mattaj, and I. Vernos. 2002. Chromosome-induced microtubule assembly mediated by TPX2 is required for spindle formation in HeLa cells. *Nat Cell Biol*. 4:871-9.

Gunawardane, R.N., O.C. Martin, and Y. Zheng. 2003. Characterization of a new gammaTuRC subunit with WD repeats. *Mol Biol Cell*. 14:1017-26.

Kollman, J.M., A. Merdes, L. Mourey, and D.A. Agard. 2011. Microtubule nucleation by gamma-tubulin complexes. *Nat Rev Mol Cell Biol*. 12:709-21.

Luders, J., U.K. Patel, and T. Stearns. 2006. GCP-WD is a gamma-tubulin targeting factor required for centrosomal and chromatin-mediated microtubule nucleation. *Nat Cell Biol*. 8:137-47.

Maxwell, C.A., J.J. Keats, A.R. Belch, L.M. Pilarski, and T. Reiman. 2005. Receptor for hyaluronan-mediated motility correlates with centrosome abnormalities in multiple myeloma and maintains mitotic integrity. *Cancer Res*. 65:850-60.

Maxwell, C.A., J.J. Keats, M. Crainie, X. Sun, T. Yen, E. Shibuya, M. Hendzel, G. Chan, and L.M. Pilarski. 2003. RHAMM is a centrosomal protein that interacts with dynein and maintains spindle pole stability. *Mol Biol Cell*. 14:2262-76.

Meunier, S., and I. Vernos. 2011. K-fibre minus ends are stabilized by a RanGTP-dependent mechanism essential for functional spindle assembly. *Nat Cell Biol*. 13:1406-14.

Moudjou, M., N. Bordes, M. Paintrand, and M. Bornens. 1996. gamma-Tubulin in mammalian cells: the centrosomal and the cytosolic forms. *J Cell Sci*. 109 (Pt 4):875-87.

Neumayer, G., C. Belzil, O.J. Gruss, and M.D. Nguyen. 2014. TPX2: of spindle assembly, DNA damage response, and cancer. *Cell Mol Life Sci*.

Ohba, T., T. Seki, Y. Azuma, and T. Nishimoto. 1996. Premature chromatin condensation induced by loss of RCC1 is inhibited by GTP- and GTPgammaS-Ran, but not GDP-Ran. *J Biol Chem*. 271:14665-7.

Peset, I., J. Seiler, T. Sardon, L.A. Bejarano, S. Rybina, and I. Vernos. 2005. Function and regulation of Maskin, a TACC family protein, in microtubule growth during mitosis. *J Cell Biol*. 170:1057-66.

Pinyol, R., J. Scrofani, and I. Vernos. 2013. The role of NEDD1 phosphorylation by Aurora A in chromosomal microtubule nucleation and spindle function. *Curr Biol*. 23:143-9.

Sardon, T., I. Peset, B. Petrova, and I. Vernos. 2008. Dissecting the role of Aurora A during spindle assembly. *EMBO J*. 27:2567-79.

Schatz, C.A., R. Santarella, A. Hoenger, E. Karsenti, I.W. Mattaj, O.J. Gruss, and R.E. Carazo-Salas. 2003. Importin alpha-regulated nucleation of microtubules by TPX2. *EMBO J*. 22:2060-70.

Sdelci, S., M. Schutz, R. Pinyol, M.T. Bertran, L. Regue, C. Caelles, I. Vernos, and J. Roig. 2012. Nek9 phosphorylation of NEDD1/GCP-WD contributes to Plk1 control of gamma-tubulin recruitment to the mitotic centrosome. *Curr Biol*. 22:1516-23.

Teixido-Travesa, N., J. Roig, and J. Luders. 2012. The where, when and how of microtubule nucleation - one ring to rule them all. *J Cell Sci*. 125:4445-56.

Thazhath, R., C. Liu, and J. Gaertig. 2002. Polyglycylation domain of beta-tubulin maintains axonemal architecture and affects cytokinesis in Tetrahymena. *Nat Cell Biol*. 4:256-9.

Tulu, U.S., C. Fagerstrom, N.P. Ferenz, and P. Wadsworth. 2006. Molecular requirements for kinetochore-associated microtubule formation in mammalian cells. *Curr Biol*. 16:536-41.

Wittmann, T., M. Wilm, E. Karsenti, and I. Vernos. 2000. TPX2, A novel xenopus MAP involved in spindle pole organization. *J Cell Biol*. 149:1405-18.

Zheng, Y., M.L. Wong, B. Alberts, and T. Mitchison. 1995. Nucleation of microtubule assembly by a gamma-tubulin-containing ring complex. *Nature*. 378:578-83.

Zhu, H., J.A. Coppinger, C.Y. Jang, J.R. Yates, 3rd, and G. Fang. 2008. FAM29A promotes microtubule amplification via recruitment of the NEDD1-gamma-tubulin complex to the mitotic spindle. *J Cell Biol*. 183:835-48.

Figure legends

Figure 1. RanGTP activates γ-TuRC MT nucleation activity

A-Western blot of control IgG and anti-NEDD1 IP from egg extract with or without RanGTP to detect the γ-TuRC components Xgrip195 and Xgrip109 and γ-tubulin as well as NEDD1, as indicated.

B- Experimental design for the experiments shown in C and D.

C- MT assembly around anti-NEDD1 beads incubated in extract containing rhodamin-tubulin. The graph shows the percentage of beads associated with MTs. Quantifications were performed on squashes. Representative images are shown (right). Beads are auto-fluorescent. Data obtained from three independent experiments counting more than 500 beads for each condition. Error bars: standard deviation. *** $p<0,001$ using X-squared test. Bars: 10 μm.

D- MT nucleation assay around anti-NEDD1 beads retrieved from egg extract and incubated in pure tubulin. Beads were spun onto cover slips and processed for IF to visualize MTs. The graph shows the percentage of beads associated with MTs. Representative images are shown (right). Beads are auto-fluorescent. Data obtained from four independent experiments counting more than 500 beads for each condition. Error bars: standard deviation. *** $p<0,001$ using X-squared test. Scale bars: 10 μm.

Figure 2. RHAMM is involved in chromosome-dependent MT nucleation

A- MT regrowth assay in control and RHAMM silenced GFP-centrin stably expressing HeLa cells. Left: IF images of control and RHAMM silenced cells. DNA (blue), MTs (red) and centrin (green, arrowheads in merge). Scale bar, 10 μm. The graph shows the average number of MT asters per cell, at the indicated times after nocodazole washout. More than 30 cells were counted at each time-point in three independent experiments. Bars: standard deviation.

B- MT regrowth assay in control and silenced cells as indicated. The graph shows the average number of MT asters per cell, 5 minutes after nocodazole washout in control and silenced cells. MCAK silencing rescues aster formation in MCRS1 silenced cells but not in TPX2, NEDD1 or RHAMM silenced cells. IF images show representative cells for each condition. DNA, blue; MTs, green. Scale bar: 10 μm. *** p<0,001%; ns: no statistical significance using X-squared test. More than 30 cells were counted in two independent experiments (TPX2i and TPX2i+MCAKi: one representative experiment).

C- Western blot analysis of control IgG and anti-XRHAMM IP from egg extract with or without RanGTP to detect the γ-TuRC components Xgrip109; Xgrip195 and γ-tubulin as well as NEDD1.

D- Centrosomal MT nucleation from sperm nuclei incubated in control or depleted extract containing rhodamine tubulin. Quantifications were done on squashes taken after 6, 8 and 10 minutes of incubation. The graph (left) shows the proportion of active centrosomes in one representative experiment out of two. Representative images are shown (right). More than 30 nuclei were counted at each time point. Scale bars: 10 μm.

Figure 3. Interaction of the RHAMM-NEDD1-γ-TuRC complex with TPX2

A- Western blot analysis of control IgG, anti-XRHAMM and anti-TPX2 IPs from egg extracts with or without RanGTP to detect XRHAMM and TPX2, as indicated.

B- Western blot analysis of control IgG and anti-NEDD1 IP from egg extracts with or without RanGTP to detect TPX2, NEDD1 and γ-tubulin, as indicated.

C- Western blot analysis of anti-NEDD1 IP from mock depleted (control) and XRHAMM depleted extracts with or without RanGTP to detect TPX2, NEDD1 and γ-tubulin, as indicated.

D- MT nucleation assay in pure tubulin of anti-NEDD1 beads retrieved from control or XRHAMM depleted extracts with or without RanGTP. The experimental design is shown (left). The graph shows the proportion of beads associated with MTs. Representative IF images of MTs and beads are shown (right). Beads are auto-fluorescent. Three independent experiments were performed, counting more than 500 beads in each condition. Error bars: standard deviation. *** p<0,001% using X-squared test. Scale bars: 10 µm.

Figure 4. NEDD1 S405 phosphorylation is essential but not sufficient for RanGTP-dependent MT nucleation

A- Western blot analysis of control IgG and anti-Aurora-A IP from egg extracts with or without RanGTP to detect TPX2, NEDD1 and Aurora A as indicated.

B- Schematic representation of TPX2 showing its Aurora A and importin (NLS) binding domains. Below, the two truncated TPX2 proteins used in C and D are shown.

C- MT assembly in the absence of RanGTP in TPX2 and NEDD1-depleted extracts containing TPX2ΔNLS and Flag-NEDD1 phospho-variants, as indicated. The experimental design is shown at the top. The graph shows the number of asters per µl of extract in one representative out of three independent experiments.

D- MT assembly in the absence of RanGTP in TPX2 and NEDD1-depleted extracts containing Δ39TPX2ΔNLS and Flag-NEDD1 phospho-variants, as indicated. The experimental design is shown at the top. The graph shows the number of asters per µl of extract in one representative out of three independent experiments.

E- MT assembly in NEDD1-depleted extracts (control) or in NEDD1 and TPX2-depleted extracts with or without RanGTP. The double depleted extract was supplemented or not with TPX2-N39, as indicated. The experimental design is shown at the top. The graph shows the number of asters per µl of extract in one representative out of three independent experiments.

F- MT assembly in NEDD1-depleted extracts by beads coated with Flag-NEDD1 phospho-variants (as indicated), with or without RanGTP. The experimental design is shown at the top. The graph shows the number of asters per µl of extract in one representative out of three independent experiments.

All the quantifications performed on squashes at 30 minutes of incubation. More than 500 beads were counted for each condition.

Figure 5. Essential role of TPX2 in promoting γTuRC recruitment

A- Western-blot analysis of control IgG and anti-GFP pull-downs from egg extracts containing GFP-TPX2 (FL) or GFP-TPX2-C-terminal (CT) with or without RanGTP. Top: GFP recombinant proteins detected with anti-GFP antibodies. Bottom: GFP-TPX2 and the endogenous TPX2 (TPX2 endo) detected with anti-TPX2 antibodies.

B- MT nucleation in pure tubulin around beads coated with Flag-NEDD1 phospho-variants retrieved from NEDD1-depleted extract. The experimental design is shown at the top. The graph shows the percentage of beads associated with MTs. Data from three independent experiments counting more than 500 beads were counted for each condition. Error bars: standard deviation. *** p<0,001%.

C- MT nucleation in pure tubulin around NEDD1 coated beads retrieved from control or TPX2 depleted extract containing or not RanGTP. The depleted extract was supplemented or not with TPX2-N39, as indicated. The experimental design is shown at the top. The graph shows the percentage of beads associated with MTs. Data from three independe experiments counting more than 500 beads were counted for each condition. Error bars: standard deviation. *** p<0,001%.

D- Model: TPX2 provides the two essential requirements for γTuRC activation by RanGTP. (a) RanGTP releases TPX2 from importins triggering the recruitment of the specific

XRHAMM-NEDD1-γTuRC MT nucleation complex on TPX2-Aurora-A promoting the phosphorylation of NEDD1 on S405 and MT nucleation. (b) In absence of TPX2, the recruitment of the phospho XRHAMM-NEDD1-γTuRC complex on beads is sufficient to trigger MT nucleation in the absence of RanGTP.

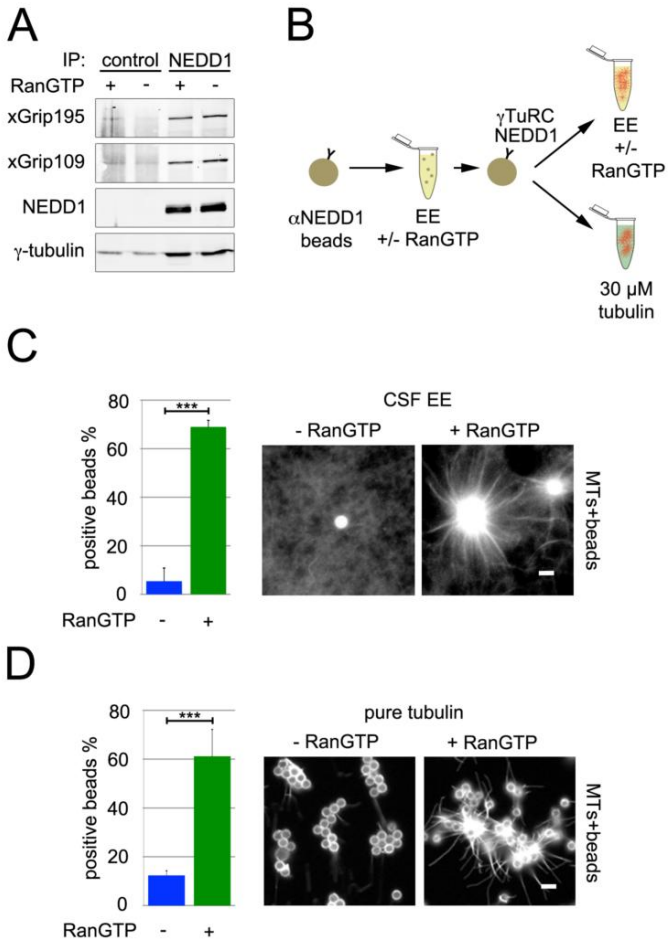
A
IP: control NEDD1
RanGTP + - + -
xGrip195
xGrip109
NEDD1
γ-tubulin
B
αNEDD1 beads
EE +/- RanGTP
γTuRC NEDD1
EE +/- RanGTP
30 μM tubulin
C
positive beads %
80
60
40
20
0
***
RanGTP - +
CSF EE
- RanGTP
+ RanGTP
MTs+beads
D
positive beads %
80
60
40
20
0
***
RanGTP - +
pure tubulin
- RanGTP
+ RanGTP
MTs+beads

Figure 1

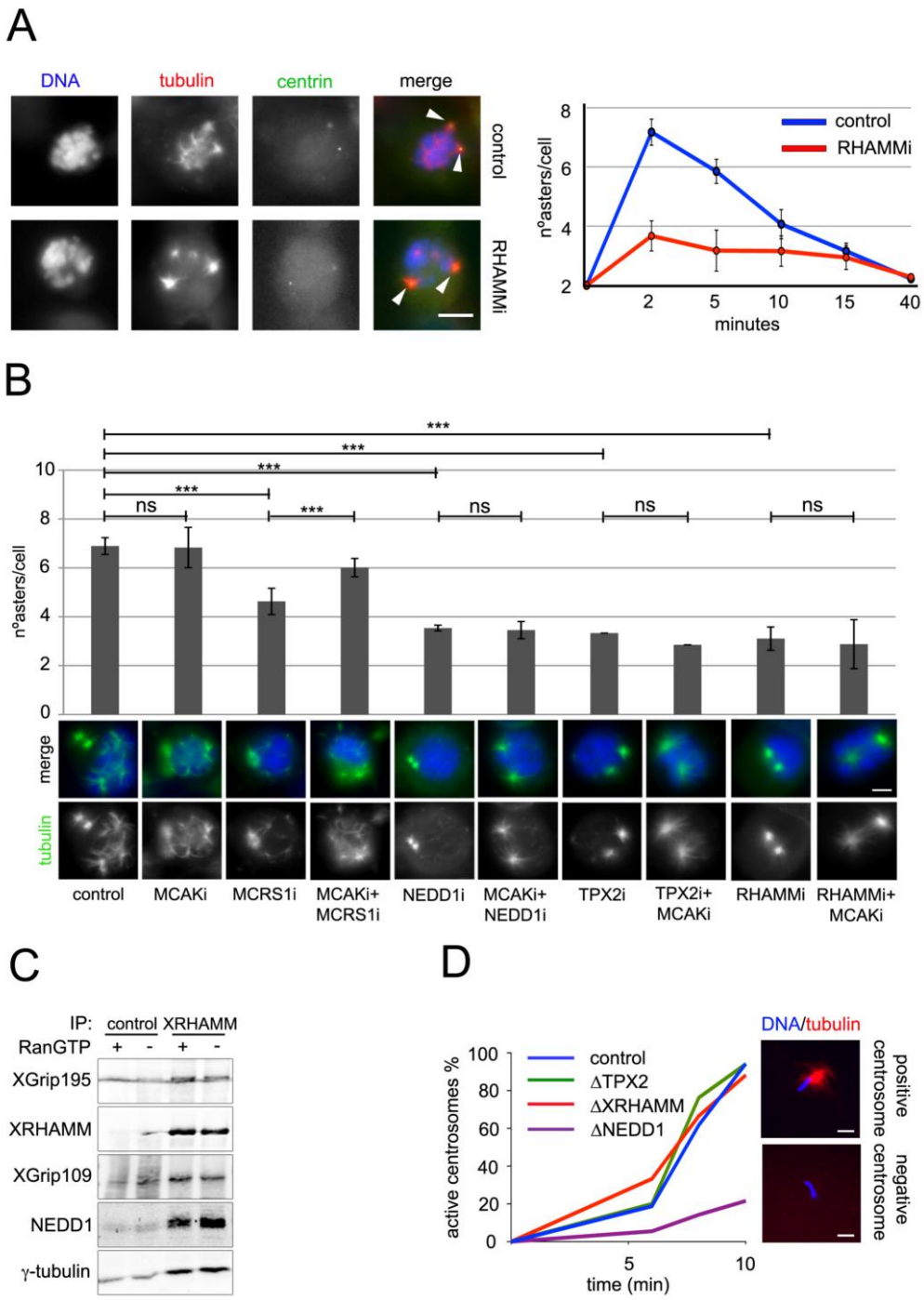
A
DNA
tubulin
centrin
merge
control
RHAMMi
nºasters/cell
control
RHAMMi
minutes
B
nºasters/cell
merge
tubulin
control
MCAKi
MCRS1i
MCAKi+ MCRS1i
NEDD1i
MCAKi+ NEDD1i
TPX2i
TPX2i+ MCAKi
RHAMMi
RHAMMi+ MCAKi
ns
C
IP:
control
XRHAMM
RanGTP
XGrip195
XRHAMM
XGrip109
NEDD1
γ-tubulin
D
DNA/tubulin
active centrosomes %
control
ΔTPX2
ΔXRHAMM
ΔNEDD1
time (min)
positive centrosome
negative centrosome

Figure 2

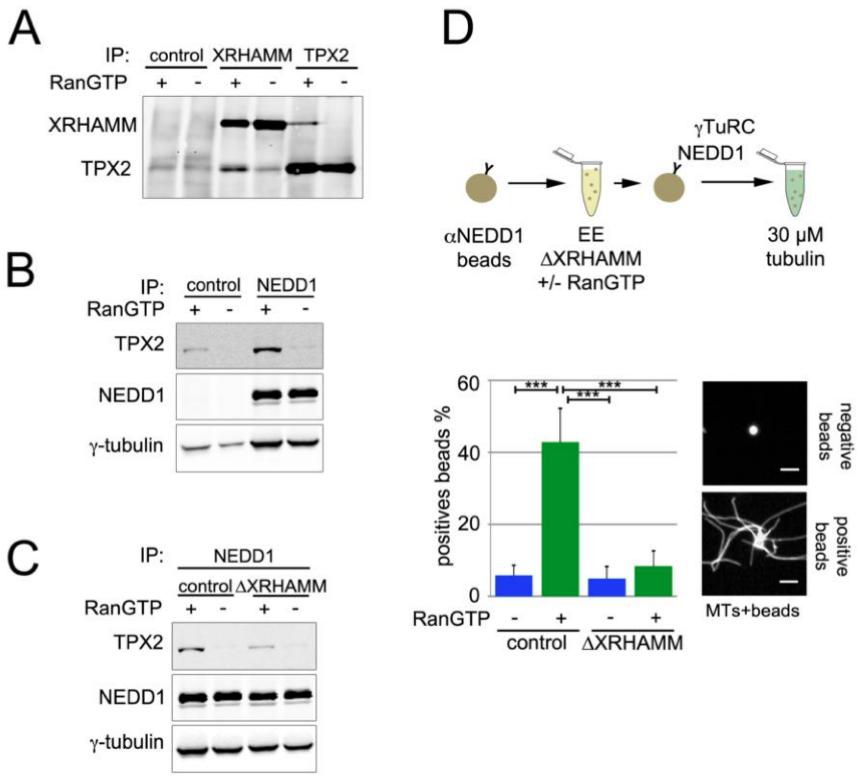
A
IP: control XRHAMM TPX2
RanGTP + - + - + -
XRHAMM
TPX2
B
IP: control NEDD1
RanGTP + - + -
TPX2
NEDD1
γ-tubulin
C
IP: NEDD1
control ΔXRHAMM
RanGTP + - + -
TPX2
NEDD1
γ-tubulin
D
γTuRC
NEDD1
αNEDD1 beads
EE ΔXRHAMM +/- RanGTP
30 μM tubulin
positives beads %
60
40
20
0
***
***
***
RanGTP - + - +
control ΔXRHAMM
negative beads
positive beads
MTs+beads

Figure 3

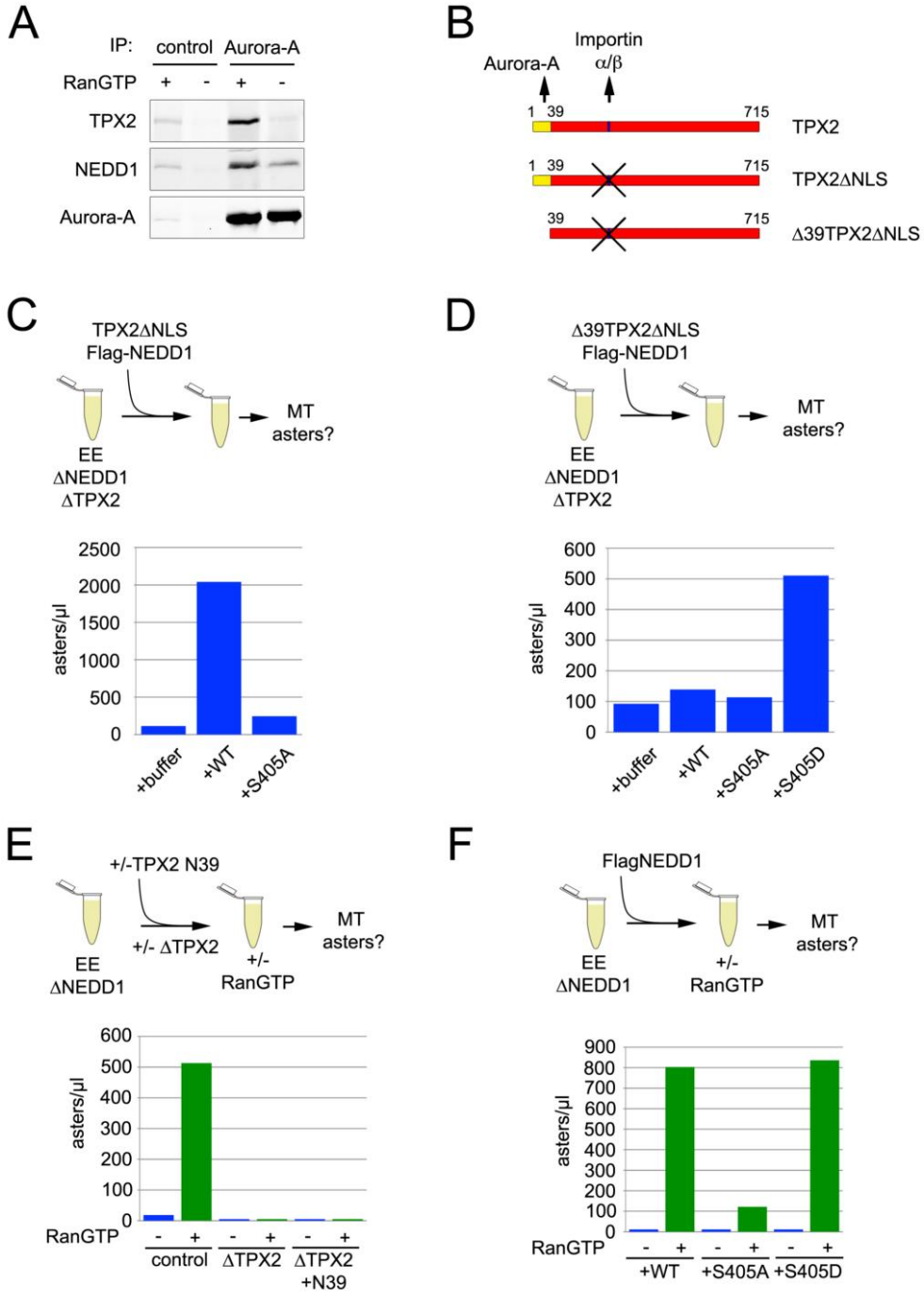
A
IP:
control
Aurora-A
RanGTP
+
-
+
-
TPX2
NEDD1
Aurora-A
B
Importin
α/β
Aurora-A
1
39
715
TPX2
TPX2ΔNLS
Δ39TPX2ΔNLS
C
TPX2ΔNLS
Flag-NEDD1
EE
ΔNEDD1
ΔTPX2
MT
asters?
asters/µl
2500
2000
1500
1000
500
0
+buffer
+WT
+S405A
D
Δ39TPX2ΔNLS
Flag-NEDD1
EE
ΔNEDD1
ΔTPX2
MT
asters?
asters/µl
600
500
400
300
200
100
0
+buffer
+WT
+S405A
+S405D
E
+/-TPX2 N39
EE
ΔNEDD1
+/- ΔTPX2
+/-
RanGTP
MT
asters?
asters/µl
600
500
400
300
200
100
0
RanGTP
-
+
control
ΔTPX2
ΔTPX2
+N39
F
FlagNEDD1
EE
ΔNEDD1
+/-
RanGTP
MT
asters?
asters/µl
900
800
700
600
500
400
300
200
100
0
RanGTP
+WT
+S405A
+S405D

Figure 4

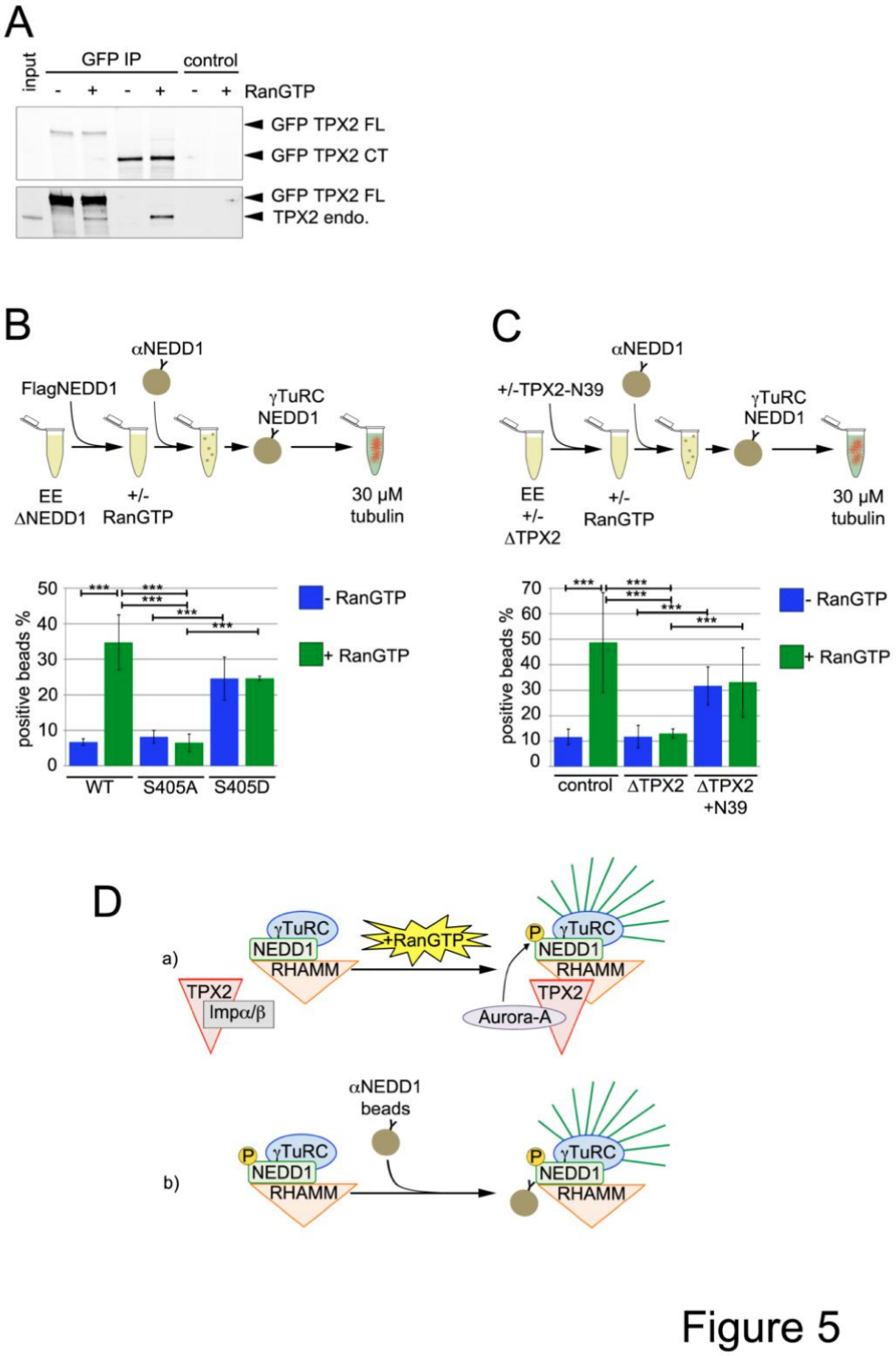
A
input
GFP IP
control
- + - + - + RanGTP
GFP TPX2 FL
GFP TPX2 CT
GFP TPX2 FL
TPX2 endo.
B
αNEDD1
FlagNEDD1
γTuRC
NEDD1
EE
ΔNEDD1
+/-
RanGTP
30 μM
tubulin
positive beads %
- RanGTP
+ RanGTP
WT
S405A
S405D
C
αNEDD1
+/-TPX2-N39
γTuRC
NEDD1
EE
+/-
ΔTPX2
+/-
RanGTP
30 μM
tubulin
positive beads %
- RanGTP
+ RanGTP
control
ΔTPX2
ΔTPX2
+N39
D
a)
γTuRC
NEDD1
RHAMM
+RanGTP
TPX2
Impα/β
Aurora-A
b)
αNEDD1
beads

Figure 5

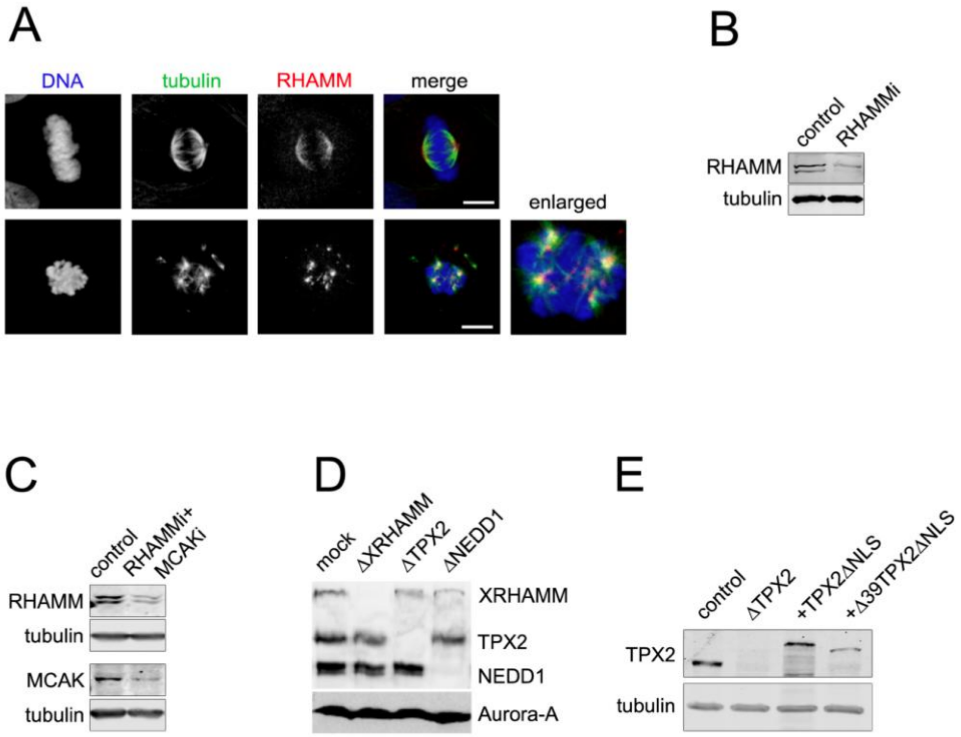

Supplemental Fig 1

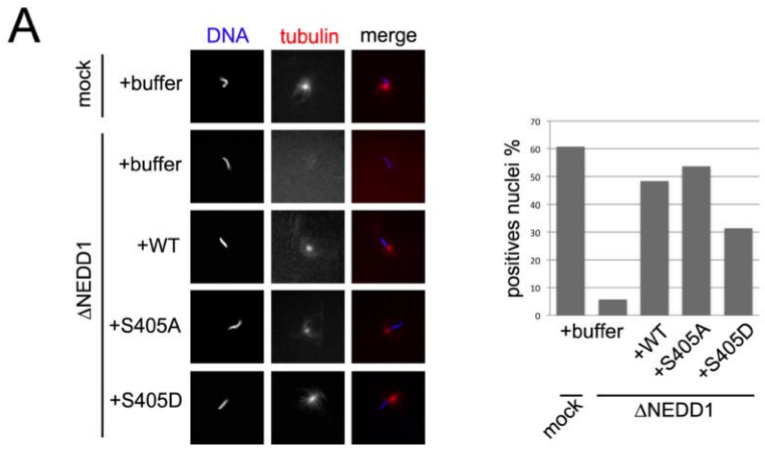

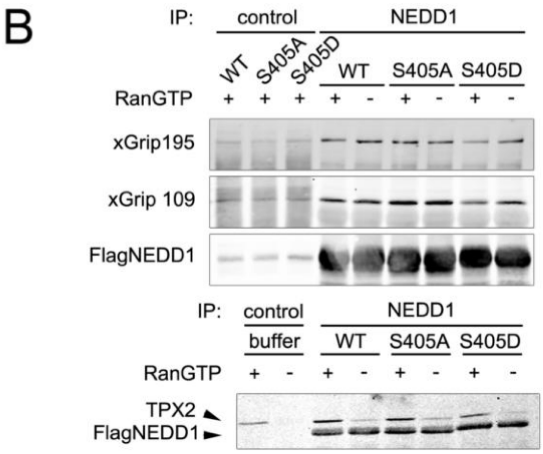

Supplemental Fig. 2

2.3. RHAMM silencing phenotype in mitotic HeLa cells

Our work showed that XRHAMM plays an essential role in RanGTP dependent MT nucleation by promoting TPX2-γTuRC interaction and indirectly Aurora-A phosphorylation on NEDD1 S405. We therefore asked if XRHAMM could have a similar conserved role in human HeLa cells. To do that, we started studying RHAMM mitotic localization. IF analysis showed that like the *Xenopus* protein the human

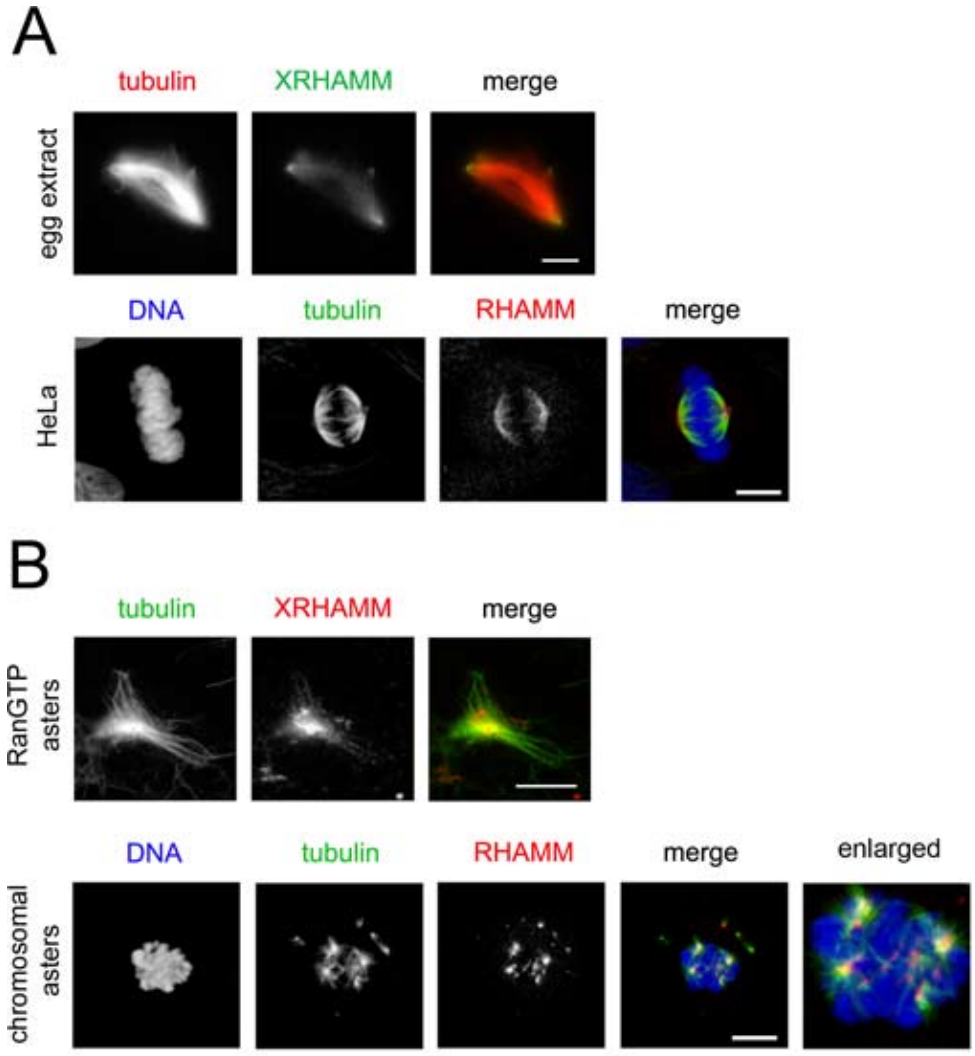

Figure 15. RHAMM mitotic localization in *Xenopus* egg extract and human HeLa cells

A) Top panel: IF on sperm assembled spindle in CSF egg extract. A small amount of rhodamine labelled tubulin was added to stain microtubules (red). XRHAMM (green). Bottom panel: IF on HeLa cells. DNA (blue), tubulin (green), RHAMM (red). Scale bars: 10 µm. B) Top panel: IF on RanGTP induced microtubules asters. A small amount of rhodamine labelled tubulin was added to stain microtubules (red). XRHAMM (green). Bottom panel: IF on HeLa cells fixed 5 minutes after nocodazole washout in MT regrowth assay. DNA (blue), tubulin (green), RHAMM (red). Scale bars: 10 µm.

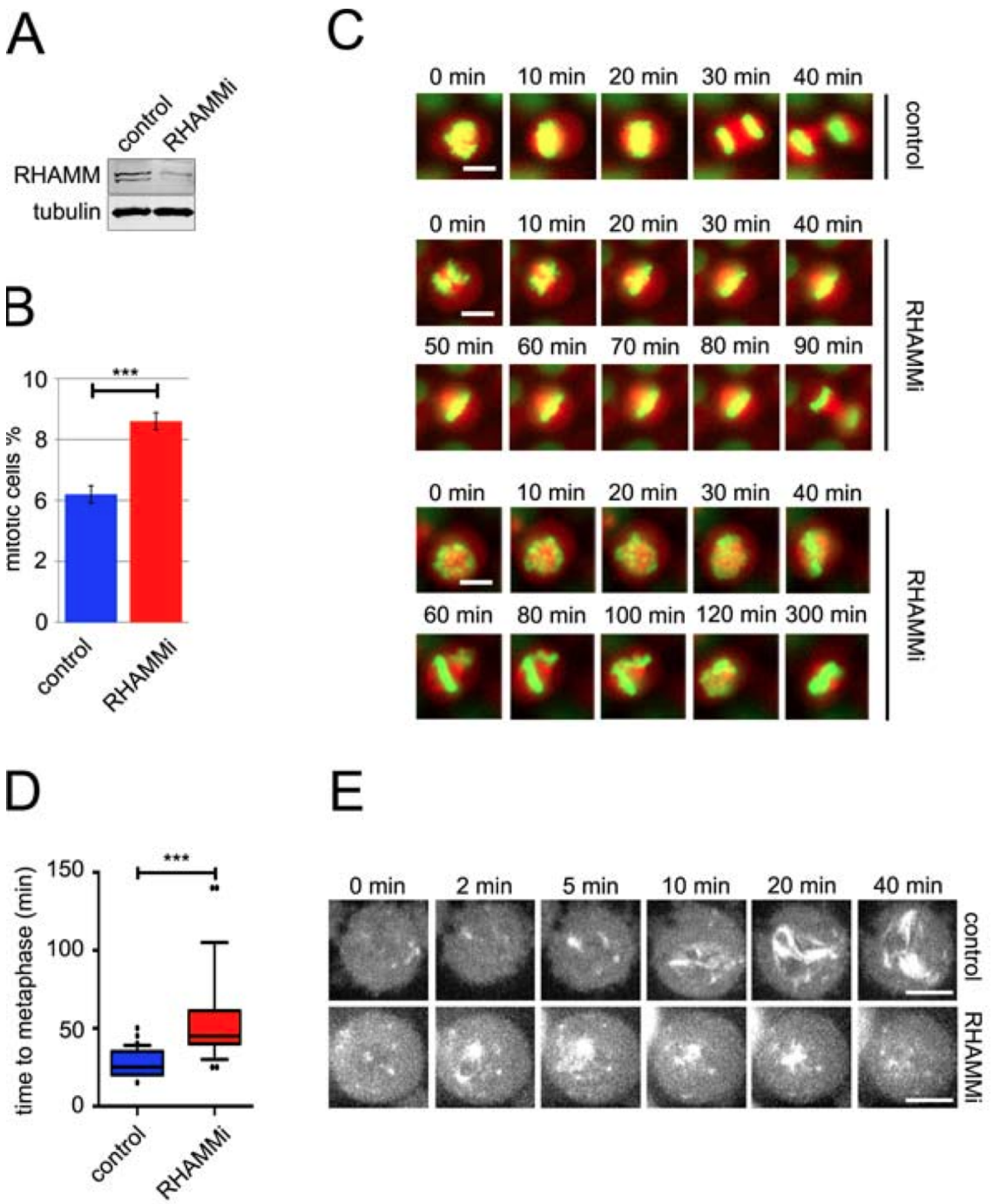

Figure 16. RHAMM role in mitotic HeLa cells

A) Western blot analysis of control and RHAMM silenced HeLa cells after 48 hours of transfection. B) Quantification of mitotic cells (percentage over the total number of cells) in control and RHAMM silenced HeLa cells. More than 500 cells were counted for each condition in two independent experiments. Error bars: standard deviation. *** $p<0,01$ using X-squared test. C) Live microscopy on control and RHAMM silenced GFP-histone RFP-tubulin stably expressing HeLa cells. One cell completing cell division (upper panel) and one cell dying before anaphase (lower panel) are representative examples of RHAMM silenced samples. Scale bars: 10 µm. D) Quantification of time from prophase to anaphase onset in control and RHAMM silenced cells. The analysis has been performed on live microscopy data. More than 30 cells were analysed for each condition in two independent

experiments. *** p<0,001 using t-test. E) Live microscopy on control and RHAMM silenced cells recovering from nocodazole in MT regrowth assay. HeLa cells express RFP tubulin. Scale bars: 10 μm.

RHAMM localized to the mitotic spindle with a strong enrichment at the spindle poles (Fig. 15A). Interestingly, RHAMM localization is conserved also on RanGTP-asters in egg extract and chromosomal MTs in HeLa cells where it localizes close to the center of all these structures (Fig. 15B). We then asked if RHAMM function in spindle assembly could be conserved in HeLa cells. Silencing RHAMM by siRNA (Fig. 16A) in asynchronous cells resulted in a significant accumulation of cells in mitosis suggesting a slower mitotic progression (Fig. 16B). To better understand which mitotic stage was affected we performed live cell imaging on control and RHAMMi cells. The analysis revealed severe problems in chromosome recruitment and congression to the metaphase plate that in many cases resulted in apoptotic cell death before anaphase onset (Fig. 16C). Consistently, quantifications of the time spent by the cells to reach anaphase showed a dramatic delay (Fig. 16D). Considering RHAMM function in *Xenopus* we asked if the phenotype observed in HeLa cells could also be due to defects in chromosomal dependent MT nucleation. We therefore performed live cell microscopy on mitotic cells released from nocodazole. Our movies clearly showed that, in absence of RHAMM, chromosomal MTs cannot form and no bipolar structures appear at early time points (Fig. 16E). This phenotype mimics the TPX2 silencing phenotype (Tulu et al., 2006) and it is in agreement with previous observations (Chen et al., 2014) suggesting that affecting chromosomal MT nucleation results in recruiting and aligning chromosomes to reach metaphase.

2.4. TPX2 and Aurora-A are essential to trigger RanGTP dependent MT nucleation.

Consistently with our model we report that both TPX2 and Aurora-A depletions from the egg extract (Fig. 17A) strongly affect RanGTP dependent MT nucleation activity of NEDD1 beads in pure tubulin (Fig. 17B). These results further support the essential role of TPX2 dependent Aurora-A activation. Promoting the interaction of TPX2 with the RHAMM-NEDD1-γTuRC complex, RanGTP may indirectly favor the phosphorylation of NEDD1 on S405 by Aurora-A. This event is affected both in ΔTPX2 and ΔAurora-A conditions.

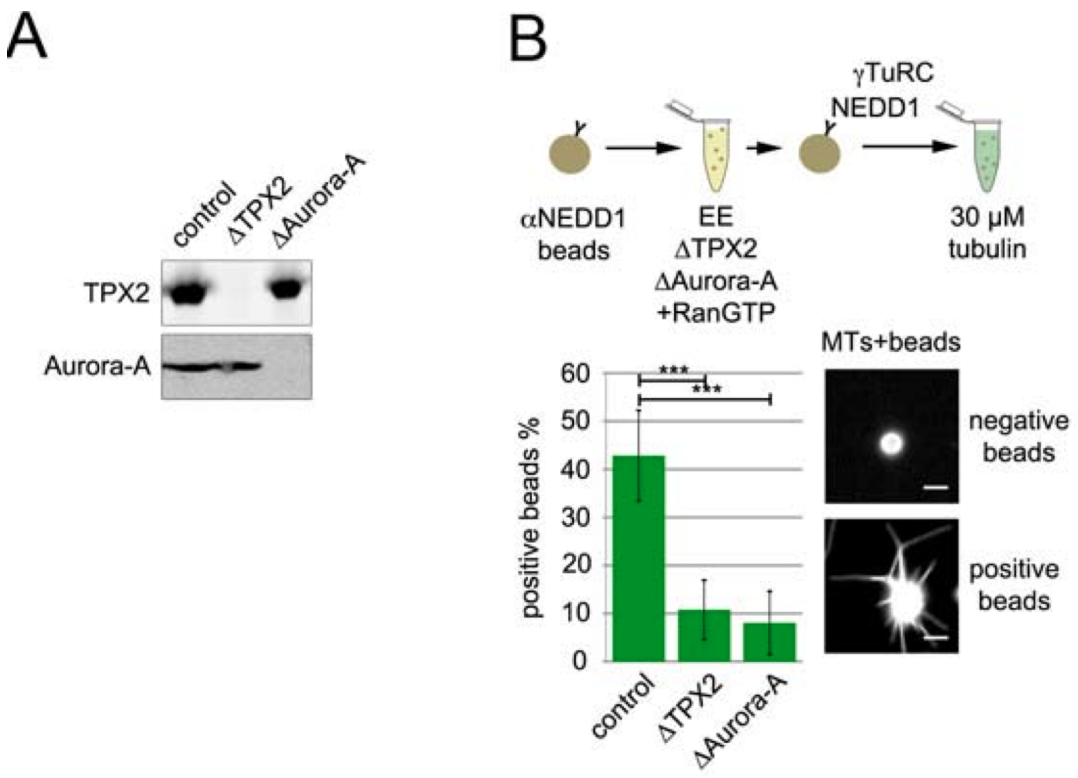

Figure 17. TPX2 and Aurora-A are essential to promote RanGTP dependent MT nucleation

A) Western blot analysis of control, TPX2 and Aurora-A depleted egg extracts. B) MT nucleation assay in pure tubulin. Beads were prepared by IP of NEDD1 from control, ΔTPX2 and ΔAurora-A egg extracts treated with RanGTP. The beads were assayed for their ability to nucleate MTs in 30 μM pure tubulin solution. A schematic representation of the experimental procedure is shown on the top. Quantifications represent the percentage of beads attached to MTs over the total number of beads. Representative IF images of MTs and beads are shown on the right. More than 500 beads were counted for each condition in three independent experiments. Error bars: standard deviation. *** p<0,001%.

2.5. Conclusion

Here, we have shown that RanGTP induces the activation of a specific pool of γTuRC associated with RHAMM, dramatically increasing its MT nucleation activity. RanGTP, by releasing TPX2 from its inhibitory binding to importins, promotes its association with the RHAMM-NEDD1-γTuRC complex. In this complex, TPX2 provides two essential requirements for RanGTP-dependent MT nucleation: the activation of Aurora-A promoting the efficient phosphorylation of NEDD1 on S405, and a scaffolding activity for the recruitment of the RHAMM-NEDD1-γTuRC complexes. We show that TPX2 is the unique RanGTP regulated factor required and NEDD1 the only essential target of Aurora A for this pathway. TPX2 is therefore the central player of the

RanGTP-dependent γTuRC activation mechanism leading to the nucleation of MTs around the chromosomes in mitosis.

3. Contribution of RanGTP-dependent microtubules to spindle assembly

Our data provide new important insights on the mechanism driving the nucleation of MTs close to the chromosomes. Because it is now well established that this class of MTs is essential for cell division (Gruss et al., 2001; Gruss et al., 2002; Tulu et al., 2006) we decided to investigate further their contribution to spindle assembly. In the next paragraphs I will report our preliminary observations suggesting that there is a link between chromosomal MTs and k-fibers assembly.

3.1. The localization of proteins involved in the RanGTP pathway suggest a link to k-fiber assembly

We screened by IF many known spindle assembly factors involved in the RanGTP pathway looking for other factors with MCRS1-like localization. Interestingly, we found that NuSAP (Ribbeck et al., 2006; Ribbeck et al., 2007) and NuMA (Radulescu and Cleveland, 2010) localize to spindle poles and to k-fibers minus ends in metaphase. Strikingly, both of them also localize to the center of chromosomal MT asters in HeLa cells during MT regrowth assays (Fig. 18A and 18B). Interestingly, this localization pattern is similar to RHAMM as it also localizes on k-fibers minus ends in HeLa cells (Fig. 18C). Preliminary observations further suggest that other members of the chromosomal MT nucleation machinery could have the same localization during mitosis. Interestingly, NuMA, NuSAP and RHAMM localization to chromosomal MT asters was not unique as they also localize to centrosomal MTs. However, the similar localization among proteins involved in the RanGTP pathway fits a model where chromosomal MTs asters could become k-fibers during spindle assembly.

3.2. New insights on chromosomal aster structure

As underlined before k-fiber assembly could involve two different mechanisms acting on the opposites ends of chromosomal MTs: the transport of chromosomal asters minus ends towards spindle poles and the recruitment of their plus ends to kinetochores. To provide more insight we therefore asked how a poleward transport mechanism could act

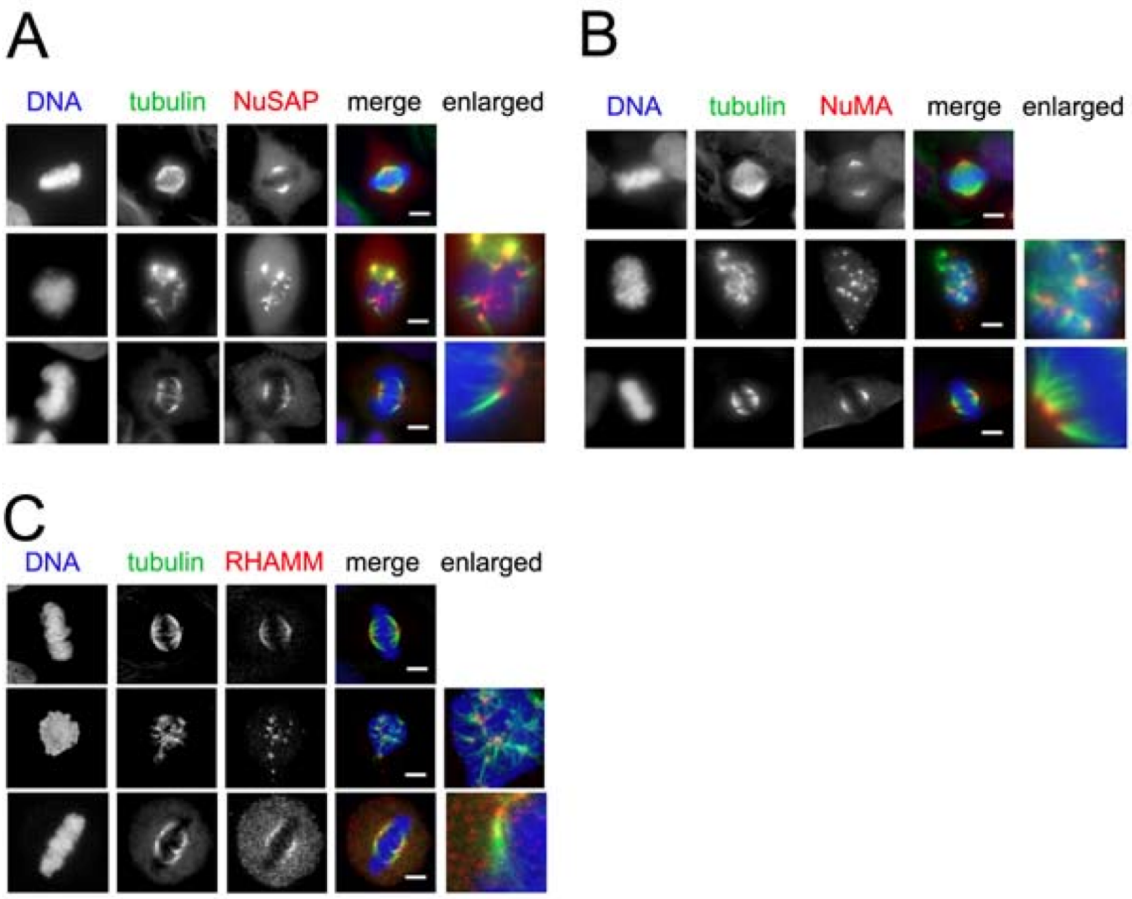

Figure 18. NuSAP, NuMA and RHAMM localization on k-fibers and chromosomal microtubules asters

A) NuSAP localization on different classes of MTs in mitotic HeLa cells. Normal mitotic cells (upper panel), chromosomal MT asters (middle panel) and k-fibers (lower panel) were processed for IF. DNA (blue), tubulin (green), NuSAP (red). Scale bars: 10 µm. B) NuMA localization on different classes of MTs in mitotic HeLa cells. Normal mitotic cells (upper panel), chromosomal MT asters (middle panel) and k-fibers (lower panel) were processed for IF. DNA (blue), tubulin (green), NuMA (red). Scale bars: 10 µm. C) RHAMM localization on different classes of MTs in mitotic HeLa cells. Normal mitotic cells (upper panel), chromosomal MT asters (middle panel) and k-fibers (lower panel) were processed for IF. DNA (blue), tubulin (green), RHAMM (red). Scale bars: 10 µm.

on chromosomal aster structures. Particularly as many proteins specifically mark the center of these MT structures we hypothesized they constitute a specific structure that could be transported trailing all the linked MT minus ends. We then performed MT regrowth experiments on HeLa cells followed by ice induced MT depolymerization (Fig. 19A). Anti-tubulin staining confirmed that newly assembled MTs were completely disassembled by the cold treatment (Fig. 19B). Strikingly, TPX2 and RHAMM were localized on defined dot-like structures at the chromosomal surface (Fig. 19C). We excluded that this dotted configuration was an indirect effect of the IF as both RHAMM

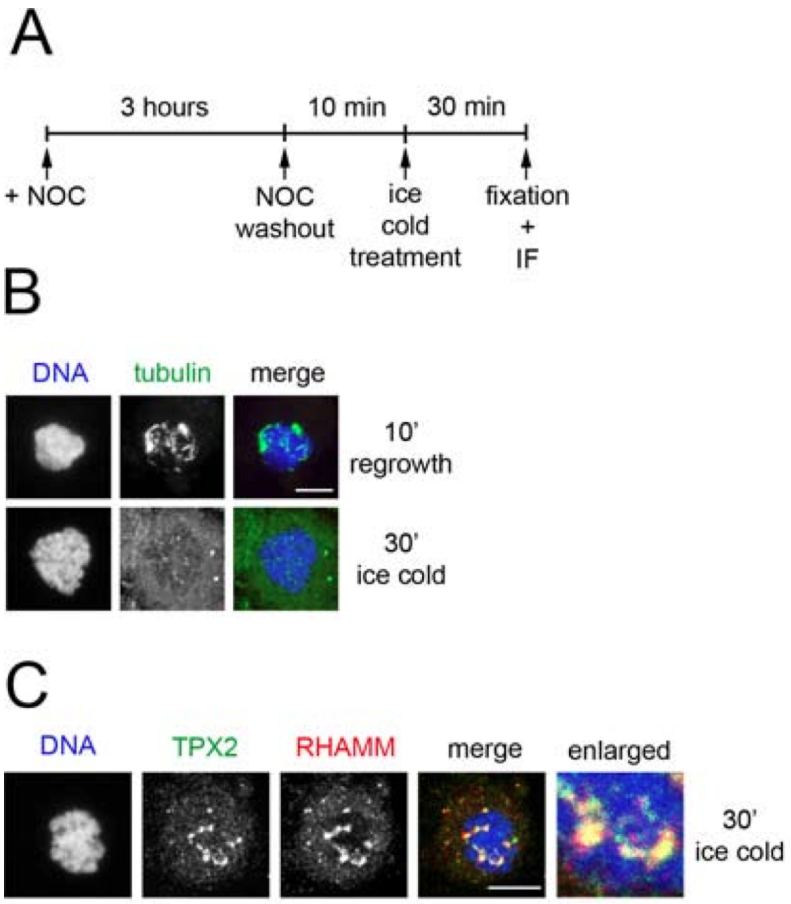

Figure 19. TPX2 and RHAMM co-localize on cold stable structures during MT regrowth in mitotic HeLa cells

A) Schematic representation of the protocol used for MT regrowth in HeLa cells. After 10 minutes from nocodazole washout cells were incubated on ice for 30 minutes. IF were then performed. B) Control IF on HeLa cells fixed after 10 minutes of MT regrowth (top) and after 30 minutes of ice-cold MT depolymerization. DNA (blue), tubulin (green). Scale bars: 10 µm. C) IF analysis of RHAMM and TPX2 localization in HeLa cells treated as described in (A). DNA (blue), TPX2 (green) and RHAMM (red). Scale bars: 10 µm.

and TPX2 appear precisely co-localized on these structures. These data suggest that some MT independent and cold resistant structures exist in the middle of chromosomal aster MTs. However, the function and the composition of such structures remain completely unknown.

Speculating on the possible k-fibers assembly process we thought that chromosomal MTs minus ends recruitment to the poles could not be sufficient if plus ends do not undergo to a kinetochores recruitment process. Because no evidences support this idea we performed MT regrowth in HeLa cells in presence of a small concentration of nocodazole (Fig.20A). In these conditions the MT density in the cytoplasm was reduced

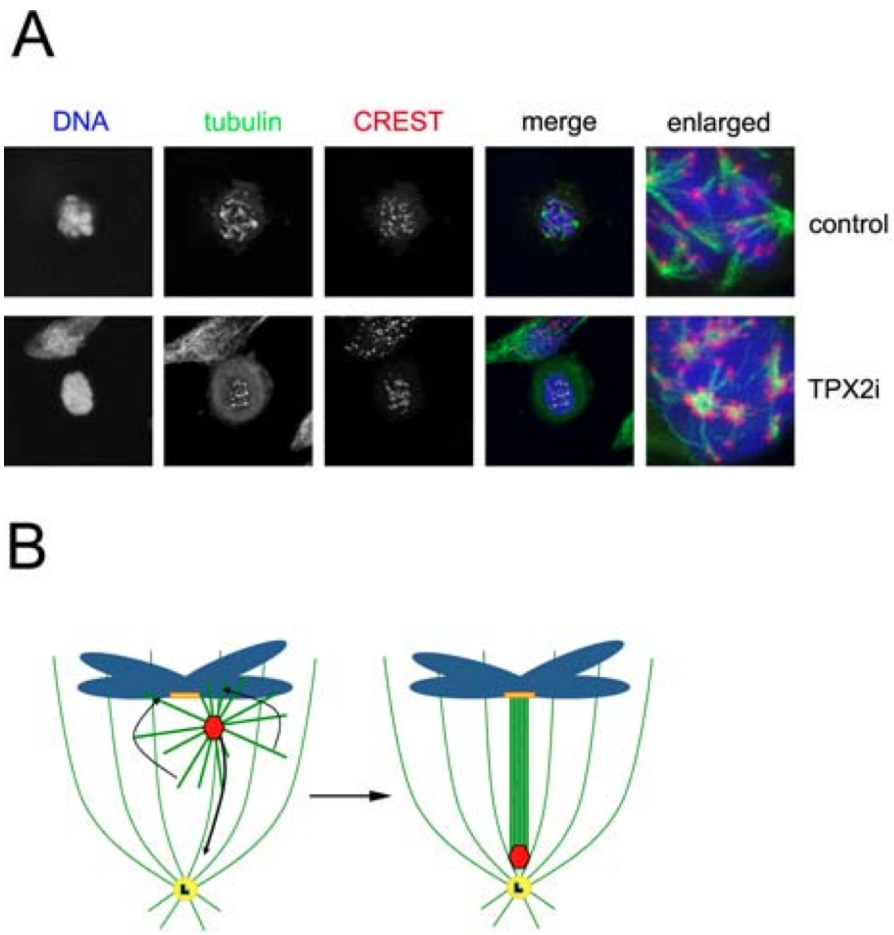

Figure 20. Chromosomal MTs are connected to kinetochores during MT regrowth assay in HeLa cells.

A) IF analysis of control and TPX2 silenced HeLa cells fixed after 5 minutes from nocodazole washout in MT regrowth assay. DNA (blue), tubulin (green). Anti human CREST stains kinetochores (red). B) Schematic model of the k-fiber assembly process. Two processes could be required to assemble k-fibers from chromosomal nucleated MTs: i) the transport of chromosomal MT asters minus ends towards spindle poles and ii) the recruitment of MTs plus ends to kinetochores.

and we were able to look for connections between chromosomal MTs plus ends and kinetochores. Strikingly, all the MTs emanating from the chromosomal asters were clearly connected with kinetochores therefore supporting our hypothesis. To exclude that these connected MTs were not coming from the two active centrosomes we silenced TPX2. In this condition the majority of chromosomal MTs were lost and MT-kinetochores connections disappeared (Fig. 20A).

All these observation support the idea that during spindle assembly chromosomal MTs asters are involved in a polar and kinetochores recruitment process (Fig. 20B).

3.3. Chromosomal MT nucleation is essential for proper k-fiber assembly

To test if k-fibers are mainly constituted by chromosomal MTs we abolished chromosomal-dependent MT nucleation, targeting by siRNA its specific machinery, and studied k-fiber mechanical properties and dynamics. To do that we first silenced RHAMM in HeLa cells and we tested then the resistance of k-fibers to ice-cold treatment. Strikingly we found that RHAMM silenced cells have less stable k-fibers suggesting that the MT bundles could be mechanically less resistant (Fig. 21A). We then asked if also k-fiber dynamics were different. To do that we first prepared monopolar spindles treating HeLa cells with monastrol and then we depolymerized non-k-fibers MTs incubating the cells on ice. Quantifications revealed that k-fibers are dramatically shorter in RHAMM silenced cells (Fig. 21B). These data suggest that impairing chromosomal dependent MT nucleation leads to defective k-fibers assembly. To further strengthen this hypothesis we performed the same experiment targeting TPX2, another essential component of the chromosomal-dependent MT nucleation machinery. Strikingly TPX2 silenced cells showed an even stronger phenotype as k-fibers started to depolymerize after a short incubation on ice (Fig. 21C). Particularly TPX2 silenced cells showed high abundance of monopolar spindles with short and poorly organized k-fibers (Fig. 21D). To have a more direct proof that these phenotypes on k-fibers are consequence of the lack of chromosomal MTs we asked if MCRS1 localization on minus ends was affected. Strikingly we observed that in RHAMM silenced cells MCRS1 could not localize on spindle poles and k-fiber minus ends (Fig. 22A). Differently in MCRS1 silenced cells RHAMM mitotic localization was not affected (Fig. 22B). Altogether these results strongly suggest that affecting chromosomal MT assembly, by targeting its specific MT nucleation machinery, we severely compromise k-fibers formation. The absence of the chromosomal MT specific marker MCRS1 on k-fibers in RHAMM silenced cells further supports this hypothesis.

3.4. Conclusion

Altogether our preliminary results provide new insight on k-fiber assembly. Particularly we showed that proteins involved in the RanGTP pathway localize similarly to the center of chromosomal asters and k-fiber minus ends. This localization pattern supports

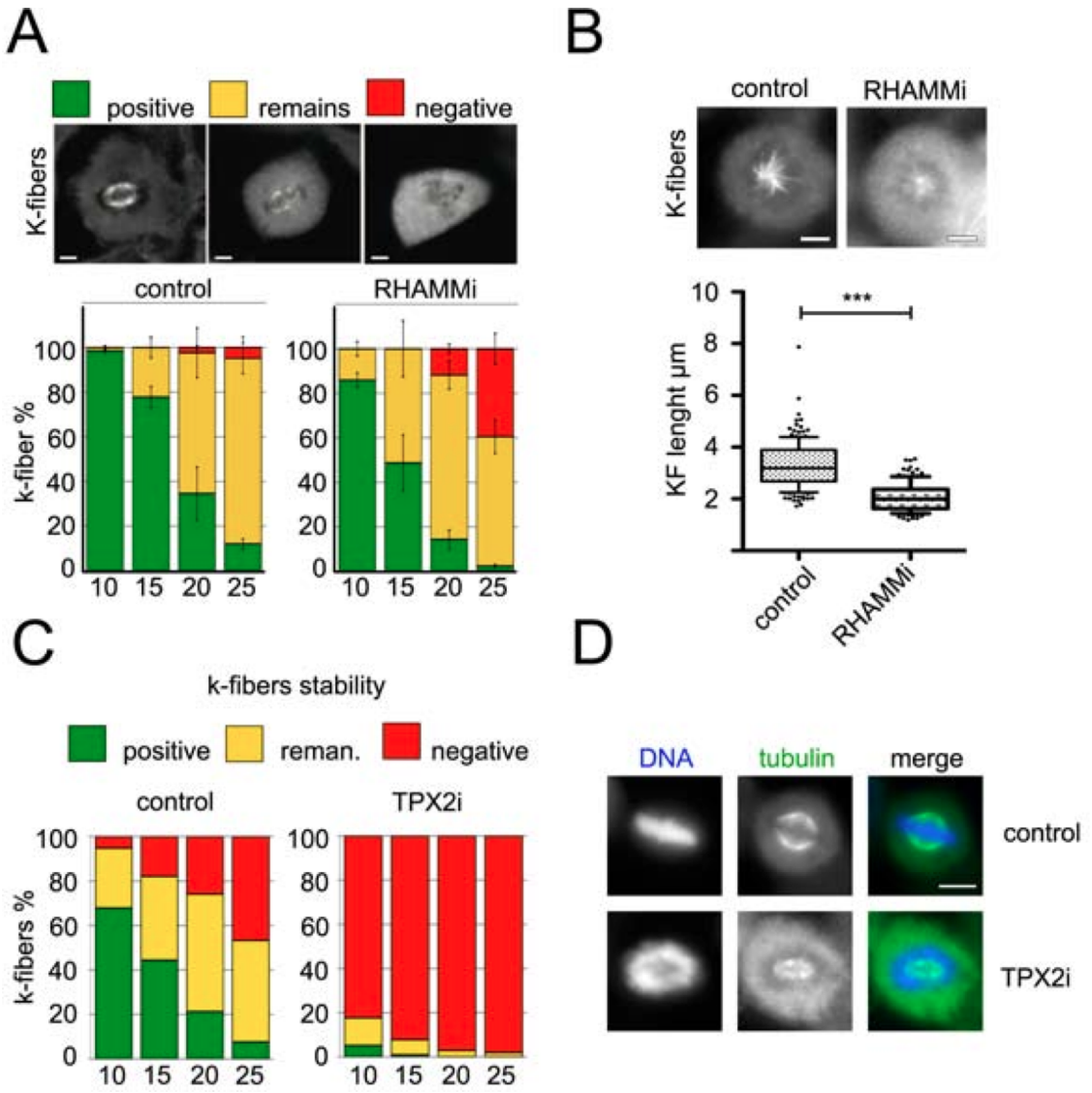

Figure 21. Chromosomal microtubule nucleation is essential for proper k-fiber assembly

A) K-fiber stability assay on control and RHAMM silenced HeLa cells. Cells were incubated on ice and samples collected after 10, 15, 20 and 25 minutes. IF shows selected examples of cells with intact k-fibers (green; positive), partially depolymerised (yellow; remains) and completely depolymerised (red; negative). Anti-tubulin stains MTs. Scale bars: 10 µm. Quantifications represent the percentage of cells observed in each category over the total number of counted cells. More than 100 cells were counted at each time point. Two independent experiments were performed. Error bars: standard deviation. B) K-fiber length in control and RHAMM silenced HeLa cells. Cells were incubated overnight in monastrol and then incubated 10 minutes on ice. Each visible MT was then measured. IF shows selected examples of one control and one RHAMM silenced cell. Anti-tubulin stains MTs. Quantifications report the length of individual k-fibers in one representative experiment out of two. More than 150 MTs were counted in 30 individual for each condition. *** $p<0,001$ using t-test. C) K-fibers stability assay on control and TPX2 silenced HeLa cells. Cells were processed like in (A). Quantifications represent the percentage of cells observed in each category over the total number of counted cells. More than 100 cells were counted in two independent experiment. Error bars: standard deviation. D) IF analysis of control and TPX2 silenced HeLa cells after 10 minutes incubation on ice. DNA (blue), tubulin (green). Scale bar: 10 µm.

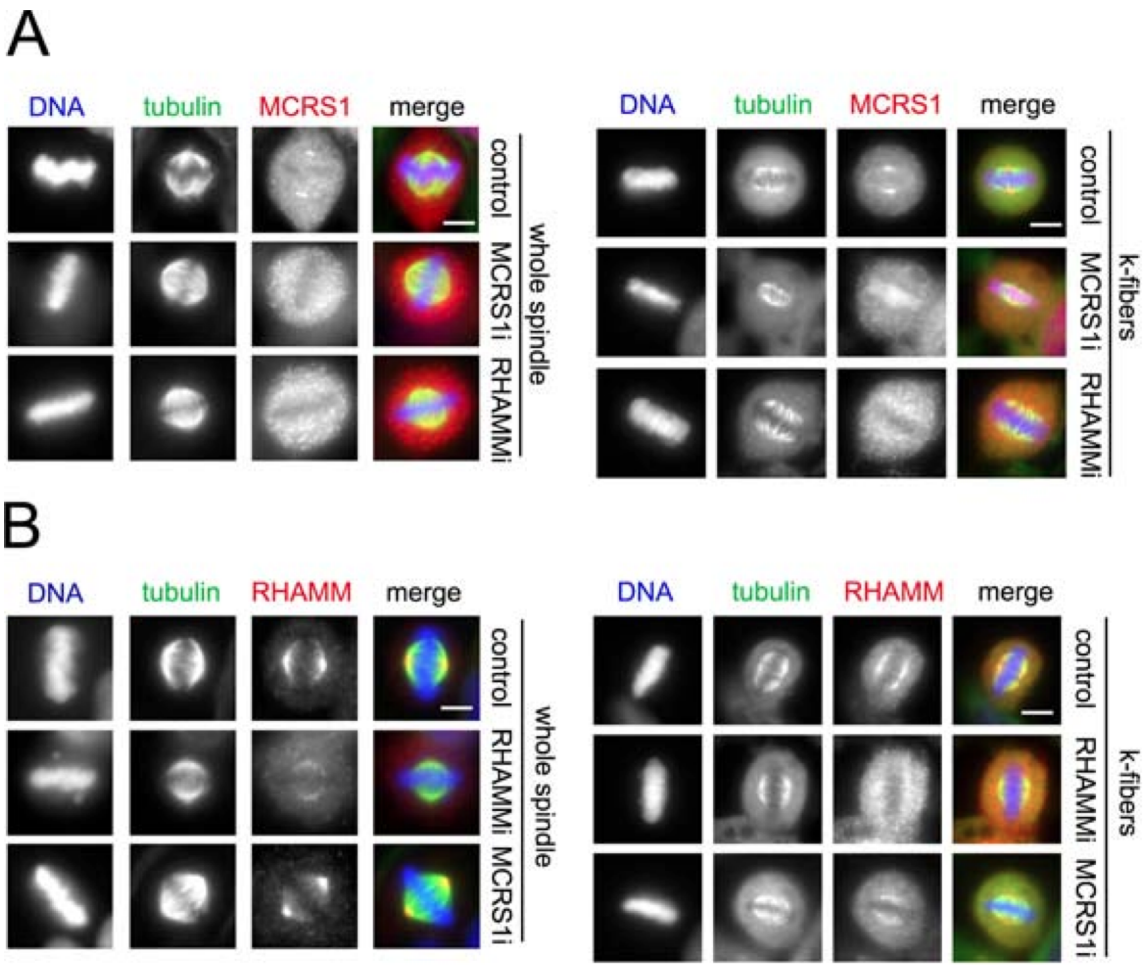

Figure 22. MCRS1 mitotic localization is lost in RHAMM silenced HeLa cells

A) IF analysis of control, MCRS1 and RHAMM silenced HeLa cells. Control mitotic HeLa cells are shown on the left. HeLa cells after 10 minutes incubation on ice are shown on the right. DNA (blue), tubulin (green) and MCRS1 (red). Scale bars: 10 µm. B) IF analysis of control, MCRS1 and RHAMM silenced HeLa cells. Normal mitotic HeLa cells are shown on the left. HeLa cells after 10 minutes incubation on ice are shown on the right. DNA (blue), tubulin (green) and RHAMM (red). Scale bars: 10 µm.

the idea that, during spindle assembly, chromosomal MT asters could be transported to spindle poles. Supporting this hypothesis we showed that proteins that localized to the center of chromosomal MT asters could constitute new structures resistant to ice-cold MT depolymerization. We speculate that an active dynein and NuMA dependent mechanism could act on these new elements. Furthermore, we presented some evidences that chromosome-dependent MT nucleation is essential to properly assemble k-fibers and therefore to faithfully segregate chromosomes. However, despite our preliminary data the exact mechanism describing k-fibers assembly remains unclear.

IV. DISCUSSION

1. A new approach to discriminate between microtubule stabilization and nucleation

DNA coated beads and recombinant RanGTP in *Xenopus laevis* egg extract as well as the MT regrowth assay in cells are the most common experimental approaches to study the chromosomal pathway of MT assembly (Heald et al., 1996; Heald et al., 1997; Tulu et al., 2006). Taking advantage of these tools many proteins involved in the assembly of chromosomal MTs have been identified. However, for many of them, their exact role is still unclear (Meunier and Vernos, 2012).

MT regrowth experiments in HeLa cells showed that silencing components of the MT nucleation machinery like RHAMM, TPX2 and NEDD1 results in the complete lack of chromosomal MTs. Interestingly, several quantifications allowed us to define this phenotype slightly stronger than the silencing of MCRS1. However, even an accurate quantification of chromosomal MT asters after nocodazole washout is not enough to establish if MT nucleation rather than MT stabilization is affected. In fact a major challenge for the identification of novel factors involved in microtubule nucleation is to distinguish them from those that promote microtubule stabilization.

To address this problem we set up an experiment that clearly discriminates between components involved in microtubule nucleation, like NEDD1 and TPX2 from others that play a role in microtubule dynamics/stabilization like MCRS1 (Fig. 22). In fact, as previously shown MCAK silencing rescues MCRS1 phenotype in MT regrowth assay (Meunier and Vernos, 2011). We therefore hypothesized that the same experimental approach could not rescue the phenotype if the MT assembly process is affected upstream to MT stabilization. In fact, RHAMM, TPX2 and NEDD1 silencing phenotypes on chromosomal MT assembly cannot be rescued by silencing the MT depolymerase MCAK. Interestingly, also pontin scored as involved in chromosomal

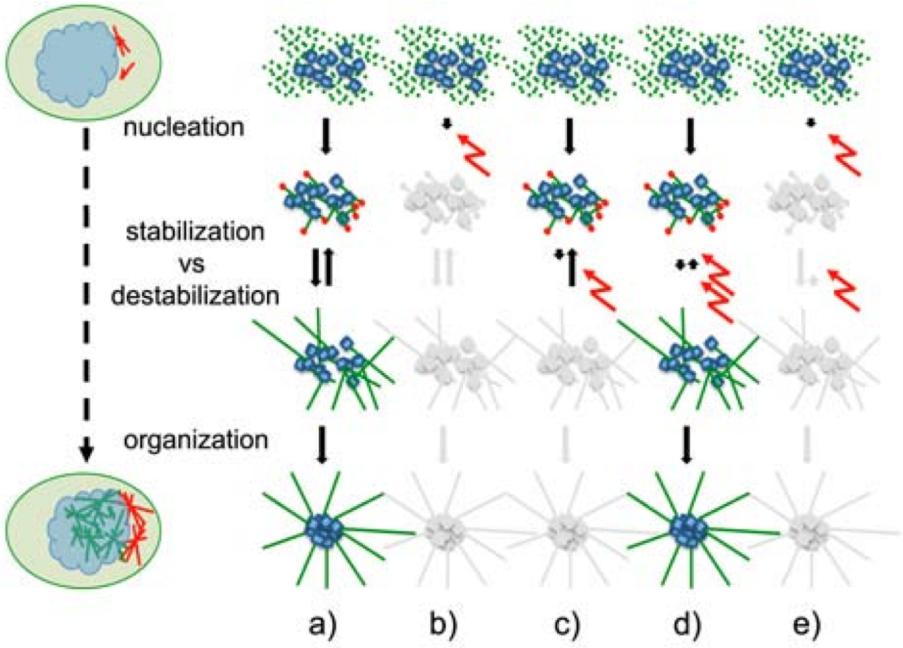

Figure 23. How to discriminate between microtubule stabilization and nucleation

Schematic representation of the approach adopted to discriminate between MT stabilization and nucleation. On the left one cell is recovering after nocodazole washout in MT regrowth assay. Chromosomal MTs asters are represented in green, centrosomal asters in red. (a) Initially, MT nucleation complexes (blue) promote the polymerization of tubulin (green) and the assembly of MTs. Later, stabilizing factors (red) promote MT growth. Finally, MTs are organized into aster-like structures. Interfering with MT nucleation (b) or MT stabilization (c) prevent MT aster formation around the chromosomes. (d) MCAK co-silencing (MT destabilizing factor) can rescue MT stabilization restoring MT aster formation whereas (e) it cannot when MT nucleation has not occurred. This approach therefore allows defining precisely the role of any candidate protein in the MT assembly process.

dependent MT nucleation confirming previous results (Ducat et al., 2008). Consistently with our data the same result has also been reported for Aurora-A (Katayama et al., 2008).

Altogether these results validate the MCAK rescue experiment as a powerful tool to discriminate between MT nucleation and stabilization. Particularly, it could be interesting to combine this experiment with a proteomic approach in order to directly look for new proteins involved in chromosomal dependent MT nucleation.

2. RanGTP triggers the activation of the γTuRC

Adding RanGTP to a CSF-arrested egg extract triggers MT aster formation suggesting that MT nucleation is activated (Carazo-Salas et al., 1999). By IP of the endogenous NEDD1 from the egg extract we were able to efficiently recruit the entire γTuRC core complex on beads. Interestingly we did not observe any difference in the γTuRC composition in extracts treated or not with RanGTP. However, NEDD1-beads do not promote MT assembly in CSF egg extract (Liu and Wiese, 2008). Strikingly, we showed that RanGTP strongly stimulates the assembly of MT asters around the NEDD1-beads.

Because RanGTP activates several targets in the egg extract we retrieved the NEDD1-beads from the egg extract and incubated them in pure tubulin. Strikingly, also in this condition, RanGTP strongly stimulates NEDD1-beads suggesting that the assembly of MTs is the consequence of the activation of MT nucleation rather than MT stabilization. We therefore concluded that RanGTP acts by stimulating γTuRC MT nucleation activity. Even if purified γTuRCs promote MT nucleation *in vitro*, in absence of any additional factor (Wiese and Zheng, 2000; Zheng et al., 1995), our data are in agreement with previous works (Carazo-Salas et al., 2001) suggesting that indeed RanGTP somehow activates the γTuRC activity. Altogether these data could suggest that in the cell cytoplasm, some inhibitory mechanism impairs γTuRC activity in nucleating MTs. Although we cannot totally exclude this hypothesis, we consider it quite unlikely, as we demonstrated that even in absence of RanGTP, the phosphorylation of NEDD1 on S405 and the recruitment of various γTuRC on beads are sufficient to activate its MT nucleation activity. Our results strongly suggest that the only inhibition that is suppressed upon RanGTP activation is the binding between importins and TPX2 (Gruss et al., 2001).

Our results seem to be contradictory with previous experiments done by recruiting the γTuRC using anti GCP2-beads. In this condition, the γTuRC is active and does not respond to RanGTP (Mishra et al., 2010). However, the two approaches differ in the γTuRC components that have been targeted by antibodies to load the complex on beads. Therefore we hypothesise that the antibody epitopes in GCP2 could interfere with the properties of the γTuRC to respond to RanGTP pathway activation.

3. RHAMM characterizes a pool of γTuRC specifically involved in RanGTP dependent MT nucleation

Consistently with previous results (Groen et al., 2004), our immunoprecipitations in egg extract showed that RHAMM interaction with the NEDD1-γTuRC is not RanGTP dependent. Moreover RHAMM depletion from the egg extract does not affect NEDD1-γTuRC levels meaning that the RHAMM-NEDD1-γTuRC represents a small sub population of γTuRCs and that different pools of γTuRC co-exist in the mitotic cell. As RHAMM depletion affects RanGTP dependent MT nucleation (Groen et al., 2004) without affecting centrosomes activity we concluded that the RHAMM-NEDD1-γTuRC is specific for the RanGTP dependent MT nucleation. However, how RHAMM is bound to only one pool of γTuRCs remains unclear. We speculate that RHAMM intracellular concentration could be limiting or alternatively a γTuRC specification mechanism for the RanGTP pathway through a still unidentified factor. It is important to note that although RHAMM is involved in the RanGTP MT assembly pathway it is not a direct RanGTP target (Groen et al., 2004).

The existence of a RHAMM-NEDD1-γTuRC complex subjected to RanGTP regulation suggests that others γTuRC populations may be at play for MT nucleation at the centrosomes or through the Augmin complex (Goshima et al., 2008). Recent results showed that branching MTs nucleation is also stimulated by RanGTP and its effector TPX2 (Petry et al., 2013) suggesting that a TPX2-γTuRC complex could also be involved in this pathway. Although apparently in contrast with our data, these results may fit in our model because the MT amplification pathway is subjected to RanGTP regulation (Petry et al., 2013). We could therefore speculate that the complex that we described to nucleate MTs close to the chromosomes could be required in the amplification through the Augmin pathway by providing the necessary template MTs (Goshima et al., 2008).

Despite all the fragmented information about RHAMM mitotic role (Chen et al., 2014; Groen et al., 2004; Joukov et al., 2006; Maxwell et al., 2005; Tolg et al., 2003) our data suggest a functional explanation of RHAMM function in spindle assembly. In fact, we strikingly showed that RHAMM is essential to promote NEDD1-γTuRC interaction

with TPX2 therefore triggering MT nucleation. A recent work characterized the minimum domains in RHAMM and TPX2 that are required for their interaction although this was not demonstrated *in vitro* (Chen et al., 2014). Interestingly, the domain on TPX2 maps to a N-terminal region containing its primary nuclear localization signal. Consistently with that but in contrast with previous observations (Groen et al., 2004) we found that RHAMM-TPX2 interaction is RanGTP dependent.

As RHAMM depletion prevents NEDD1-TPX2 interaction, we proposed that RHAMM-NEDD1-γTuRC pool is the only one that can bind TPX2, and thereby the only one potentially regulated by RanGTP. Interestingly this mechanism in RanGTP-dependent MT nucleation may help to understand the oncogenic role of this protein (Maxwell et al., 2008). However how a protein with membrane receptor activity (Turley, 1992) could also play such specific role in γTuRC regulation still remain an intriguing mystery.

4. TPX2 provides all the essential requirements for RanGTP dependent γTuRC activation

TPX2 is a well-established factor critical for RanGTP-dependent MT nucleation (Wittmann et al., 2000; Gruss et al., 2001; Neumayer et al., 2014) however the exact mechanism by which it operates is still unclear. Our results strikingly link TPX2 recruitment on RHAMM-NEDD1-γTuRC and the activation of RanGTP-dependent MT nucleation. As shown by our lab, the TPX2 ΔNLS construct, constitutively released from importins, can promote MT nucleation in absence of RanGTP (Brunet et al., 2004). This important data suggests that TPX2 is the only RanGTP target essential to trigger the activation of γTuRC MT nucleation. Strikingly, we found that the same construct, truncated in its first 39 amino acids (Δ39 TPX2 ΔNLS), was not able to promote MT nucleation in absence of RanGTP strongly indicating that Aurora-A activation plays an essential function in this process.

Interestingly we showed that also Aurora-A is recruited on the NEDD1-γTuRC most likely in complex with its major activator TPX2 (Bayliss et al., 2003). Recent results

showed that RHAMM-TPX2 interaction promotes the localization of the active Aurora-A kinase to spindle poles and chromosomal MT asters in HeLa cells (Chen et al., 2014). These data are consistent with our model strengthening the idea that RHAMM could recruit the TPX2-Aurora-A complex to sites of MT nucleation. We then propose that, with this mechanism, RHAMM indirectly triggers NEDD1 S405 phosphorylation therefore contributing to γTuRC activation. In fact we showed that NEDD1 S405 phosphorylation is essential for the RanGTP dependent MT nucleation although the mechanism remains unclear.

NEDD1 S405 phosphorylation has been demonstrated to be Aurora-A dependent. Although we showed that it is required for chromosomal MT nucleation, no direct evidence linked it initially to the RanGTP pathway (Pinyol et al., 2013). Our add back experiments in egg extracts not complemented with RanGTP clearly showed for the first time that S405 phosphorylation depends on TPX2 dependent Aurora-A activation. Providing ΔNEDD1ΔTPX2 extracts with both NEDD1 WT and TPX2 ΔNLS triggers MT nucleation. On the contrary no MTs are nucleated if the Δ39 TPX2 ΔNLS construct, that cannot activate Aurora-A, is added instead. As in these experimental conditions TPX2 ΔNLS is the only direct RanGTP target we can conclude that NEDD1 S405 phosphorylation requires RanGTP that promotes Aurora-A activation by TPX2.

However, we observed that this phosphorylation was not sufficient to promote MT nucleation both in absence of RanGTP or TPX2. This strongly suggests that TPX2 plays another essential role in γTuRC activation apart from promoting NEDD1 S405 phosphorylation. Interestingly our experiments revealed a radical difference between the MT nucleation activity of NEDD1-γTuRC soluble in CSF egg extract and the same complex recruited on beads. Particularly, we observed that NEDD1 S405 phosphorylated γTuRCs, loaded on beads, can overcome TPX2 and RanGTP requirement for MT nucleation. Therefore we propose that the RanGTP pathway, through TPX2, not only triggers NEDD1 S405 phosphorylation but also stimulates the recruitment of multiple γTuRCs. How TPX2 carries out this function and how this event can participate in γTuRC activation are still two essential questions for the field. Interestingly pull down experiments revealed RanGTP dependent TPX2-TPX2 interactions in egg extract. Even if this approach does not prove any direct interaction it suggests the formation of complexes including multiple TPX2 molecules. We then

proposed that this property of TPX2, coming from its C-terminal part, could be the second essential requirement essential to promote RanGTP dependent MT nucleation.

Our work strongly suggests that the gathering of multiple γTuRCs is an essential activation mechanism valid not only for centrosomal MT nucleation but also for the RanGTP pathway. However, we also showed that this mechanism is not sufficient if NEDD1 is not phosphorylated on S405. We found that the γTuRCs remain inactive when loaded on beads in absence of RanGTP. This data points out that the recruitment mechanism described for centrosomal MT nucleation is most probably not sufficient for RanGTP dependent MT nucleation.

5. NEDD1 S405 phosphorylation role in γTuRC microtubule nucleation activity

NEDD1 has recently emerged as a targeting factor for the γTuRC essential for all the known MT assembly pathways in mitosis (Luders et al., 2006; Zhu et al., 2008). NEDD1, targets the nucleation complex to the centrosomes and pre-existing MTs. Specific phosphorylations on NEDD1 are the key mechanism driving this process (Johmura et al., 2011; Sdelci et al., 2012). NEDD1 and the γTuRC are also essential for the chromosomal dependent MT nucleation although the mechanism is still unclear (Luders et al., 2006). Our data showed that also in this pathway one specific phosphorylation on NEDD1 S405 is essential to trigger MT nucleation close to the chromosomes. This phosphorylation site is surprisingly close to the once that determine γTuRC targeting to the centrosomes and the MTs branching points (S377 and S411). However, unlike in the other MT assembly pathways, chromosomal MT nucleation does not seem to arise from a specific site, making targeting an unlikely mechanism. The function of NEDD1 S405 phosphorylation is therefore an intriguing question.

Our data showed that the gathering of multiple γTuRCs is essential for their activation. Therefore, we speculated that the formation of a multi protein complex could act as MTOC and NEDD1 S405 phosphorylation could promote γTuRC recruitment. Our results suggest that oligomers containing multiple copies of TPX2 could play as

molecular platforms to recruit and activate γTuRCs. Pull down experiments of NEDD1 S405 phospho mutants discarded that TPX2 essential binding to the γTuRC was regulated by the NEDD1 S405 phosphorylation state. However, we cannot exclude that an interaction with a still unknown factor could be triggered by this phosphorylation. Interestingly, our beads experiments strongly suggest that such unknown regulatory factor cannot be a direct RanGTP target. In fact, the recruitment of the phospho-mimicking mutant (NEDD1 S405D) on beads is sufficient to activate the γTuRC. This is true also when the beads are prepared in extracts not complemented with RanGTP where all the RanGTP regulated proteins are inhibited by importins.

A second hypothesis to explain the role of NEDD1 S405 phosphorylation is the direct activation of the γTuRC MT nucleation activity. This idea is based on a predicted flexibility in GCP3 resulting in a conformational activation of the γTuRC (Kollman et al., 2011). Our pull downs of NEDD1 S405 phospho mutants did not reveal any major change in the γTuRC core complex composition. As small conformational changes will not be detected with this approach we cannot discard the possibility that NEDD1 S405 phosphorylation works by optimizing the γTuRC template function.

Our data clearly showed that NEDD1 S405 phosphorylation is an essential event to activate RanGTP dependent MT nucleation. However it is not sufficient to promote this activity in CSF egg extract if the RanGTP pathway is not active. This observation strikingly suggested that others events are required to promote γTuRC MT nucleation activity. As discussed before these unknown essential events are provided by TPX2.

6. Chromosomal microtubules role in spindle assembly

It is well established that chromosomal nucleated MTs are essential for spindle assembly and therefore for correct chromosome segregation. However, the precise contribution of this class of MTs to spindle assembly is still unclear. The kinetochores fibers (k-fibers) are bundles of MTs that connect sister kinetochores to the opposite spindle poles and drive their segregation to the two daughter cells (McEwen et al., 1997; Rieder, 1981). MCRS1 is a new RanGTP-target that protects k-fibers minus ends from

depolymerization. During spindle assembly, MCRS1 decorates the center of chromosomal MT asters and in metaphase localizes to k-fibers minus-ends (Meunier and Vernos, 2011). This peculiar localization suggests that during spindle assembly chromosomal MTs could be recruited to spindle poles while forming k-fibers. Consistently with this idea, non-centrosomal asters are recruited to spindle poles by an active transport that involve the minus-end directed motor dynein and NuMA (Khodjakov et al., 2003). Therefore, our current model is that chromosomal MTs minus-ends could be transported towards spindle poles while a different mechanism recruits the plus-ends on kinetochores. The combination of these two processes could explain how k-fibers form during spindle assembly (Meunier and Vernos, 2012). Our preliminary data provided new evidences that chromosomal nucleated MTs participate in k-fiber assembly.

Studying the mitotic localization of proteins involved in the chromosomal pathway we noticed a similar localization pattern to chromosomal MTs. NuSAP, NuMA, RHAMM and MCRS1 do not completely co-localize with the MTs. In fact they appear as dots in the middle of chromosomal MT asters. Interestingly ice-cold depolymerization of chromosomal MT asters showed that these proteins keep their localization independently of the presence of MTs. These data suggest that chromosomal MT asters are organized around cold-stable and MT-independent structures. The mechanism of assembly and the function of these macro-complexes are unclear. However, as we observed the same proteins localized on similar structures on k-fibers minus ends we speculate a transport towards the spindle poles. During this process MTs minus ends could also be recruited.

Our observation also raise an intriguing question on the biological role of chromosomal MT. Why chromosomal nucleated MTs are organized in a variable number of asters-like structures before being recruited on spindle poles? In fact, evidence in cells suggests that chromosomal MT asters are not artefacts derived from MT regrowth protocols (Mahoney et al., 2006). We could speculate that these structures may play an essential mechanical function during spindle and k-fibers assembly.

Another important observation made in the context of k-fibers assembly is that many proteins involved in the RanGTP pathway manifest a phenotype on k-fibers when silenced in cells (Meunier and Vernos, 2012). Our data report that silencing components

of the chromosomal dependent MT nucleation machinery like RHAMM and TPX2 strongly affect k-fibers properties like cold resistance and length. NEDD1 also shows the same phenotype when silenced in HeLa cells (Pinyol et al., 2013). Strikingly this effect was strictly dependent on NEDD1 S405 phosphorylation. Altogether our results suggest that preventing chromosomal MT nucleation interferes with k-fiber assembly. Is this k-fiber phenotype due to the absence of chromosomal MTs or to a direct γTuRC effect on the dynamics of k-fibers minus ends? In agreement with this second hypothesis it has been shown that the γTuRC also plays role in the regulation of MT minus ends dynamics inhibiting depolymerization (Wiese and Zheng, 2000). It is therefore possible that chromosomal dependent MT nucleation machinery contributes both to k-fibers biogenesis and dynamics.

7. Open questions

In this work we examined how the RanGTP pathway regulates MT nucleation through the γTuRC. Particularly we show that TPX2 together with Aurora-A and RHAMM are part of a RanGTP-dependent complex that binds and stimulates the γ-TuRC. We found that within this complex TPX2 carries out two essential events: the phosphorylation by Aurora-A of the γ-TuRC adaptor NEDD1 and the gathering of multiple γTuRCs. This efficient mechanism links γTuRCs recruitment and NEDD1 phosphorylation thereby promoting MT nucleation at the vicinity of the chromosomes. In addition to providing new exciting insights about how chromosomes regulate γTuRC MT nucleation activity, our work opens new research lines to precisely define these mechanisms of play. Some of the most interesting questions that remain to be addressed are the following:

i) Understanding the TPX2-RHAMM-NEDD1-γTuRC complex architecture. The first step will be to clearly define the hierarchy of the complex defining stoichiometry, binding domains between its components and new functional insights. It will also be essential to look for putative missing components of the RanGTP dependent MT nucleation machinery. To this aim it will be interesting to systematically test all the proteins with reported function in MT nucleation such as pontin (Ducat et al., 2008), Nup107/160 (Mishra et al., 2010) and MEL-28 (Yokoyama et al., 2014). To identify

new unknown components of the RanGTP dependent MT nucleation machinery a proteomic approach similar to the one described in this thesis could be used. Particularly, it could be useful to combine it with the MCAK rescue experiment in MT regrowth assay that we showed effective in the identification of proteins involved in chromosomal dependent MT nucleation.

ii) Unraveling the exact function of NEDD1 S405 phosphorylation, defining its molecular role within the γTuRC structure. The first step will be to discriminate between a role in recruitment of unknown γTuRC activators/repressors and a direct action on the γTuRC conformation. To look for new regulatory factors responsive to NEDD1 S405 phosphorylation state we prepared HeLa cell lines stably expressing inducible NEDD1 WT, S405A and S405D. With these tools we will perform SILAC mass spectrometry experiments aimed at the identification of phospho specific interactors of NEDD1. On the other hand, *in vitro* phosphorylation experiments on NEDD1 S405 on γTuRC could be useful to discriminate between activation and recruitment mechanisms. In case of activation effect of S405 phosphorylation on the γTuRC it will be essential to investigate γTuRC conformational changes. The aim will be to get a better understanding on the RHAMM-NEDD1-γTuRC complex architecture and the influence of NEDD1 phosphorylation.

iii) Investigating TPX2 function in promoting γTuRC recruitment and therefore activation. To answer this question, it will be essential to get new insights on TPX2 structure focusing on its possible ability to form oligomers. To this aim, it will be useful to take advantage of both traditional biochemical approaches and high resolution imaging. The combination of this approach with functional experiments in egg extract will be essential to validate the data and get support to our model.

iv) Reconstituting the RanGTP dependent MT nucleation machinery. This is a long term and challenging project that will require a complete definition of all the components of the machinery and their expression and purification. It will be then possible to define the minimal γTuRC composition responsible for MT nucleation through the RanGTP pathway.

v) Understanding the contribution of chromosomes nucleated MTs in spindle assembly. Our preliminary results suggest that chromosomal MTs are the principal k-fibers components. It will be interesting to develop an imaging technique to specifically track chromosomal nucleated MTs to determine if they are indeed essential components of k-fibers.

V. CONCLUSIONS

i) Using a the proteomic based approach we have identified eight novel candidates with a putative role in the RanGTP pathway of MT assembly. Preliminary results on three of them (SET, pontin and DNAJB6) strongly encourage further investigations on their mitotic role.

ii) Aurora-A phosphorylation on NEDD1 S405 is specific, essential but not sufficient for RanGTP dependent MT nucleation in human HeLa cells and *Xenopus laevis* egg extract.

iii) Different subsets of γTuRCs coexist in mitosis, one of them includes RHAMM and is specifically required for RanGTP dependent MT nucleation.

iv) RHAMM plays a conserved role promoting TPX2-γTuRC interaction and therefore stimulating RanGTP dependent MT nucleation.

v) TPX2 is the only RanGTP target essential for the chromosome-dependent MT nucleation activity.

vi) RanGTP dependent γTuRC activation requires two main events both provided by TPX2: the Aurora-A phosphorylation on NEDD1 S405 and the gathering of multiple γTuRCs.

vii) Preliminary experiments in HeLa cells suggest that MTs nucleated close to the chromosomes are essential for k-fibers assembly.

VI. MATERIAL AND METHODS

1. DNA constructs

1.1. NEDD1

The cDNA of human NEDD1 (hNEDD1, GI:206597464) was obtained from RZPD - German Science Centre for Genome Research. Full-length hNEDD1 (1-660 aa) was cloned into pFLAG-CMVTM-2 (Sigma-Aldrich) using the primers 5'-CCATAGATCTGATGCAGGAAAACCTC-3' and 5'-AAGTCGACTCAAAAGTGGGCCCGTAAT-3'. hNEDD1 Ser405 was mutated into Alanine or Aspartic acid by site directed mutagenesis. All the constructs were controlled by sequencing.

1.2. TPX2

Xenopus laevis TPX2 FL ΔNLS and Δ39 TPX2 ΔNLS (bringing Lys284 to Ala mutation) were generated as described previously (Brunet et al., 2004). TPX2 CT has been prepared as described previously (Brunet et al., 2004). GST-N39 TPX2 constructs has been generated and purified as described previously (Bayliss et al., 2003).

1.3. Candidates

Candidates identified in our proteomic screen (Results section 3) were cloned into pFLAG-CMV (Sigma-Aldrich) by PCR on total HeLa cells RNA extract. For long genes two PCR amplified the two half portion of the sequence. A common restriction enzyme site in the forward and direct primers tail allowed cloning the full sequence. The following primers and restriction sites were used:

Gene Name	Ensemble Gene ID	Primers Sequence and Restriction Enzymes
Small nuclear ribonucleoprotein 200kDa (U5)	ENSG00000144028	5'-EcoRI-ATGGCGGATGTAACCGC-3' 5'-CTGGAGAGGGTGCCTATCCCT-ClaI-3' 5'-ClaI-TCACAGCTGAAATTGGAGGGC-3' 5'-GAGACAGACAGTGATTCAGATTGA-XbaI-3'

C5orf24	ENSG00000181904	5'-HindIII-TGATGCATCCTGTTGCCAGC-3' 5'-TCAAAACCACCCAATGAGTGA-XbaI-3'
Elongation factor Tu GTP binding domain containing 2	ENSG00000108883	5'-ClaI-ATGGATACCGACTTATATGATGAG-3' 5'-ACTAAGATGTACAGCACAGATGAT-SalI-3' 5'-SalI-GGAGTCCAGTTTCACGCCTTT-3' 5'-CTCAATTACCCCATGTGA-XbaI-3'
PRP19/PSO4 pre-mRNA processing factor 19 homolog	ENSG00000110107	5'-EcoRI-ATGTCCCTAATCTGCTCCATC-3' 5'-CTCAAGTTCTACAGCCTGTAG-XbaI-3'
C12orf41	ENSG00000139620	5'-HindIII-ATGAACAGGATTCGGATTCACGT-3' 5'-CCAGAACCCACTTCTATTAGTTGA-XbaI-3'
Chaperonin containing TCP1, subunit 8 (theta)	ENSG00000156261	5'-EcoRI-ATGGCGCTTCACGTTCCCAAG-3' 5'-TGGGATGATGACCAAAATGATTGA-XbaI-3'
Isoleucil-tRNA synthetase	ENSG00000196305	5'-HindIII-ATGCTTCAACAAGTTCCAGAAAACA-3' 5'-AGTTTCCATCATCCAGAAG-EcoRI-3' 5'-EcoRI-TATGGTGCTGATGCCCTCAGA-3' 5'-TACCAACAACAGCAGACTTCTAG-XbaI-3'
Small nucleolar RNA, H/ACA box 29	ENSG00000120438	5'-KpnI-ATGGAGGGGCCTTTGTCCGTGTT-3' 5'-CACTCTGGAGCCCTTAATGATTGA-XbaI-3'

Candidates selected from the nuclear proteome (LifeDB) were kindly gift from Dr. Stefan Wiemann. All these genes are cloned in fusion with different CFP/YFP both in C and N terminal.

1.4. Construct for antibody production

To make anti DNAJB6 (ENSG00000105993) and anti SET (ENSG00000119335) antibodies different fragment were cloned in pMAL-C2 vector (New England BioLabs). A schematic of the constructs is reported in (Fig.12 and Fig.14). The following primers and restriction sites were used:

Gene Name	Construct Name	Primer sequence and Restriction Enzymes
SET	SET alpha	5'-EcoRI-ATGGCCCCTAAACGCCAGTCT-3' 5'-GCAGGCTTGCCGAAGAAGGGATAA-XbaI-3'
	SET beta	5'-EcoRI-ATGTCGGCGCCGGCGGCCAAA-3' 5'-TCCAACCACGACGGGGCCGAC-XbaI-3'
	SET FL	5'-EcoRI-ATGTCGGCGCCGGCGGCC-5' 5'-GAGGAGGATGAAGGAGAAGATGACTAA-XbaI

	SET GLOB	5'EcoRI-GAGACCTCAGAAAAAGAACAGCAAGAA-3' 5'-GAAAATAAAGTTCTCTCCAAAGAATTTCATTAA-XbaI-3'
	SET CT	5'-EcoRI-CTGAATGAGAGTGGTGATCCATCT-3' 5'-GAGGAGGATGAAGGAGAAGATGACTAA-XbaI
DNAJB6	DNAJB6 CT	5'-EcoRI-CGGGACATCTATGACAAATATGGC-3' 5'-AAGTCGACCAAAGGCAATCACTAG-XbaI
	DNAJB6 DIS1	5'-EcoRI-CGGGACATCTATGACAAATATGGC-3' 5'-TCAACTTCAACTAAAATGGTTAATGGCTAA-XbaI-3'
	DNAJB6 DIS2	5'-EcoRI-AGAAAAATCACTACAAAGAGAATTGTCGAG-3' 5'-AAGTCGACCAAAGGCAATCACTAG-XbaI

2. Expression and purification of recombinant proteins

Constructs were expressed using the FreeStyle-293 Expression System (Life Technologies) and purified as described previously (Pinyol et al., 2013).

3. siRNA

All the siRNA were purchased from Dharmacon Inc. The following siRNA were used:
RHAMM: 5'-GGUGCUUAUGAUGUUAAAAUU-3'.
TPX2: 5'-GAAUGGAACUGGAGGCUUUU-3'.
MCRS1: GAGGAAGAAGUUCGAUGAUUU-3'.
MCAK: 5'-GAUCCAACGCAGUAAUGGUUU-3'
NEDD1: 5'- GGGCAAAAGCAGACATGTG-3'
Pontin pool of 4 siRNA: 5'-AUAAGGUGGUGAACAAGUA-3' 5'-GGGAAGGACAGCAUUGAGA-3' 5'-CAGGAUAAGUACAUGAAGU-3' 5'-CUCAGGAGCUGGGUAGUAA-3'
SET: oligo1 5'-GAAGUCCACCGAAAUCAAAUU-3'; oligo2 5'-AGGAGAAGAUGACUAAAUAUU-3'
DNAJB6: oligo1 5'-AGCAAGUAGCGGAGGCAUA-3'; oligo2 5'-CUAUGAAGUUCUAGGCGUG-3'
Control (scrambled): 5'-CGUACGCGGAAUACUUCGAUU-3'

4. Antibodies

4.1. Human antibodies

The rabbit polyclonal antibody against human RHAMM was made against three different peptides (1. CAPSPGAYDVKTLEVL; 2. CKVLGIKHFDPSKAFH 3. CYDSMVQSLEDVTAQF). The human rabbit polyclonal antibody against MCRS1 was raised against the following peptide: CTAKSLQVHWQLMKQY (Meunier and Vernos, 2011). The commercial human CREST antibodies was from Antibody Incorporated. The rabbit polyclonal antibody against human NuMA was made against three different peptides (1. CNSLHVADPVEAVLQL; 2. CGASKKALSKASPNTR 3. CEHTSTQALVSELLPA). The rabbit polyclonal antibody against human NuSAP was made against three different peptides.

4.2. *Xenopus laevis* antibodies

The rabbit polyclonal antibody against *Xenopus* TPX2 was raised against recombinant GST-TPX2 (Wittmann et al., 2000) and affinity purified against the full-length protein. The rabbit polyclonal antibody against *Xenopus* NEDD1 was raised against GST-NEDD1 (371-655) and affinity purified against the same NEDD1 fragment (Sdelci et al., 2012). The mouse monoclonal antibody against *Xenopus* TPX2 was produced by Abyntek Biopharma. The rabbit polyclonal antibody against *Xenopus* RHAMM was raised against GST-RHAMM (137 C-terminal amino acids) and affinity purified against the same fragment (Groen et al., 2004). The mouse 1C1 monoclonal antibody against *Xenopus* Eg2 (Aurora-A) was a kind gift from C. Prigent (CNRS Université de Rennes, Rennes, France). Polyclonal antibodies against XGrip195, XGrip109 and pontin were kind gifts from Yixian Zheng (Carnegie Institution for Science, Baltimore, USA).

4.3. General antibodies

GFP polyclonal antibody was raised in rabbit and affinity purified. The monoclonal mouse antibody against γ-tubulin (GTU-88) was from Sigma-Aldrich. The monoclonal mouse antibody against α-tubulin (DM1A) was from Sigma-Aldrich The monoclonal anti human NEDD1 (cross-reacts with *Xenopus* NEDD1) was from Abcam. The mouse monoclonal anti tubulin (12G10) was from the Developmental Studyes Hybridoma Bank (Thazhath et al., 2002).

5. Cell culture

HeLa cell lines were maintained and transfected as described previously (Meunier and Vernos, 2011). The stable HeLa cell line expressing GFP–centrin-1 was a gift from A. Khodjakov (Wadsworth Center, Albany, NY). The stable HeLa cell line expressing histone H2B-GFP and tubulin-RFP was a kind gift from P. Meraldi (ETH, Zurich).

6. Gene silencing

MCAK, MCRS1, TPX2 and NEDD1 genes were silenced as described before (Gruss et al., 2002; Meunier and Vernos, 2011; Pinyol et al., 2013). RHAMM gene was silenced as explained previously (Maxwell et al., 2005). Pontin gene was silenced incubating cells 72h with a pool of four individual siRNA (Dharmacon). SET gene silencing was optimized to work efficiently at 96 hour of incubation. DNAJB6 gene silencing was optimized to work efficiently at 48 hour of incubation. In all the siRNA experiment cells were transfected with Lipofectamine 2000 (Invitrogen) using 100 pmol of siRNAs per well in six-well plates according to the manufacturer's protocol and analysed 48 h after transfection. For double siRNA experiments 100 pmol of each siRNAs were transfected with the double amount of Lipofectamine 2000 in six well plates. To transfect the pool of four 25 pmol of each siRNA were transfected.

7. MT regrowth assay

MT regrowth was performed as previously described (Meunier and Vernos, 2011). MTs were depolymerised by incubating cells in media containing 3μM of nocodazole for 3h and washed two times in PBS and two times in DMEM medium. Cells were incubated at 37 ºC and fixed at different time points.

To visualize TPX2 and RHAMM structures at the center of chromosomal MT asters cells were released from nocodazole 10 minutes an than incubated 30 minutes on ice to completely depolymerise MTs.

To visualize chromosomal MTs interaction with kinetochores cells were released from nocodazole for 15 minutes in presence of nocodazol at 100 mM concentration.

8. Immunofluorescence and fixation

Cells were incubated in pre-warmed medium from 2 to 40 min and fixed in MeOH for 10 min at -20 ºC and than processed for immunofluorescence. Cells grown on coverslips were fixed in −20 °C methanol for 10 min. Blocking and antibody dilution buffer was 0.5% BSA (Sigma), 0.1% Triton-X100 (Sigma). Coverslips were mounted in 10% Mowiol (Calbiochem) in 0.1 M TrisHCl at pH 8.2; 25% glycerol (Merck).

9. K-fiber assay

For cold-stable assays, cells were washed twice with PBS, incubated on ice for 10–25 min in L15 medium (Sigma) supplemented with 20 mM HEPES at pH 7.3 and washed once with cold PBS before fixation. To assay k-fibers stability cells were fixed after 10, 15, 20, 25 minutes of incubation on ice. To assay k-fibers length cells were incubated overnight with 5 μM STLC (Sigma) and then incubated 10 minutes on ice. Microtubules were measured and processed with the imaging and processing software ImageJ.

10. *Xenopus laevis* egg extract

Cytostatic factor arrested egg extracts (CSF-arrested egg extracts) from *Xenopus laevis* were prepared as previously described (Peset et al., 2005). Recombinant RanQ69L-GTP was expressed and purified as described before (Brunet et al., 2004). RanGTP asters were induced by adding 15 μM of RanQ69L-GTP to CSF-arrested extracts containing 0.2 mg/ml of rhodamine-labeled tubulin. Extracts were incubated at 20ºC and squashes of 3 μl were collected at the indicated time points. Quantifications were made counting the total number of MT asters in 10 random lines for each cover slip (40X magnification

with Leica DMI6000B microscope equipped with a Leica DFC 350FX camera). Data were normalized to obtain the number of aster per µl of extract.

DNA-coated beads were prepared as described previously (Brunet et al., 2004). To induce DNA-beads induced MT assembly, CSF arrested egg extract containing 0,2 mg/ml of Rhodamine-labelled tubulin were incubated with DNA-coated beads and sent to interphase by adding 0,4 mM Ca2+. The extract was then cycled back to mitosis by addition of one volume of fresh CSF egg extract. MT assembly was followed taking squashes every 10 minutes. Quantifications were made at 30 minutes. Images were taken at 40X magnification and the total tubulin signal for each beads cluster measured and normalized for the cluster size.

Centrosome MT assembly was studied adding Xenopus sperm nuclei at a concentration of approx. 1000 nuclei/µl to CSF-arrested extract containing 0.2 mg/ml of rhodamine-labeled tubulin. Extracts were incubated at 20ºC and squashes of 3 µl were collected after 6, 8 and 10 minutes of incubation. MT nucleation from sperm centrosomes was evaluated counting 100 nuclei for each condition at every time point.

11. Immunodepletions and immunoprecipitations

For NEDD1, TPX2 and RHAMM immunodepletions, one volume of antibodies-coated protein A dynabeads (Life Technologies) was incubated in 2,5 volumes of CSF-arrested egg extract. Dynabeads were prepared following manufacturer's recommendations. Two rounds of immunodepletion of 30 min each at 4°C completely depleted the endogenous proteins from the CSF-arrested extract. Mock control depletions were performed in the same conditions using unspecific anti-rabbit IgG coated protein-A dynabeads. Experiments aimed to compare samples treated or not with RanGTP immunodepletions were performed before adding RanGTP to the extract.

For immunoprecipitations 1 volume of protein-A dynabeads (Life Technologies) were coated with antibodies (6 µg for 20 µl of beads) and incubated 1h on ice in 2,5 volumes of CSF-arrested extract. All the immunoprecipitations were performed in CSF-arrested extract after 15 min 20˚C incubation with RanGTP (+ condition) or CSF-XB buffer (- condition).

To observe RHAMM-TPX2-NEDD1 interactions beads were washed without detergent four times in TBS buffer like described previously (Groen et al., 2004). To detect NEDD1-γ-tubulin, NEDD1-GCP3, NEDD1-GCP6 and NEDD1-Eg2 interactions beads were washed three times in PBS triton 0,1%. To detect NEDD1-RHAMM, NEDD1-TPX2 and RHAMM-TPX2 interactions beads were washed without detergent (four times in TBS). For all the others IP beads were washed in TBS 0,1% Triton-X100. Proteins were eluted from beads directly in SDS PAGE loading buffer 2X.

12. MT nucleation assay (NEDD1-beads experiments)

To assay the γ-TuRC MT nucleation activity we coated beads with γ-TuRC and associated proteins through immunoprecipitation of NEDD1. One volume of anti-NEDD1 protein-A dynabeads (Life Technologies) was resuspended in a large amount of CSF-arrested extract (10 volumes) and incubated for 1h on ice. To coat beads with NEDD1 S405 phosphorylation mutants, CSF-arrested extracts were depleted of the endogenous protein, complemented with the recombinant proteins and incubated 20 min at 20ºC. IP were performed in extracts incubated (+) or not (-) with RanGTP for 15 min at 20ºC.

To evaluate MT nucleation in CSF-arrested extract beads were washed 4 times in CSF-XB buffer (10 mM Hepes [pH 7,7], 50 mM sucrose, 100 mM KCl, 0,1 mM CaCl2, and 5mM EGTA) and then resuspended in the same volume of the initial beads slurry. Beads were then diluted 200-400 times in 20 µl CSF-arrested extract and incubated at 20ºC 20-30 min. The exact time point was evaluated depending on the extract quality by squashes at different time points.

To study MT nucleation *in vitro*, beads were washed 2 times in CSF-XB and 2 times in BRB80 buffer (80 mM PIPES (pH 6.8), 1 mM EGTA, 1 mM MgCl2) and then resuspended in BRB80 in the same volume of the initial beads slurry. 1-2 µl of beads was then added to a 30 µM pure tubulin solution and incubated 10 minutes at 37ºC. For both approaches the reaction mixture was fixed in 1% glutaraldehyde (in BRB80) and then spun down on cover slips and fixed in methanol 10' at -20ºC. MTs were then visualized by immunofluorescence using anti-tubulin antibody. To quantify MT

nucleation, beads associated with MTs were counted over the total in 30 random fields for each condition.

13. Fluorescence microscopy

Fixed cells were visualized with a ×63 objective on an inverted DMI-6000 Leica wide-field fluorescent microscope. Confocal images were acquired in 0.4 μm steps using a ×63 oil-immersion 1.4 numerical aperture objective lens on a Leica TCS SP5 confocal microscope. Live microscopy were performed with Zeiss Cell Observer HS microscope with x63 dry objective.

VI. BIBLIOGRAPHY

Adachi, Y., G.N. Pavlakis, and T.D. Copeland. 1994. Identification and characterization of SET, a nuclear phosphoprotein encoded by the translocation break point in acute undifferentiated leukemia. *The Journal of biological chemistry*. 269:2258-2262.

Akhmanova, A., and M.O. Steinmetz. 2008. Tracking the ends: a dynamic protein network controls the fate of microtubule tips. *Nature reviews. Molecular cell biology*. 9:309-322.

Al-Bassam, J., and F. Chang. 2011. Regulation of microtubule dynamics by TOG-domain proteins XMAP215/Dis1 and CLASP. *Trends in cell biology*. 21:604-614.

Aldaz, H., L.M. Rice, T. Stearns, and D.A. Agard. 2005. Insights into microtubule nucleation from the crystal structure of human gamma-tubulin. *Nature*. 435:523-527.

Anders, A., and K.E. Sawin. 2011. Microtubule stabilization in vivo by nucleation-incompetent gamma-tubulin complex. *Journal of cell science*. 124:1207-1213.

Asteriti, I.A., W.M. Rensen, C. Lindon, P. Lavia, and G. Guarguaglini. 2010. The Aurora-A/TPX2 complex: a novel oncogenic holoenzyme? *Biochimica et biophysica acta*. 1806:230-239.

Aylett, C.H., J. Lowe, and L.A. Amos. 2011. New insights into the mechanisms of cytomotive actin and tubulin filaments. *International review of cell and molecular biology*. 292:1-71.

Barr, A.R., and F. Gergely. 2007. Aurora-A: the maker and breaker of spindle poles. *Journal of cell science*. 120:2987-2996.

Barros, T.P., K. Kinoshita, A.A. Hyman, and J.W. Raff. 2005. Aurora A activates D-TACC-Msps complexes exclusively at centrosomes to stabilize centrosomal microtubules. *The Journal of cell biology*. 170:1039-1046.

Bayliss, R., T. Sardon, I. Vernos, and E. Conti. 2003. Structural basis of Aurora-A activation by TPX2 at the mitotic spindle. *Molecular cell*. 12:851-862.

Belmont, L., T. Mitchison, and H.W. Deacon. 1996. Catastrophic revelations about Op18/stathmin. *Trends in biochemical sciences*. 21:197-198.

Belmont, L.D., A.A. Hyman, K.E. Sawin, and T.J. Mitchison. 1990. Real-time visualization of cell cycle-dependent changes in microtubule dynamics in cytoplasmic extracts. *Cell*. 62:579-589.

Bhowmick, R., M. Li, J. Sun, S.A. Baker, C. Insinna, and J.C. Besharse. 2009. Photoreceptor IFT complexes containing chaperones, guanylyl cyclase 1 and rhodopsin. *Traffic*. 10:648-663.

Bird, A.W., and A.A. Hyman. 2008. Building a spindle of the correct length in human cells requires the interaction between TPX2 and Aurora A. *The Journal of cell biology*. 182:289-300.

Booth, D.G., F.E. Hood, I.A. Prior, and S.J. Royle. 2011. A TACC3/ch-TOG/clathrin complex stabilises kinetochore fibres by inter-microtubule bridging. *The EMBO journal*. 30:906-919.

Brunet, S., T. Sardon, T. Zimmerman, T. Wittmann, R. Pepperkok, E. Karsenti, and I. Vernos. 2004. Characterization of the TPX2 domains involved in microtubule nucleation and spindle assembly in Xenopus egg extracts. *Molecular biology of the cell*. 15:5318-5328.

Bucciarelli, E., M.G. Giansanti, S. Bonaccorsi, and M. Gatti. 2003. Spindle assembly and cytokinesis in the absence of chromosomes during Drosophila male meiosis. *The Journal of cell biology*. 160:993-999.

Burns, R.G. 1991. Assembly of chick brain MAP2-tubulin microtubule protein. Characterization of the protein and the MAP2-dependent addition of tubulin dimers. *The Biochemical journal*. 277 (Pt 1):231-238.

Carazo-Salas, R.E., O.J. Gruss, I.W. Mattaj, and E. Karsenti. 2001. Ran-GTP coordinates regulation of microtubule nucleation and dynamics during mitotic-spindle assembly. *Nature cell biology*. 3:228-234.

Carazo-Salas, R.E., G. Guarguaglini, O.J. Gruss, A. Segref, E. Karsenti, and I.W. Mattaj. 1999. Generation of GTP-bound Ran by RCC1 is required for chromatin-induced mitotic spindle formation. *Nature*. 400:178-181.

Carlier, M.F. 1989. Role of nucleotide hydrolysis in the dynamics of actin filaments and microtubules. *International review of cytology*. 115:139-170.

Cassimeris, L., D. Gard, P.T. Tran, and H.P. Erickson. 2001. XMAP215 is a long thin molecule that does not increase microtubule stiffness. *Journal of cell science*. 114:3025-3033.

Cheeseman, I.M., and A. Desai. 2008. Molecular architecture of the kinetochore-microtubule interface. *Nature reviews. Molecular cell biology*. 9:33-46.

Chen, H., P. Mohan, J. Jiang, O. Nemirovsky, D. He, M.C. Fleisch, D. Niederacher, L.M. Pilarski, C.J. Lim, and C.A. Maxwell. 2014. Spatial regulation of Aurora A activity during mitotic spindle assembly requires RHAMM to correctly localize TPX2. *Cell cycle*. 13.

Chretien, D., F. Metoz, F. Verde, E. Karsenti, and R.H. Wade. 1992. Lattice defects in microtubules: protofilament numbers vary within individual microtubules. *The Journal of cell biology*. 117:1031-1040.

Cross, R.A., and A. McAinsh. 2014. Prime movers: the mechanochemistry of mitotic kinesins. *Nature reviews. Molecular cell biology*. 15:257-271.

De Luca, M., P. Lavia, and G. Guarguaglini. 2006. A functional interplay between Aurora-A, Plk1 and TPX2 at spindle poles: Plk1 controls centrosomal localization of Aurora-A and TPX2 spindle association. *Cell cycle*. 5:296-303.

Delaval, B., A. Bright, N.D. Lawson, and S. Doxsey. 2011. The cilia protein IFT88 is required for spindle orientation in mitosis. *Nature cell biology*. 13:461-468.

Desai, A., and T.J. Mitchison. 1997. Microtubule polymerization dynamics. *Annual review of cell and developmental biology*. 13:83-117.

Dogterom, M., J.W. Kerssemakers, G. Romet-Lemonne, and M.E. Janson. 2005. Force generation by dynamic microtubules. *Current opinion in cell biology*. 17:67-74.

Doree, M., and S. Galas. 1994. The cyclin-dependent protein kinases and the control of cell division. *FASEB journal : official publication of the Federation of American Societies for Experimental Biology*. 8:1114-1121.

Ducat, D., S. Kawaguchi, H. Liu, J.R. Yates, 3rd, and Y. Zheng. 2008. Regulation of microtubule assembly and organization in mitosis by the AAA+ ATPase Pontin. *Molecular biology of the cell*. 19:3097-3110.

Erickson, H.P. 2000. Gamma-tubulin nucleation: template or protofilament? *Nature cell biology*. 2:E93-96.

Gadde, S., and R. Heald. 2004. Mechanisms and molecules of the mitotic spindle. *Current biology : CB*. 14:R797-805.

Gallant, P. 2007. Control of transcription by Pontin and Reptin. *Trends in cell biology*. 17:187-192.

Gard, D.L., and M.W. Kirschner. 1987. A microtubule-associated protein from Xenopus eggs that specifically promotes assembly at the plus-end. *The Journal of cell biology*. 105:2203-2215.

Garrett, S., K. Auer, D.A. Compton, and T.M. Kapoor. 2002. hTPX2 is required for normal spindle morphology and centrosome integrity during vertebrate cell division. *Current biology : CB*. 12:2055-2059.

Giubettini, M., I.A. Asteriti, J. Scrofani, M. De Luca, C. Lindon, P. Lavia, and G. Guarguaglini. 2011. Control of Aurora-A stability through interaction with TPX2. *Journal of cell science*. 124:113-122.

Golias, C.H., A. Charalabopoulos, and K. Charalabopoulos. 2004. Cell proliferation and cell cycle control: a mini review. *International journal of clinical practice*. 58:1134-1141.

Goodwin, S.S., and R.D. Vale. 2010. Patronin regulates the microtubule network by protecting microtubule minus ends. *Cell*. 143:263-274.

Goshima, G. 2011. Identification of a TPX2-like microtubule-associated protein in Drosophila. *PloS one*. 6:e28120.

Goshima, G., M. Mayer, N. Zhang, N. Stuurman, and R.D. Vale. 2008. Augmin: a protein complex required for centrosome-independent microtubule generation within the spindle. *The Journal of cell biology*. 181:421-429.

Groen, A.C., L.A. Cameron, M. Coughlin, D.T. Miyamoto, T.J. Mitchison, and R. Ohi. 2004. XRHAMM functions in ran-dependent microtubule nucleation and pole formation during anastral spindle assembly. *Current biology : CB*. 14:1801-1811.

Gruss, O.J., R.E. Carazo-Salas, C.A. Schatz, G. Guarguaglini, J. Kast, M. Wilm, N. Le Bot, I. Vernos, E. Karsenti, and I.W. Mattaj. 2001. Ran induces spindle assembly by reversing the inhibitory effect of importin alpha on TPX2 activity. *Cell*. 104:83-93.

Gruss, O.J., and I. Vernos. 2004. The mechanism of spindle assembly: functions of Ran and its target TPX2. *The Journal of cell biology*. 166:949-955.

Gruss, O.J., M. Wittmann, H. Yokoyama, R. Pepperkok, T. Kufer, H. Sillje, E. Karsenti, I.W. Mattaj, and I. Vernos. 2002. Chromosome-induced microtubule assembly mediated by TPX2 is required for spindle formation in HeLa cells. *Nature cell biology*. 4:871-879.

Guillet, V., M. Knibiehler, L. Gregory-Pauron, M.H. Remy, C. Chemin, B. Raynaud-Messina, C. Bon, J.M. Kollman, D.A. Agard, A. Merdes, and L. Mourey. 2011. Crystal structure of gamma-tubulin complex protein GCP4 provides insight into microtubule nucleation. *Nature structural & molecular biology*. 18:915-919.

Gunawardane, R.N., O.C. Martin, and Y. Zheng. 2003. Characterization of a new gammaTuRC subunit with WD repeats. *Molecular biology of the cell*. 14:1017-1026.

Hannak, E., M. Kirkham, A.A. Hyman, and K. Oegema. 2001. Aurora-A kinase is required for centrosome maturation in Caenorhabditis elegans. *The Journal of cell biology*. 155:1109-1116.

Hartwell, L.H. 1978. Cell division from a genetic perspective. *The Journal of cell biology*. 77:627-637.

Heald, R., R. Tournebize, T. Blank, R. Sandaltzopoulos, P. Becker, A. Hyman, and E. Karsenti. 1996. Self-organization of microtubules into bipolar spindles around artificial chromosomes in Xenopus egg extracts. *Nature*. 382:420-425.

Heald, R., R. Tournebize, A. Habermann, E. Karsenti, and A. Hyman. 1997. Spindle assembly in Xenopus egg extracts: respective roles of centrosomes and microtubule self-organization. *The Journal of cell biology*. 138:615-628.

Hendershott, M.C., and R.D. Vale. 2014. Regulation of microtubule minus-end dynamics by CAMSAPs and Patronin. *Proceedings of the National Academy of Sciences of the United States of America*. 111:5860-5865.

Howard, J., and A.A. Hyman. 2007. Microtubule polymerases and depolymerases. *Current opinion in cell biology*. 19:31-35.

Hunt, T. 1989. Maturation promoting factor, cyclin and the control of M-phase. *Current opinion in cell biology*. 1:268-274.

Hunt, T. 1991. Cyclins and their partners: from a simple idea to complicated reality. *Seminars in cell biology*. 2:213-222.

Hutchins, J.R., Y. Toyoda, B. Hegemann, I. Poser, J.K. Heriche, M.M. Sykora, M. Augsburg, O. Hudecz, B.A. Buschhorn, J. Bulkescher, C. Conrad, D. Comartin, A. Schleiffer, M. Sarov, A. Pozniakovsky, M.M. Slabicki, S. Schloissnig, I. Steinmacher, M. Leuschner, A. Ssykor, S. Lawo, L. Pelletier, H. Stark, K. Nasmyth, J. Ellenberg, R. Durbin, F. Buchholz, K. Mechtler, A.A. Hyman, and J.M. Peters. 2010. Systematic analysis of human protein complexes identifies chromosome segregation proteins. *Science*. 328:593-599.

Jiang, K., and A. Akhmanova. 2011. Microtubule tip-interacting proteins: a view from both ends. *Current opinion in cell biology*. 23:94-101.

Jiang, K., S. Hua, R. Mohan, I. Grigoriev, K.W. Yau, Q. Liu, E.A. Katrukha, A.F. Altelaar, A.J. Heck, C.C. Hoogenraad, and A. Akhmanova. 2014. Microtubule minus-end stabilization by polymerization-driven CAMSAP deposition. *Developmental cell*. 28:295-309.

Johmura, Y., N.K. Soung, J.E. Park, L.R. Yu, M. Zhou, J.K. Bang, B.Y. Kim, T.D. Veenstra, R.L. Erikson, and K.S. Lee. 2011. Regulation of microtubule-based microtubule nucleation by mammalian polo-like kinase 1. *Proceedings of the National Academy of Sciences of the United States of America*. 108:11446-11451.

Joukov, V., A.C. Groen, T. Prokhorova, R. Gerson, E. White, A. Rodriguez, J.C. Walter, and D.M. Livingston. 2006. The BRCA1/BARD1 heterodimer modulates ran-dependent mitotic spindle assembly. *Cell*. 127:539-552.

Kalab, P., R.T. Pu, and M. Dasso. 1999. The ran GTPase regulates mitotic spindle assembly. *Current biology : CB*. 9:481-484.

Kalab, P., K. Weis, and R. Heald. 2002. Visualization of a Ran-GTP gradient in interphase and mitotic Xenopus egg extracts. *Science*. 295:2452-2456.

Karsenti, E., J. Newport, and M. Kirschner. 1984. Respective roles of centrosomes and chromatin in the conversion of microtubule arrays from interphase to metaphase. *The Journal of cell biology*. 99:47s-54s.

Karsenti, E., and I. Vernos. 2001. The mitotic spindle: a self-made machine. *Science*. 294:543-547.

Katayama, H., K. Sasai, M. Kloc, B.R. Brinkley, and S. Sen. 2008. Aurora kinase-A regulates kinetochore/chromatin associated microtubule assembly in human cells. *Cell cycle*. 7:2691-2704.

Khodjakov, A., R.W. Cole, B.R. Oakley, and C.L. Rieder. 2000. Centrosome-independent mitotic spindle formation in vertebrates. *Current biology : CB*. 10:59-67.

Khodjakov, A., L. Copenagle, M.B. Gordon, D.A. Compton, and T.M. Kapoor. 2003. Minus-end capture of preformed kinetochore fibers contributes to spindle morphogenesis. *The Journal of cell biology*. 160:671-683.

Khodjakov, A., and T. Kapoor. 2005. Microtubule flux: what is it good for? *Current biology : CB*. 15:R966-968.

Khodjakov, A., and C.L. Rieder. 1999. The sudden recruitment of gamma-tubulin to the centrosome at the onset of mitosis and its dynamic exchange throughout the cell cycle, do not require microtubules. *The Journal of cell biology*. 146:585-596.

Kinoshita, K., T.L. Noetzel, I. Arnal, D.N. Drechsel, and A.A. Hyman. 2006. Global and local control of microtubule destabilization promoted by a catastrophe kinesin MCAK/XKCM1. *Journal of muscle research and cell motility*. 27:107-114.

Kirschner, M.W., and T. Mitchison. 1986. Microtubule dynamics. *Nature*. 324:621.

Kline-Smith, S.L., and C.E. Walczak. 2004. Mitotic spindle assembly and chromosome segregation: refocusing on microtubule dynamics. *Molecular cell*. 15:317-327.

Knoblich, J.A. 2010. Asymmetric cell division: recent developments and their implications for tumour biology. *Nature reviews. Molecular cell biology*. 11:849-860.

Kollman, J.M., A. Merdes, L. Mourey, and D.A. Agard. 2011. Microtubule nucleation by gamma-tubulin complexes. *Nature reviews. Molecular cell biology*. 12:709-721.

Kollman, J.M., J.K. Polka, A. Zelter, T.N. Davis, and D.A. Agard. 2010. Microtubule nucleating gamma-TuSC assembles structures with 13-fold microtubule-like symmetry. *Nature*. 466:879-882.

Kotak, S., and P. Gonczy. 2013. Mechanisms of spindle positioning: cortical force generators in the limelight. *Current opinion in cell biology*. 25:741-748.

Kufer, T.A., H.H. Sillje, R. Korner, O.J. Gruss, P. Meraldi, and E.A. Nigg. 2002. Human TPX2 is required for targeting Aurora-A kinase to the spindle. *The Journal of cell biology*. 158:617-623.

Lawler, S. 1998. Microtubule dynamics: if you need a shrink try stathmin/Op18. *Current biology : CB*. 8:R212-214.

Leung, J.W., A. Leitch, J.L. Wood, C. Shaw-Smith, K. Metcalfe, L.S. Bicknell, A.P. Jackson, and J. Chen. 2011. SET nuclear oncogene associates with microcephalin/MCPH1 and regulates chromosome condensation. *The Journal of biological chemistry*. 286:21393-21400.

Li, M., A. Makkinje, and Z. Damuni. 1996. The myeloid leukemia-associated protein SET is a potent inhibitor of protein phosphatase 2A. *The Journal of biological chemistry*. 271:11059-11062.

Liu, L., and C. Wiese. 2008. Xenopus NEDD1 is required for microtubule organization in Xenopus egg extracts. *Journal of cell science*. 121:578-589.

Luders, J., U.K. Patel, and T. Stearns. 2006. GCP-WD is a gamma-tubulin targeting factor required for centrosomal and chromatin-mediated microtubule nucleation. *Nature cell biology*. 8:137-147.

Mahoney, N.M., G. Goshima, A.D. Douglass, and R.D. Vale. 2006. Making microtubules and mitotic spindles in cells without functional centrosomes. *Current biology : CB*. 16:564-569.

Maia, A.R., X. Zhu, P. Miller, G. Gu, H. Maiato, and I. Kaverina. 2013. Modulation of Golgi-associated microtubule nucleation throughout the cell cycle. *Cytoskeleton*. 70:32-43.

Maiato, H., C.L. Rieder, and A. Khodjakov. 2004. Kinetochore-driven formation of kinetochore fibers contributes to spindle assembly during animal mitosis. *The Journal of cell biology*. 167:831-840.

Margolis, R.L., and L. Wilson. 1978. Opposite end assembly and disassembly of microtubules at steady state in vitro. *Cell*. 13:1-8.

Maurer, S.P., N.I. Cade, G. Bohner, N. Gustafsson, E. Boutant, and T. Surrey. 2014. EB1 accelerates two conformational transitions important for microtubule maturation and dynamics. *Current biology : CB*. 24:372-384.

Maxwell, C.A., J.J. Keats, A.R. Belch, L.M. Pilarski, and T. Reiman. 2005. Receptor for hyaluronan-mediated motility correlates with centrosome abnormalities in multiple myeloma and maintains mitotic integrity. *Cancer research*. 65:850-860.

Maxwell, C.A., J. McCarthy, and E. Turley. 2008. Cell-surface and mitotic-spindle RHAMM: moonlighting or dual oncogenic functions? *Journal of cell science*. 121:925-932.

McEwen, B.F., A.B. Heagle, G.O. Cassels, K.F. Buttle, and C.L. Rieder. 1997. Kinetochore fiber maturation in PtK1 cells and its implications for the mechanisms of chromosome congression and anaphase onset. *The Journal of cell biology*. 137:1567-1580.

Mehrle, A., H. Rosenfelder, I. Schupp, C. del Val, D. Arlt, F. Hahne, S. Bechtel, J. Simpson, O. Hofmann, W. Hide, K.H. Glatting, W. Huber, R. Pepperkok, A. Poustka, and S. Wiemann. 2006. The LIFEdb database in 2006. *Nucleic acids research*. 34:D415-418.

Meunier, S., and I. Vernos. 2011. K-fibre minus ends are stabilized by a RanGTP-dependent mechanism essential for functional spindle assembly. *Nature cell biology*. 13:1406-1414.

Meunier, S., and I. Vernos. 2012. Microtubule assembly during mitosis - from distinct origins to distinct functions? *Journal of cell science*. 125:2805-2814.

Mishra, R.K., P. Chakraborty, A. Arnaoutov, B.M. Fontoura, and M. Dasso. 2010. The Nup107-160 complex and gamma-TuRC regulate microtubule polymerization at kinetochores. *Nature cell biology*. 12:164-169.

Mitchison, T., and M. Kirschner. 1984a. Dynamic instability of microtubule growth. *Nature*. 312:237-242.

Mitchison, T., and M. Kirschner. 1984b. Microtubule assembly nucleated by isolated centrosomes. *Nature*. 312:232-237.

Mitchison, T.J. 1989. Polewards microtubule flux in the mitotic spindle: evidence from photoactivation of fluorescence. *The Journal of cell biology*. 109:637-652.

Moritz, M., Y. Zheng, B.M. Alberts, and K. Oegema. 1998. Recruitment of the gamma-tubulin ring complex to Drosophila salt-stripped centrosome scaffolds. *The Journal of cell biology*. 142:775-786.

Moutinho-Pereira, S., A. Debec, and H. Maiato. 2009. Microtubule cytoskeleton remodeling by acentriolar microtubule-organizing centers at the entry and exit from mitosis in Drosophila somatic cells. *Molecular biology of the cell*. 20:2796-2808.

Murphy, S.M., L. Urbani, and T. Stearns. 1998. The mammalian gamma-tubulin complex contains homologues of the yeast spindle pole body components spc97p and spc98p. *The Journal of cell biology*. 141:663-674.

Murray, A.W., M.J. Solomon, and M.W. Kirschner. 1989. The role of cyclin synthesis and degradation in the control of maturation promoting factor activity. *Nature*. 339:280-286.

Noetzel, T.L., D.N. Drechsel, A.A. Hyman, and K. Kinoshita. 2005. A comparison of the ability of XMAP215 and tau to inhibit the microtubule destabilizing activity of XKCM1. *Philosophical transactions of the Royal Society of London. Series B, Biological sciences*. 360:591-594.

O'Connell, C.B., J. Loncarek, P. Kalab, and A. Khodjakov. 2009. Relative contributions of chromatin and kinetochores to mitotic spindle assembly. *The Journal of cell biology*. 187:43-51.

Oakley, C.E., and B.R. Oakley. 1989. Identification of gamma-tubulin, a new member of the tubulin superfamily encoded by mipA gene of Aspergillus nidulans. *Nature*. 338:662-664.

Oegema, K., C. Wiese, O.C. Martin, R.A. Milligan, A. Iwamatsu, T.J. Mitchison, and Y. Zheng. 1999. Characterization of two related Drosophila gamma-tubulin complexes that differ in their ability to nucleate microtubules. *The Journal of cell biology*. 144:721-733.

Peset, I., J. Seiler, T. Sardon, L.A. Bejarano, S. Rybina, and I. Vernos. 2005. Function and regulation of Maskin, a TACC family protein, in microtubule growth during mitosis. *The Journal of cell biology*. 170:1057-1066.

Petry, S., A.C. Groen, K. Ishihara, T.J. Mitchison, and R.D. Vale. 2013. Branching microtubule nucleation in Xenopus egg extracts mediated by augmin and TPX2. *Cell*. 152:768-777.

Pierson, G.B., P.R. Burton, and R.H. Himes. 1978. Alterations in number of protofilaments in microtubules assembled in vitro. *The Journal of cell biology*. 76:223-228.

Pines, J. 2006. Mitosis: a matter of getting rid of the right protein at the right time. *Trends in cell biology*. 16:55-63.

Pines, J., and C.L. Rieder. 2001. Re-staging mitosis: a contemporary view of mitotic progression. *Nature cell biology*. 3:E3-6.

Pinyol, R., J. Scrofani, and I. Vernos. 2013. The role of NEDD1 phosphorylation by Aurora A in chromosomal microtubule nucleation and spindle function. *Current biology : CB*. 23:143-149.

Radulescu, A.E., and D.W. Cleveland. 2010. NuMA after 30 years: the matrix revisited. *Trends in cell biology*. 20:214-222.

Rebollo, E., S. Llamazares, J. Reina, and C. Gonzalez. 2004. Contribution of noncentrosomal microtubules to spindle assembly in Drosophila spermatocytes. *PLoS biology*. 2:E8.

Remy, M.H., A. Merdes, and L. Gregory-Pauron. 2013. Assembly of gamma-tubulin ring complexes: implications for cell biology and disease. *Progress in molecular biology and translational science*. 117:511-530.

Ribbeck, K., A.C. Groen, R. Santarella, M.T. Bohnsack, T. Raemaekers, T. Kocher, M. Gentzel, D. Gorlich, M. Wilm, G. Carmeliet, T.J. Mitchison, J. Ellenberg, A. Hoenger, and I.W. Mattaj. 2006. NuSAP, a mitotic RanGTP target that stabilizes and cross-links microtubules. *Molecular biology of the cell*. 17:2646-2660.

Ribbeck, K., T. Raemaekers, G. Carmeliet, and I.W. Mattaj. 2007. A role for NuSAP in linking microtubules to mitotic chromosomes. *Current biology : CB*. 17:230-236.

Rice, L.M., E.A. Montabana, and D.A. Agard. 2008. The lattice as allosteric effector: structural studies of alphabeta- and gamma-tubulin clarify the role of GTP in

microtubule assembly. *Proceedings of the National Academy of Sciences of the United States of America*. 105:5378-5383.
Rieder, C.L. 1981. The structure of the cold-stable kinetochore fiber in metaphase PtK1 cells. *Chromosoma*. 84:145-158.
Rieder, C.L. 2005. Kinetochore fiber formation in animal somatic cells: dueling mechanisms come to a draw. *Chromosoma*. 114:310-318.
Rieder, C.L., and A. Khodjakov. 2003. Mitosis through the microscope: advances in seeing inside live dividing cells. *Science*. 300:91-96.
Roberts, A.J., T. Kon, P.J. Knight, K. Sutoh, and S.A. Burgess. 2013. Functions and mechanics of dynein motor proteins. *Nature reviews. Molecular cell biology*. 14:713-726.
Rogers, G.C., S.L. Rogers, and D.J. Sharp. 2005. Spindle microtubules in flux. *Journal of cell science*. 118:1105-1116.
Roll-Mecak, A., and F.J. McNally. 2010. Microtubule-severing enzymes. *Current opinion in cell biology*. 22:96-103.
Rosenblatt, J. 2005. Spindle assembly: asters part their separate ways. *Nature cell biology*. 7:219-222.
Rusan, N.M., U.S. Tulu, C. Fagerstrom, and P. Wadsworth. 2002. Reorganization of the microtubule array in prophase/prometaphase requires cytoplasmic dynein-dependent microtubule transport. *The Journal of cell biology*. 158:997-1003.
Sampath, S.C., R. Ohi, O. Leismann, A. Salic, A. Pozniakovski, and H. Funabiki. 2004. The chromosomal passenger complex is required for chromatin-induced microtubule stabilization and spindle assembly. *Cell*. 118:187-202.
Sanchez, T., D.T. Chen, S.J. DeCamp, M. Heymann, and Z. Dogic. 2012. Spontaneous motion in hierarchically assembled active matter. *Nature*. 491:431-434.
Sanchez, T., and Z. Dogic. 2013. Engineering oscillating microtubule bundles. *Methods in enzymology*. 524:205-224.
Sanchez, T., D. Welch, D. Nicastro, and Z. Dogic. 2011. Cilia-like beating of active microtubule bundles. *Science*. 333:456-459.
Sauer, G., R. Korner, A. Hanisch, A. Ries, E.A. Nigg, and H.H. Sillje. 2005. Proteome analysis of the human mitotic spindle. *Molecular & cellular proteomics : MCP*. 4:35-43.
Schatz, C.A., R. Santarella, A. Hoenger, E. Karsenti, I.W. Mattaj, O.J. Gruss, and R.E. Carazo-Salas. 2003. Importin alpha-regulated nucleation of microtubules by TPX2. *The EMBO journal*. 22:2060-2070.
Schorderet-Slatkine, S., and K.C. Drury. 1973. Progesterone induced maturation in oocytes of Xenopus laevis. Appearance of a 'maturation promoting factor' in enucleated oocytes. *Cell differentiation*. 2:247-254.
Schweizer, N., M. Weiss, and H. Maiato. 2014. The dynamic spindle matrix. *Current opinion in cell biology*. 28C:1-7.
Sdelci, S., M. Schutz, R. Pinyol, M.T. Bertran, L. Regue, C. Caelles, I. Vernos, and J. Roig. 2012. Nek9 phosphorylation of NEDD1/GCP-WD contributes to Plk1 control of gamma-tubulin recruitment to the mitotic centrosome. *Current biology : CB*. 22:1516-1523.
Seo, S.B., P. McNamara, S. Heo, A. Turner, W.S. Lane, and D. Chakravarti. 2001. Regulation of histone acetylation and transcription by INHAT, a human cellular complex containing the set oncoprotein. *Cell*. 104:119-130.
Sigala, B., M. Edwards, T. Puri, and I.R. Tsaneva. 2005. Relocalization of human chromatin remodeling cofactor TIP48 in mitosis. *Experimental cell research*. 310:357-369.

Slep, K.C. 2010. Structural and mechanistic insights into microtubule end-binding proteins. *Current opinion in cell biology*. 22:88-95.

Sorokin, A.V., E.R. Kim, and L.P. Ovchinnikov. 2007. Nucleocytoplasmic transport of proteins. *Biochemistry. Biokhimiia*. 72:1439-1457.

Stewart, S., and G. Fang. 2005. Anaphase-promoting complex/cyclosome controls the stability of TPX2 during mitotic exit. *Molecular and cellular biology*. 25:10516-10527.

Teixido-Travesa, N., J. Roig, and J. Luders. 2012. The where, when and how of microtubule nucleation - one ring to rule them all. *Journal of cell science*. 125:4445-4456.

Teixido-Travesa, N., J. Villen, C. Lacasa, M.T. Bertran, M. Archinti, S.P. Gygi, C. Caelles, J. Roig, and J. Luders. 2010. The gammaTuRC revisited: a comparative analysis of interphase and mitotic human gammaTuRC redefines the set of core components and identifies the novel subunit GCP8. *Molecular biology of the cell*. 21:3963-3972.

Thazhath, R., C. Liu, and J. Gaertig. 2002. Polyglycylation domain of beta-tubulin maintains axonemal architecture and affects cytokinesis in Tetrahymena. *Nature cell biology*. 4:256-259.

Tolg, C., R. Poon, R. Fodde, E.A. Turley, and B.A. Alman. 2003. Genetic deletion of receptor for hyaluronan-mediated motility (Rhamm) attenuates the formation of aggressive fibromatosis (desmoid tumor). *Oncogene*. 22:6873-6882.

Toso, A., J.R. Winter, A.J. Garrod, A.C. Amaro, P. Meraldi, and A.D. McAinsh. 2009. Kinetochore-generated pushing forces separate centrosomes during bipolar spindle assembly. *The Journal of cell biology*. 184:365-372.

Tsai, M.Y., C. Wiese, K. Cao, O. Martin, P. Donovan, J. Ruderman, C. Prigent, and Y. Zheng. 2003. A Ran signalling pathway mediated by the mitotic kinase Aurora A in spindle assembly. *Nature cell biology*. 5:242-248.

Tsai, M.Y., and Y. Zheng. 2005. Aurora A kinase-coated beads function as microtubule-organizing centers and enhance RanGTP-induced spindle assembly. *Current biology : CB*. 15:2156-2163.

Tulu, U.S., C. Fagerstrom, N.P. Ferenz, and P. Wadsworth. 2006. Molecular requirements for kinetochore-associated microtubule formation in mammalian cells. *Current biology : CB*. 16:536-541.

Turley, E.A. 1992. Hyaluronan and cell locomotion. *Cancer metastasis reviews*. 11:21-30.

Vale, R.D., C.M. Coppin, F. Malik, F.J. Kull, and R.A. Milligan. 1994. Tubulin GTP hydrolysis influences the structure, mechanical properties, and kinesin-driven transport of microtubules. *The Journal of biological chemistry*. 269:23769-23775.

Vanneste, D., V. Ferreira, and I. Vernos. 2011. Chromokinesins: localization-dependent functions and regulation during cell division. *Biochemical Society transactions*. 39:1154-1160.

Varga, V., J. Helenius, K. Tanaka, A.A. Hyman, T.U. Tanaka, and J. Howard. 2006. Yeast kinesin-8 depolymerizes microtubules in a length-dependent manner. *Nature cell biology*. 8:957-962.

von Lindern, M., S. van Baal, J. Wiegant, A. Raap, A. Hagemeijer, and G. Grosveld. 1992. Can, a putative oncogene associated with myeloid leukemogenesis, may be activated by fusion of its 3' half to different genes: characterization of the set gene. *Molecular and cellular biology*. 12:3346-3355.

Vos, J.W., L. Pieuchot, J.L. Evrard, N. Janski, M. Bergdoll, D. de Ronde, L.H. Perez, T. Sardon, I. Vernos, and A.C. Schmit. 2008. The plant TPX2 protein regulates prospindle assembly before nuclear envelope breakdown. *The Plant cell*. 20:2783-2797.

Wainman, A., D.W. Buster, T. Duncan, J. Metz, A. Ma, D. Sharp, and J.G. Wakefield. 2009. A new Augmin subunit, Msd1, demonstrates the importance of mitotic spindle-templated microtubule nucleation in the absence of functioning centrosomes. *Genes & development*. 23:1876-1881.

Wiese, C., and Y. Zheng. 2000. A new function for the gamma-tubulin ring complex as a microtubule minus-end cap. *Nature cell biology*. 2:358-364.

Wittmann, T., H. Boleti, C. Antony, E. Karsenti, and I. Vernos. 1998. Localization of the kinesin-like protein Xklp2 to spindle poles requires a leucine zipper, a microtubule-associated protein, and dynein. *The Journal of cell biology*. 143:673-685.

Wittmann, T., M. Wilm, E. Karsenti, and I. Vernos. 2000. TPX2, A novel xenopus MAP involved in spindle pole organization. *The Journal of cell biology*. 149:1405-1418.

Wollman, R., E.N. Cytrynbaum, J.T. Jones, T. Meyer, J.M. Scholey, and A. Mogilner. 2005. Efficient chromosome capture requires a bias in the 'search-and-capture' process during mitotic-spindle assembly. *Current biology : CB*. 15:828-832.

Yang, G., B.R. Houghtaling, J. Gaetz, J.Z. Liu, G. Danuser, and T.M. Kapoor. 2007. Architectural dynamics of the meiotic spindle revealed by single-fluorophore imaging. *Nature cell biology*. 9:1233-1242.

Yokoyama, H., B. Koch, R. Walczak, F. Ciray-Duygu, J.C. Gonzalez-Sanchez, D.P. Devos, I.W. Mattaj, and O.J. Gruss. 2014. The nucleoporin MEL-28 promotes RanGTP-dependent gamma-tubulin recruitment and microtubule nucleation in mitotic spindle formation. *Nature communications*. 5:3270.

Zheng, Y., M.L. Wong, B. Alberts, and T. Mitchison. 1995. Nucleation of microtubule assembly by a gamma-tubulin-containing ring complex. *Nature*. 378:578-583.

Zhu, H., J.A. Coppinger, C.Y. Jang, J.R. Yates, 3rd, and G. Fang. 2008. FAM29A promotes microtubule amplification via recruitment of the NEDD1-gamma-tubulin complex to the mitotic spindle. *The Journal of cell biology*. 183:835-848.